

# 4-(Difluoromethyl)-5-(4-((3*R*,5*S*)-3,5-dimethylmorpholino)-6-((*R*)-3-methylmorpholino)-1,3,5-triazin-2-yl)pyridin-2-amine (PQR626), a Potent, Orally Available, and Brain-Penetrant mTOR Inhibitor for the Treatment of Neurological Disorders

Chiara Borsari, Erhan Keles, Denise Rageot, Andrea Treyer, Thomas Bohnacker, Lukas Bissegger, Martina De Pascale, Anna Melone, Rohitha Sriramaratnam, Florent Beauflis, Matthias Hamburger, Paul Hebeisen, Wolfgang Löscher, Doriano Fabbro, Petra Hillmann, and Matthias P. Wymann\*



Cite This: *J. Med. Chem.* 2020, 63, 13595–13617



Read Online

ACCESS |



Metrics & More

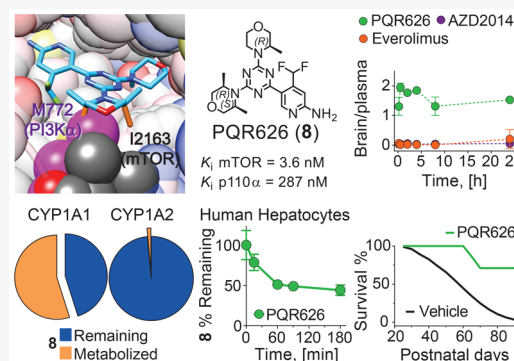


Article Recommendations



Supporting Information

**ABSTRACT:** The mechanistic target of rapamycin (mTOR) pathway is hyperactivated in cancer and neurological disorders. Rapalogs and mTOR kinase inhibitors (TORKi) have recently been applied to alleviate epileptic seizures in tuberous sclerosis complex (TSC). Herein, we describe a pharmacophore exploration to identify a highly potent, selective, brain penetrant TORKi. An extensive investigation of the morpholine ring engaging the mTOR solvent exposed region led to the discovery of PQR626 (**8**). **8** displayed excellent brain penetration and was well-tolerated in mice. In mice with a conditionally inactivated *Tsc1* gene in glia, **8** significantly reduced the loss of *Tsc1*-induced mortality at 50 mg/kg p.o. twice a day. **8** overcomes the metabolic liabilities of PQR620 (**52**), the first-in-class brain penetrant TORKi showing efficacy in a TSC mouse model. The improved stability in human hepatocytes, excellent brain penetration, and efficacy in *Tsc1*<sup>GFAP</sup>CKO mice qualify **8** as a potential therapeutic candidate for the treatment of neurological disorders.



## INTRODUCTION

The mechanistic target of rapamycin (mTOR) is activated downstream of phosphoinositide 3-kinase (PI3K). The mTOR kinase is a part of two functionally distinct multiprotein complexes, mTOR complex 1 (mTORC1) and mTOR complex 2 (mTORC2).<sup>1,2</sup> TORC1 monitors the availability of cellular energy, oxygen and amino acids, surface receptor ligation, and stress levels. Cell surface receptor-mediated activation of PI3K triggers PtdIns(3,4,5)P<sub>3</sub> production, which is recognized by the pleckstrin homology domains in protein kinase B (PKB/Akt), phosphoinositide-dependent protein kinase 1 (PDK1), and the TORC2 component SIN1. Thr308 is phosphorylated by PDK1 and at Ser473 in the hydrophobic motif by mTORC2.<sup>3,4</sup> TORC1 regulates lipid and protein synthesis through phosphorylation of S6 kinase (S6K), resulting in phosphorylation of the downstream effector ribosomal protein S6.<sup>5</sup> Moreover, TORC1 modulates lysosome function and inhibits autophagy. TORC2 controls cytoskeletal rearrangements, cell cycle progression, and survival.<sup>6</sup> A critical negative regulator of TORC1 is the suppressor protein tuberous sclerosis complex (TSC), composed of hamartin (TSC1) and tuberin (tuberous sclerosis 2, TSC2). PKB/Akt regulates TSC *via* phosphorylation of tuberin on multiple sites.

Phosphorylation of TSC2 blocks its GTPase-activating function, resulting in active Ras homolog enriched in brain and TORC1.<sup>6,7</sup>

The mTOR pathway is dysregulated in many diseases such as neurological disorders, cancer, and type 2 diabetes.<sup>4,8</sup> In central nervous system (CNS) disorders, mTOR is supposed to be implicated in Parkinson's, Alzheimer's, and Huntington's disease, epilepsy, stroke, and trauma.<sup>9</sup> TSC loss of function triggers hyperactivation of TORC1, causing hyperplastic lesions in multiple organs. In ~90% of TSC patients, epilepsy, behavioral problems, and cognitive impairment dominate the patient's morbidity, which have made mTOR kinase a target for TSC treatment in the CNS.<sup>10</sup>

Rapamycin (**55**) and its derivatives (dubbed rapalogs; Figure 1) are allosteric inhibitors of TORC1 and form *via*

Received: April 15, 2020

Published: November 9, 2020



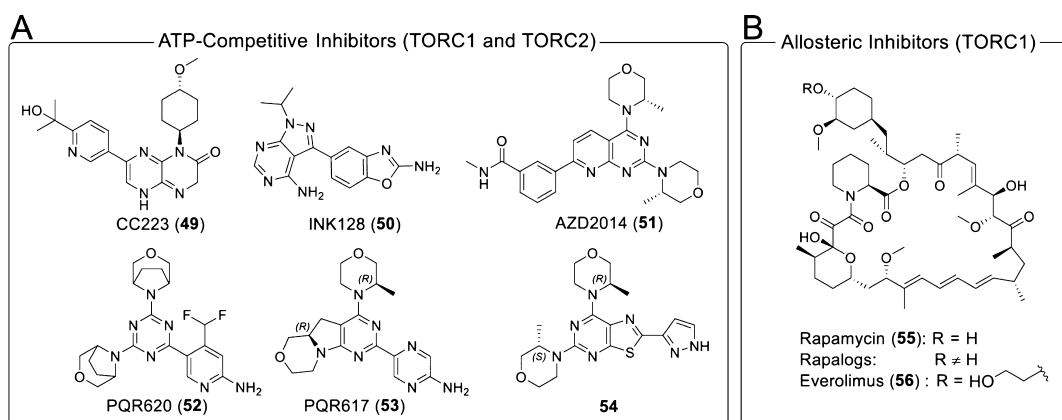
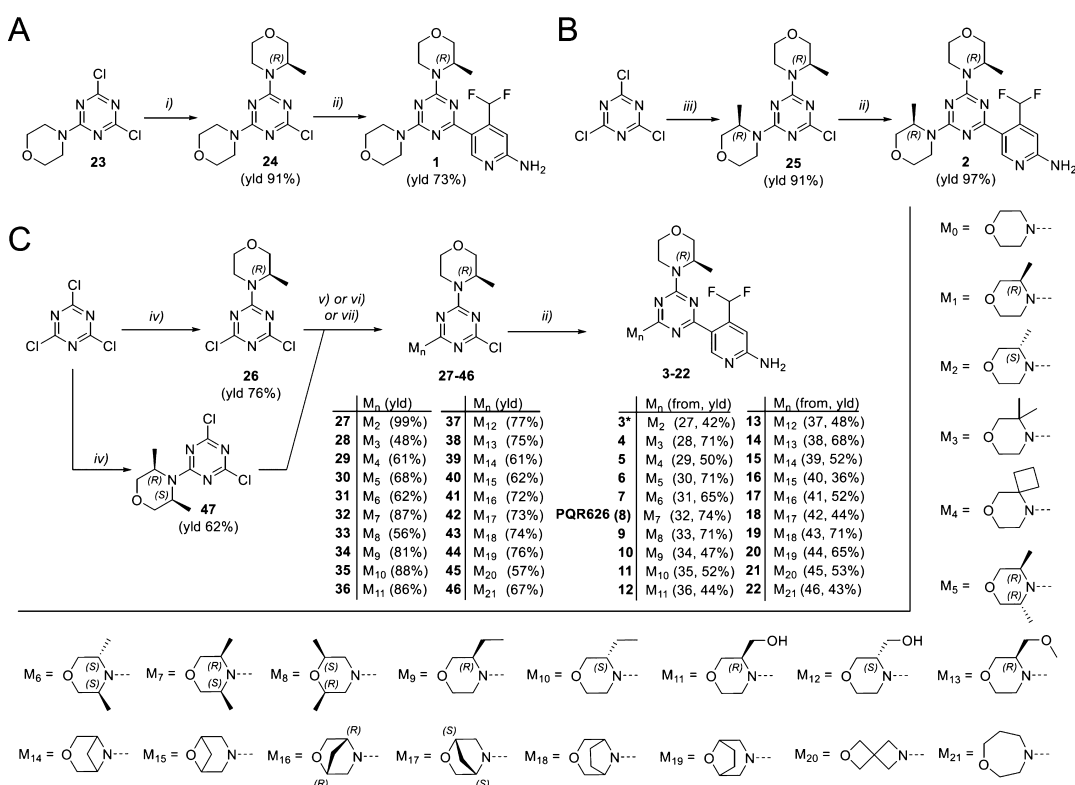


**Figure 1.** (A) Chemical structures of selected TORKi, including 49,<sup>23</sup> 50,<sup>24</sup> 51,<sup>25</sup> 52,<sup>26</sup> 53,<sup>27</sup> and a thiazolopyrimidine derivative (54).<sup>28</sup> (B) Chemical structures of 55 and rapalogs (e.g., 56), which function as allosteric inhibitors of TORC1, forming a TORC1-rapalog-FKBP12 complex.<sup>11</sup>

**Scheme 1. (A–C) Synthesis of the Compound Library (1–22)<sup>4a</sup>**



<sup>a</sup>Reagents and conditions: (i) morpholine, *N,N*-diisopropylethylamine (DIPEA), EtOH, 0 °C → rt, o/n as reported in the literature;<sup>26</sup> (ii) (1) boronate 48, XPhosPdG2 (cat.), K<sub>3</sub>PO<sub>4</sub>, dioxane/H<sub>2</sub>O, 95 °C, 2–16 h; (2) HCl, H<sub>2</sub>O, 60 °C, 3–16 h; (iii) morpholine derivative (M<sub>n</sub>-H), DIPEA, DCM, 0 °C → rt, o/n as reported in the literature;<sup>26</sup> (iv) morpholine derivative (M<sub>n</sub>-H), DCM, -50 °C, 2 h; (v) M<sub>n</sub>-H, DIPEA, DCM, 0 °C → rt, o/n (for 27–29, 32, 34–46); (vi) M<sub>n</sub>-H, DIPEA, THF, 0 °C → rt → 70 °C, o/n (for 30 and 31); (vii) see (i) for intermediate 33. \*Compound 3 is reported in ref 35.

the FKBP-rapamycin binding domain (FRB domain) of TORC1 a stable complex with FK506 binding protein 12 (FKBP12) bound to rapamycin.<sup>11</sup> Chronic exposure to rapalogs has been proposed to disrupt mTORC2 after long exposure.<sup>12</sup> The beneficial effects of 55 or rapalogs alleviating epileptic seizures caused by loss-of-function in mTOR signaling have been recently explored. Sirolimus (55) and everolimus (56, RAD001) significantly decreased seizures in mice with tissue-specific inactivation of the *Tsc1* gene primarily in glia (*Tsc1*<sup>GFAP</sup>CKO mice) and prolonged their survival.<sup>13,14</sup> Moreover, rapalogs displayed efficacy in reducing frequency of

seizures and TSC-associated solid tumor size in TSC patients, leading to the approval of 56 for the treatment of TSC-associated seizures in 2018.<sup>15,16</sup> The ability of mTOR inhibitors to induce autophagy and to reduce detrimental protein aggregates in neurons may be exploited for the treatment of other neurological disorders including Huntington's,<sup>17,18</sup> Alzheimer's,<sup>19</sup> and Parkinson's diseases.<sup>20</sup> However, TORC1 inhibition by rapalogs is not efficient in all TSC patients, and significant adverse side effects due to immune suppression often demand the termination of further treatment.<sup>21</sup> The adverse side effects are pronounced because

Table 1. SAR Investigation on the Exploration of Substituted Morpholines

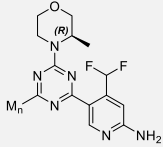
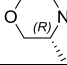
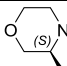
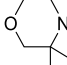
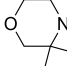
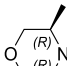
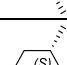
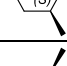
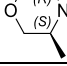
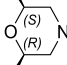
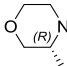
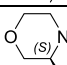
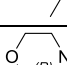
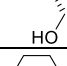
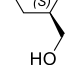
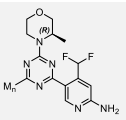
Name	M <sub>n</sub>	Cellular Assays IC <sub>50</sub> [nM] <sup>a</sup>		<i>in vitro</i> Binding Assays K <sub>i</sub> [nM] <sup>b</sup>		Selectivity K <sub>i</sub> (p110α)/ K <sub>i</sub> (mTOR)	clogP <sup>c</sup>	PSA <sup>c</sup>
		pPKB S473	pS6 S235/236	p110α	mTOR			
<b>1</b>		147 ± 14	138 ± 23	19 ± 0.89	8.0 ± 2.5	2.5	2.80	102.52
<b>2</b>		436 ± 65	261 ± 75	469 ± 1.7	14 ± 2.7	39	3.22	102.52
<b>3</b>		173 ± 6.8	137 ± 8.3	33 ± 8.4	11 ± 4.6	2.9	3.22	102.52
<b>4</b>		191 ± 11	61 ± 9.8	469 ± 250	4.7 ± 0.38	100	3.30	102.52
<b>5</b>		271 ± 27	192 ± 13	404 ± 21	11 ± 0.88	36	3.63	102.52
<b>6</b>		506 ± 45	392 ± 20	>1000	25 ± 1.7	>43	3.63	102.52
<b>7</b>		200 ± 13	136 ± 3.7	233 ± 17	6.4 ± 1.9	37	3.63	102.52
<b>PQR626 (8)</b>		96 ± 9.6	71 ± 11	287 ± 37	3.6 ± 0.98	80	3.63	102.52
<b>9</b>		1338 ± 280	561 ± 43	>1000	42 ± 13	>24	3.63	102.52
<b>10</b>		231 ± 8.9	238 ± 50	65 ± 5.0	18 ± 3.8	3.6	3.69	102.52
<b>11</b>		248 ± 20	241 ± 23	63 ± 28	67 ± 36	0.9	3.69	102.52
<b>12</b>		1483 ± 227	>1000	>1000	50 ± 7.7	>20	2.13	122.75
<b>13</b>		524 ± 45	471 ± 52	>1000	28 ± 2.9	>35	2.13	122.75
<b>14</b>		956 ± 123	426 ± 89	>1000	23 ± 12	>43	2.71	111.75
<b>15</b>		1561 ± 145	407 ± 33	>1000	73 ± 0.82	>14	2.82	102.52

Table 1. continued

		Cellular Assays IC <sub>50</sub> [nM] <sup>a</sup>		<i>in vitro</i> Binding Assays K <sub>i</sub> [nM] <sup>b</sup>		Selectivity K <sub>i</sub> (p110α)/ K <sub>i</sub> (mTOR)	clogP <sup>c</sup>	PSA <sup>c</sup>
Name	M <sub>n</sub>	pPKB S473	pS6 S235/236	p110α	mTOR			

<sup>a</sup>Phosphorylation of PKB (Ser473) and S6 (Ser235/236) were measured in A2058 cells treated with inhibitors. Subsequent detection of phosphoproteins was done using in-cell western assays. IC<sub>50</sub>s were measured using a 7- or 11-point 1:2 serial dilution and each concentration was measured in independent triplicate (7-point dilution) or independent duplicate (11-point dilution) experiments. Data are reported as mean ± SD. Log IC<sub>50</sub>s are reported in Table S1 in the Supporting Information. <sup>b</sup>The *in vitro* binding of the compounds to the ATP-binding site of p110α and mTOR was evaluated with a commercially available time-resolved Förster resonance energy transfer (TR-FRET) displacement assay. IC<sub>50</sub>s were measured using a 10-point 1:4 serial dilution and each concentration was performed in independent duplicate experiments. Data are reported as mean ± SD. IC<sub>50</sub>s and log IC<sub>50</sub>s are reported in Table S1. <sup>c</sup>Marvin/JChem 20.9 was used to calculate logP (partition coefficient) and PSA (polar surface area) values, ChemAxon (<https://www.chemaxon.com>).

rapalogs have a limited ability to penetrate the blood–brain barrier (BBB). Only when high plasma levels are reached, mTOR in the brain can be efficiently inhibited.<sup>22</sup>

For these reasons, the identification of mTOR inhibitors with optimized brain permeability is an ongoing challenge for the treatment of CNS disorders.

mTOR kinase inhibitors (TORKi) that bind to the ATP-pocket inhibit mTOR kinase and thus target the function of both mTORC1 and mTORC2. mTOR-selective inhibitors covering different chemical spaces have been discovered, including CC-223 (49),<sup>23</sup> sapanisertib/INK128<sup>24</sup> (50), and vistusertib/AZD2014<sup>25</sup> (51; Figure 1), and have been explored to treat a variety of human cancers.

We have recently disclosed PQR620 (52, Figure 1), a brain penetrable inhibitor of mTOR kinase with excellent selectivity.<sup>26</sup> Compound 52, bearing two ethylene bridged morpholines, is the first-in-class selective catalytic mTOR inhibitor able to cross the BBB. It has been identified through chemical modifications of PQR309 (57, bimiralisib; see the Supporting Information for chemical structure),<sup>29–32</sup> a pan-PI3K inhibitor with moderate mTOR affinity, currently evaluated in Phase II trials of solid tumors and lymphomas.<sup>33</sup> In 2020, Novartis has proposed a novel brain-penetrant TORKi bearing a thiazolopyrimidine scaffold (54, Figure 1).<sup>28</sup> Very recently, we have explored a novel chemical space and disclosed a tricyclic pyrimido-pyrrolo-oxazine, PQR617 (53, Figure 1), showing selectivity for mTOR over class I PI3Ks of ~450-fold. However, this compound showed only minimal brain penetration,<sup>27</sup> preventing application in the treatment of CNS disorders.

Because the ethylene bridge on the two morpholines in 52 has been identified as a primary site of metabolism in human liver microsomes<sup>34</sup> and human hepatocytes, 52 has been characterized as an optimal proof-of-concept molecule for rodent models<sup>22</sup> but is expected to have a short half-life in human patients. Pharmacokinetic studies of 52 in male cynomolgous monkeys showed a rapid compound degradation (Figure S1). The metabolic reactions occurred mainly by oxidation of 52 at the bridged morpholines, while the triazine core and the 4-(difluoromethyl)pyridin-2-amine did not show metabolic sensitivity (Figure S2). We therefore focused on the modification of both morpholines of 52 and on the development of a follow-up compound for 52 with improved metabolic stability in humans. We built up a broad structure–activity relationship (SAR) study to develop novel, brain-penetrable, and orally bioavailable mTORC1/2 inhibitors. Evaluation of metabolic stability and pharmacokinetic proper-

ties pinpointed PQR626 (8) as a promising candidate for CNS indications.

## RESULTS AND DISCUSSION

**Chemistry.** The library of triazine compounds was synthesized as depicted in Scheme 1. (*R*)-4-(4-Chloro-6-morpholino-1,3,5-triazin-2-yl)-3-methylmorpholine (24) was prepared from 2,4-dichloro-6-(morpholin-4-yl)-1,3,5-triazine (23), and later compound 1 was generated from intermediate 24 and boronate 48 (see Experimental Section for the chemical structure) using a Suzuki cross-coupling (Scheme 1A). The first step in the synthesis of compound 2 involved the di-substitution of cyanuric chloride with the same morpholine moiety (M<sub>1</sub>, (*R*)-3-methylmorpholine) to generate intermediate 25 (Scheme 1B). All other final compounds were synthesized starting from cyanuric chloride by following substitution with two different morpholine derivatives: first (*R*)-3-methylmorpholine was introduced (76% yield), followed by substituted morpholine M<sub>n</sub> (M<sub>2</sub>–M<sub>6</sub> and M<sub>8</sub>–M<sub>21</sub>, Scheme 1C). Influenced by the first morpholine derivative introduced, the second nucleophilic substitution yielded the desired intermediates with moderate to excellent yields (48–99%). As depicted in Scheme 1C, the synthesis of intermediate 32 was optimized introducing first the highest sterically hindered morpholine [(3*S*,5*R*)-3,5-dimethylmorpholine, 62% yield], followed by (*R*)-3-methylmorpholine (87% yield). The last synthetic step involved the displacement of the chlorine of intermediates (24, 25, 27–46) by the heteroaryl moiety using a palladium-catalyzed Suzuki cross-coupling with boronate 48. Yields for final compounds (1–22) were moderate to excellent (36–97%).

**Combining Pharmacophore Features.** The triazine core of 52 was selected as the primary building block, and chemical features of 52 and 53 inspired scaffold explorations. The 4-(difluoromethyl)pyridin-2-amine was chosen as a heteroaromatic ring because it was found to be an essential feature for mTOR affinity. As previously suggested, the CHF<sub>2</sub>-moiety potentially (i) interacts with a nitrogen atom of the triazine core or (ii) with Glu2190 in mTOR, leading to highly potent compounds *in vitro* and in cells.<sup>26</sup> In addition, the pyridine ring displayed a higher mTOR potency compared to the pyrimidine moiety.<sup>32</sup> The (*R*)-3-methylmorpholine represented the third pharmacophoric feature in our drug design process. This substituted morpholine provided selectivity for mTOR over the closely related PI3K family, as highlighted by the development of 53 and 54 (Figure 1).<sup>27,28</sup>



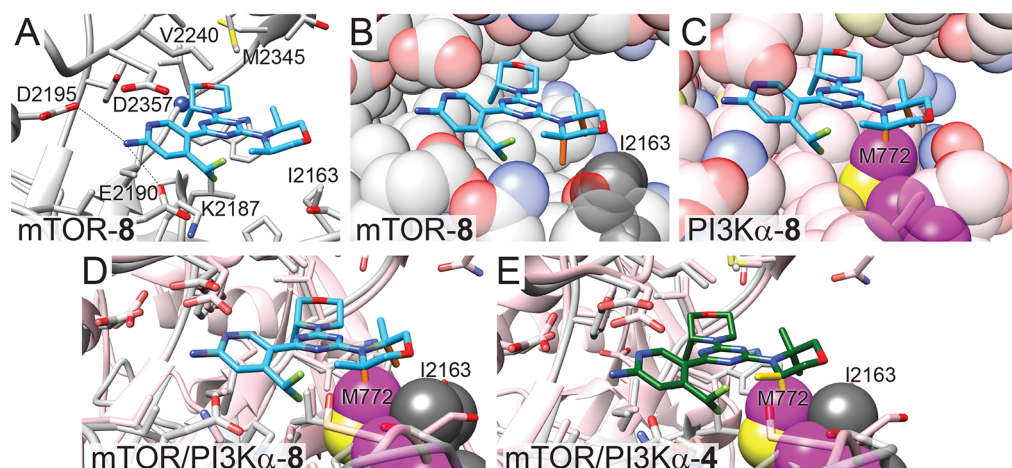


**Figure 2.** (A) Docking of **8** (light blue) to mTOR (gray) starting from PDB: 4JT6. H-bonds are represented as dashed black lines. The backbone amide (Val2240) essential for binding is shown in a ball-and-stick representation. (B) Sphere representation of mTOR-8 complex and (C) of PI3K $\alpha$ -8 complex. Ile2163 (mTOR) is depicted as dark gray while Met772 (PI3K $\alpha$ ) in magenta. Both conformations (“methyl-up” in light blue and “methyl-down” in orange) are displayed. Docking of **8** (light blue) to PI3K $\alpha$  (pink) was performed starting from PDB: 6OAC. (D) Superimposition of mTOR-8 and PI3K $\alpha$ -8 complex; mTOR (gray) and PI3K $\alpha$  (pink). (E) Superimposition of mTOR-4 and PI3K $\alpha$ -4 complexes; mTOR (gray) and PI3K $\alpha$  (pink). Both conformations (“methyl-right” in green and “methyl-left” in yellow) are displayed.

### Assessment of Cellular Efficacy and PI3K/mTOR Affinity.

To identify novel brain penetrant TORKi with optimized metabolic stability, we focused our SAR study on the exploration of substituted morpholines. With the exception of **1**, which bears one unsubstituted morpholine, we synthesized a library of compounds bearing differently substituted morpholines ( $M_n$  substituents, Scheme 1), namely, 3-methylmorpholine [ $M_1$ : (R) and  $M_2$ : (S)], 3,3-dimethylmorpholine ( $M_3$ ), 8-oxa-5-azaspiro[3.5]nonane ( $M_4$ ), 3,5-dimethylmorpholine [ $M_5$ : (3R,5R);  $M_6$ : (3S,5S);  $M_7$ : (3S,5R)], (2R,6S)-2,6-dimethylmorpholine ( $M_8$ ), 3-ethylmorpholine [ $M_9$ : (R) and  $M_{10}$ : (S)], morpholin-3-ylmethanol [ $M_{11}$ : (R) and  $M_{12}$ : (S)], (R)-3-(methoxymethyl)morpholine ( $M_{13}$ ), 3-oxa-6-azabicyclo[3.1.1]heptane ( $M_{14}$ ), 6-oxa-3-azabicyclo[3.1.1]heptane ( $M_{15}$ ), 2-oxa-5-azabicyclo[2.2.1]heptane [ $M_{16}$ : (1R,4R) and  $M_{17}$ : (1S,4S)], 3-oxa-8-azabicyclo[3.2.1]octane ( $M_{18}$ ), 8-oxa-3-azabicyclo[3.2.1]octane ( $M_{19}$ ), 2-oxa-6-azaspiro[3.3]heptane ( $M_{20}$ ), and 1,4-oxazepane ( $M_{21}$ ). The compounds were tested for *in vitro* binding to the catalytic subunit of mTOR and PI3K $\alpha$  (p110 $\alpha$ ) and for inhibition of PI3K/mTOR pathway in A2058 cells [phosphorylation of S6 and protein kinase B (PKB/Akt) on Ser473 to detect mTORC1 and mTORC2 activity, respectively]. Whereas **1** bearing an unsubstituted morpholine showed a selectivity for mTOR versus PI3K $\alpha$  of 2.5-fold, increasing the steric demand of the morpholine substituents significantly enhanced the compounds' selectivity (see compounds **2**, **4**–**9**, **12**–**14**; Table 1). Sterically hindered morpholines had previously been reported to enhance the selectivity for mTOR over PI3K.<sup>26,27,36</sup> The presence of a bridged morpholine resulted in a decrease in mTOR affinity, with the exception of 3-oxa-8-azabicyclo[3.2.1]octane ( $M_{18}$ ) and 8-oxa-3-azabicyclo[3.2.1]octane ( $M_{19}$ ) that led to a significant activity toward mTOR ( $K_i$  for **19** and **20** = 13 and 24 nM, respectively). Ring-enlargement from a morpholine to a 1,4-oxazepane maintained strong mTOR affinity ( $K_i$  for **1** and **22** = 8 and 15 nM, respectively). Compounds **4** and **8** showed a high potency for mTOR kinase [ $K_i$  **4** = 4.7 nM; **8** = 3.6 nM] together with a 100-/80-fold selectivity for mTOR over PI3K $\alpha$ . Sterically hindered morpholines caused a decrease

in cellular activity (Table 1), with the exception of  $M_3$  (3,3-dimethylmorpholine) and  $M_7$  [(3S,5R)-3,5-dimethylmorpholine]. Bridged-morpholine derivatives (**15**–**20**) had poor cellular activity, apart from **19** bearing a 3-oxa-8-azabicyclo[3.2.1]octane ( $M_{18}$ , Scheme 1) and showing moderate potency in cells (IC<sub>50</sub> for pPKB/Akt = 157 nM and for pS6 = 282 nM). The 3-oxa-8-azabicyclo[3.2.1]octane is also present in the lead compound **52**. Compounds **4** and **8** displayed the best cellular activity (IC<sub>50</sub> for pPKB/Akt = 191 and 96 nM, and for pS6 = 61 and 71 nM, respectively) and were selected for additional studies.

**Clarification of Inhibitor–Protein Interactions.** Because the presence of a sterically hindered morpholine increased the mTOR selectivity over PI3K, computational modeling studies for compounds **8** and **4** were performed. To explain the compounds' different affinity for mTOR and PI3K $\alpha$ , we investigated the inhibitors' interactions with the ATP-binding site of the respective kinase. As previously described for **52**,<sup>26</sup> **53**,<sup>27</sup> and other morpholino-substituted PI3K inhibitors,<sup>29,30,32,37,38</sup> a pivotal interaction for mTOR and PI3K binding is the H-bond formation between the backbone amide of Val2240 in the hinge region of mTOR or of the Val851 in PI3K $\alpha$  with the oxygen atom of the morpholine moiety. The (R)-3-methylmorpholine is well accommodated in the hinge region of mTOR, providing selectivity for mTOR kinase over the structurally related PI3Ks.<sup>27,28,39</sup> We used the X-ray structure of PI103 in mTOR (see ref 40; PDB ID 4JT6, 3.6 Å resolution) and replaced PI103 with compound **8**. After energy minimization, the resulting mTOR-8 complex preserved crucial interactions including the hydrogen bonds between Asp2195/Glu2190 and the 2-aminopyridine and between the oxygen atom of the (R)-3-methylmorpholine and the Val2240 backbone amide (Figure 2A). The (3S,5R)-3,5-dimethylmorpholine points toward the solvent exposed region, and hydrophobic interactions between one of the two methyl groups and Met2345 could further stabilize the mTOR-8 complex (Figure 2A). The interaction with Met2345 has been described to play a pivotal role in inhibitor binding stabilization also for the tricyclic pyrimido-pyrrolo-oxazine scaffold.<sup>27</sup> Because of the high sequence homology of the ATP-

Table 2. Lipid Kinase and mTOR Binding Constants of 4, 8, and Reference Compounds

kinase →	inhibitor binding constants <sup>a</sup> $K_d$ [nM], ±SD							*most sensitive PI3K/mTOR
	mTOR	PI3K $\alpha$	PI3K $\beta$	PI3K $\delta$	PI3K $\gamma$	PI4K $\beta$	VPS34	fold selectivity (class I PI3K isoforms)
<b>4</b>	0.88 ± 0.17	<b>81 ± 27</b>	1350 ± 71	2450 ± 354	595 ± 106	>30 000	28 ± 1.4	90
PQR626 ( <b>8</b> )	0.67 ± 0.09	<b>110 ± 14</b>	1450 ± 71	3500 ± 424	1350 ± 71	>30 000	65 ± 3.5	164
CC223 ( <b>49</b> ) <sup>b</sup>	28 ± 11	<b>2300 ± 141</b>	18,500 ± 6364	6200 ± 0	7150 ± 919	39 ± 10	2500 ± 354	>80×
INK128 ( <b>50</b> ) <sup>b</sup>	0.092 ± 0.007	15 ± 3.5	81 ± 1.4	30 ± 13	3.7 ± 0.28	n.d.	8200 ± 707	>40×
AZD2014 ( <b>51</b> ) <sup>b</sup>	0.14 ± 0.02	33 ± 1.4	3300 ± 282	1500 ± 283	8400 ± 707	>30 000	23 000 ± 3535	>230×
PQR620 ( <b>52</b> ) <sup>b</sup>	0.27 ± 0.16	<b>980 ± 14</b>	22 000 ± 2828	23 000 ± 2828	18 000 ± 707	>30 000	1400 ± 0	>3700×
PQR617 ( <b>53</b> ) <sup>b</sup>	3.5 ± 0.49	<b>1600 ± 0</b>	7450 ± 495	12 000 ± 0	11 000 ± 1414	>30 000	3250 ± 495	457

<sup>a</sup>Dissociation constants ( $K_d$ ) were assessed with ScanMax technology from DiscoverX (11 point threefold serial dilutions of the listed compounds). Experiments were performed using an automated and standardized *in vitro* assay at DiscoverX (San Diego, USA) as technical duplicates, and  $K_d$  was calculated from dose–response curves (fitting with Hill equation).  $K_d$  is shown as mean ± SD. <sup>b</sup>Values for compounds **49**, **50**, **51**, **52**, and **53** are from ref 27. n.d. = not determined. \*Ratio of  $K_d$  of most sensitive class I PI3K isoform (indicated in bold type) over  $K_d$  for mTOR.

binding pocket of mTOR and class I PI3Ks, we can assume a similar binding mode for PI3K isoforms. Analogous computational modeling analysis was carried out starting from the X-ray structure of PI3K $\alpha$  in complex with the structurally similar triazine derivative PQR530 (see ref 35; PDB ID 6OAC, 3.15 Å resolution). After ligand energy minimization, the oxygen atom of the (*R*)-3-methylmorpholine established a H-bond with the backbone amide of Val851 in PI3K $\alpha$ , while the NH<sub>2</sub> group of the 4-(difluoromethyl)pyridin-2-amine forms H-bonds with Asp810/Asp933. Two opposing conformations are possible for the binding of (3*S*,5*R*)-3,5-dimethylmorpholine to the solvent exposed region: with the methyl groups pointing toward (i) Met2345 in mTOR (Met922 in PI3K $\alpha$ ) or (ii) Ile2163 in mTOR (Met772 in PI3K $\alpha$ ). In mTOR, both conformations are well accommodated (Figure 2B). On the contrary, only one conformation can bind to PI3K $\alpha$  because of a clash with Met772 in the “methyl-down” conformation (Figure 2C). A superimposition of mTOR and PI3K $\alpha$  ATP-binding pockets highlighted the inability of highly sterically hindered substituents to bind in the solvent exposed region of PI3K $\alpha$  because of the different orientation between Met772 (PI3K $\alpha$ ) and Ile2163 (mTOR; Figure 2D). Computational modeling studies were also performed for compound 4 and, similarly, both morpholine conformations bond with mTOR's solvent exposed region, while just the “methyl-right” conformation was accommodated in the ATP-binding site of PI3K $\alpha$  (Figure 2E).

**Profiling of Enzymatic Activity, Selectivity, and *In Vitro* ADME.** Due to their significant potency in cells, low nanomolar affinity, and high selectivity for mTOR, compounds 4 and 8 were characterized on the DiscoverX KINOMEScan platform. KdELECT assays (DiscoverX) confirmed the excellent affinity of 4 and 8 for mTOR kinase, with compound 8 showing a selectivity >150-fold for mTOR compared to class I PI3K isoforms (Table 2). The determined selectivity of 8 for mTOR kinase over class I PI3K isoforms exceeded those of previously published molecules such as CC223<sup>41</sup> (**49**, ~80×) and INK128 (**50**, ~40×) and was in the range of AZD2014 (**51**, ~230×; Table 2). Both compounds (4 and 8) displayed a low nanomolar affinity for the class III PI3K Vps34 (Table 2). Although many pharmaceutical companies have curtailed their drug discovery programs on Vps34 inhibitors,<sup>42</sup> Vps34 has been identified as a promising therapeutic target for

combination strategies in cancer treatment because of its pivotal role in autophagy.<sup>43</sup>

These data qualify 8 as a highly potent mTOR inhibitor with low to moderate activity for PI3K $\alpha$ . Moreover, the selectivity of compound 8 for mTOR over a wide range of proteins (>400) and lipid kinases was demonstrated in a DiscoverX scanMAX kinase assay panel. Compound 8 displayed negligible binding to protein kinases at a concentration of 10  $\mu$ M (Figure S3 and Table S3 in the Supporting Information). It obtained excellent selectivity scores<sup>44</sup> of  $S(35) = 0.04$  and  $S(10) = 0.017$  (corresponding to 16 and 4 hits, respectively—Table S2), compared to 50 which recorded 0.29 and 0.14 (corresponding to 118 and 55 hits, respectively—Table S2). In order to assess off-target effects, compound 8 was tested at a 10  $\mu$ M concentration in a Cerep safety pharmacology panel. No off-target interactions of 8 with the cell surface and nuclear receptors, transporters, and ion channels including hERG (Table S4) were identified. Enzyme activities such as phosphodiesterases, kinases, and proteases were also unaffected by compound 8 (Table S5).

**Metabolic Stability and CYP450 Reactive Phenotyping.** To assess its metabolic stability in comparison with 52, compound 8 was incubated with hepatocytes from mice (CD-1), rats (Sprague-Dawley), dogs (Beagle), and humans. The hepatocytes stability is strongly predictive of *in vivo* clearance across species, as previously demonstrated with 57.<sup>30</sup> Compound 8 showed a moderate stability with mouse, rat, and human hepatocytes, with 48.4, 42.3, and 44.0% compound remaining after 3 h of incubation. A moderate-to-high stability was observed with dog hepatocytes (75.6%; Table S6 and Figure 3A). 52 presented a high stability in mouse, rat, and dog hepatocytes (>59.9% remaining compound; see Table S7), characterizing it as an excellent TORKi to explore rodent models. Compound 52's limited stability in human hepatocytes (27.8% remaining compound after 3 h; Table S7) designates 52 as a candidate for topical applications, which is also supported by its lipophilic properties. 8 achieved a 52% increase in stability in human hepatocytes with respect to 52 (Table 3), providing substantial advantages for the development of novel agents targeting CNS disorders.

Both 8 and compound 4, bearing a 3,3-dimethylmorpholine, were characterized with respect to their CYP1A-related

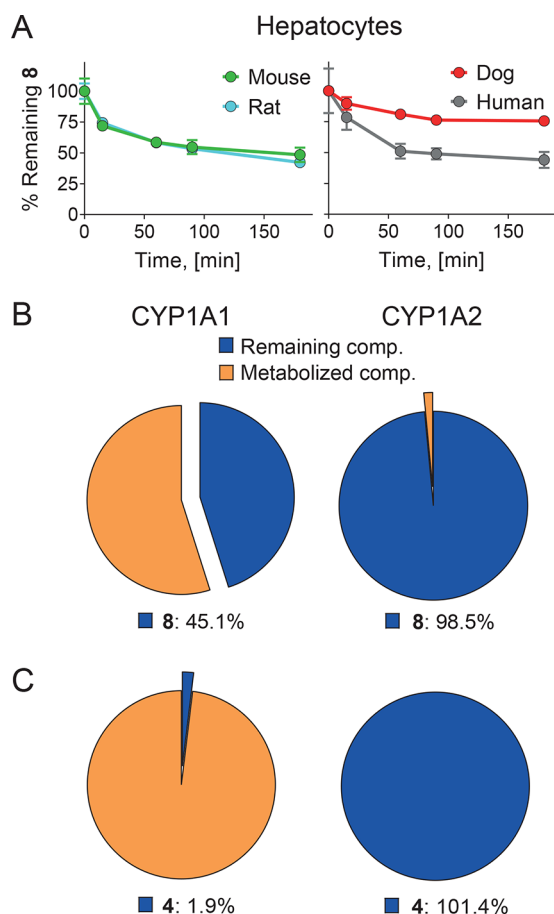


**Figure 3.** (A) Stability of **8** at 5  $\mu\text{M}$  in primary hepatocyte cultures from mice, rats, dogs, and humans ( $n = 2$ ; mean  $\pm$  SEM; error bars are not shown when smaller than symbols). Values are tabulated in Table S6 of the Supporting Information. (B,C) Pie chart displaying the % of remaining (B) compound **8** (blue) and (C) compound **4** (blue) after 60 min of incubation with the indicated human recombinant CYP isoenzymes.

metabolism, after incubation with individual human recombinant CYP isoenzymes CYP1A1 and CYP1A2. CYP1A1 is implicated in the metabolism of structurally similar molecules and the high interindividual expression of this isoenzyme hampers the establishment of a therapeutic dose. Compound **8** was moderately stable with CYP1A1 as indicated by 45.1% remaining compound after 60 min of incubation (Figure 3B), while compound **4** was extensively depleted, resulting in <2% remaining compound after 60 min (Figure 3C). Both compounds were not substrates of CYP1A2. Because the (R)-3-methylmorpholine has been suggested to protect the

compounds from extensive CYP1A1 metabolism,<sup>27</sup> the susceptibility of **4** to the CYP1A1 metabolism is related to the 3,3-dimethylmorpholine.

**In Vitro Permeability and hMDR1 Affinity.** To determine the potential for BBB penetration, compound **8** and three other molecules with high potency in biochemical and cellular assays (**1**, **3**, **4**; Table 1) were tested in an *in vitro* TransWell assay using CRISPR–Cas9-generated Madin–Darby canine kidney II (MDCK) cell lines with deleted canine MDR1 (MDCK<sup>cMDR1-ko</sup>) and one line stably expressing human MDR1 (MDCK-hMDR1<sup>cMDR1-ko</sup>).<sup>45</sup> MDCK cells differentiate to form tight junctions and monolayers that mimic the BBB. The MDCK-hMDR1 permeability assay is able to identify compounds which are multidrug resistance protein 1 (MDR1 or P-glycoprotein, P-gp) substrates and distinguish between potential CNS and non-CNS drugs. The apparent permeability ( $P_{\text{app}}$ ) and efflux ratio (ER) across cell monolayers was assessed in MDCK-hMDR1<sup>cMDR1-ko</sup>.<sup>45</sup> The ER was compared against the MDCK<sup>cMDR1-ko</sup> control cells. Compound **53** is known to have limited uptake into the brain<sup>27</sup> and displayed significantly different ER between the MDCK-hMDR1<sup>cMDR1-ko</sup> and the MDCK<sup>cMDR1-ko</sup> cells ( $p$ -value using an unpaired  $t$ -test: 0.000031, Figure 4A). Thus, **53** was

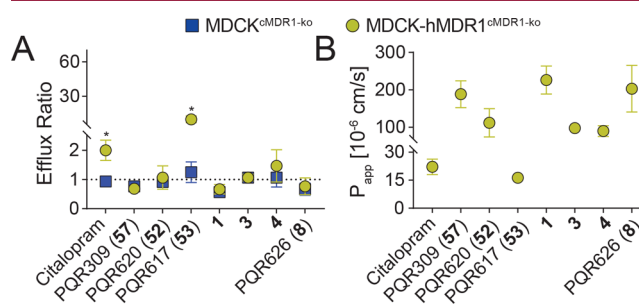


**Figure 4.** (A) ER in MDCK-hMDR1<sup>cMDR1-ko</sup> and MDCK<sup>cMDR1-ko</sup> cells. The dotted line shows ER = 1, indicative of equal apparent permeability across the cell monolayer in both directions. High ER in MDCK-hMDR1<sup>cMDR1-ko</sup> cells indicates hMDR1 affinity of the compound. Citalopram, a hMDR1 substrate,<sup>45</sup> has been used as positive control. **57** and **52** are known to have a good BBB penetration *in vivo*, while **53** has a limited BBB penetration *in vivo*. (B) Apparent permeability ( $P_{\text{app}}$ ) in direction from apical to basolateral compartment across MDCK-hMDR1<sup>cMDR1-ko</sup> monolayers seeded on TransWell plates. Results are shown as mean  $\pm$  SD ( $n > 3$ ), \* $p$ -value < 0.05 (unpaired  $t$ -test, GraphPad Prism 8.0.2).

classified as a hMDR1 substrate. Compound **52** and **57**, known for having good brain penetration *in vivo*,<sup>26,30</sup> did not show significant differences between the ER in both cell lines ( $p$ -value > 0.05), and an ER close to 1 indicated that these

**Table 3.** Stability of Compound PQR626 (**8**) and PQR620 (**52**) in Hepatocyte Cultures

cpd./species		mouse	rat	dog	human
PQR626 ( <b>8</b> )	<sup>a</sup> CL <sub>int</sub>	4.3 $\pm$ 0.33	5.3 $\pm$ 0.19	1.8 $\pm$ 0.20	5.3 $\pm$ 0.26
	$t_{1/2}$ [min]	201 $\pm$ 16	162 $\pm$ 5.7	490 $\pm$ 57	164 $\pm$ 8.22
PQR620 ( <b>52</b> ) <sup>c</sup>	CL <sub>int</sub>	2.7 $\pm$ 1.2	1.8 $\pm$ 0.35	1.6 $\pm$ 0.21	8.0 $\pm$ 0.18
	$t_{1/2}$ [min]	324 $\pm$ 177	468 $\pm$ 92	525 $\pm$ 70	108 $\pm$ 2.4
7-EC <sup>b</sup>	CL <sub>int</sub>	42 $\pm$ 0.47	16 $\pm$ 0.18	60 $\pm$ 2.1	27 $\pm$ 0.09
	$t_{1/2}$ [min]	21 $\pm$ 0.23	55 $\pm$ 0.62	14 $\pm$ 0.50	31 $\pm$ 0.10

<sup>a</sup>CL<sub>int</sub> [ $\mu\text{L}/\text{min}/10^6$  cells];  $t_{1/2}$ , [min]. <sup>b</sup>Assay reference compound: 7-EC, 7-ethoxycoumarin. Results are shown as mean  $\pm$  SEM ( $n = 2$ ). Raw data are reported in Table S6 of the Supporting Information. <sup>c</sup>The data for **52** are reprinted from ref 26.



compounds are not likely to be dependent on active transport. Similarly, none of novel tested compounds—1, 3, 4, and 8—was classified as a hMDR1 substrate. 4 showed a nonsignificant trend toward hMDR1 affinity with an ER of 1.5 in MDCK-hMDR1<sup>MDR1-ko</sup> cells (Figure 4A). Compound 8 was no hMDR1 substrate and had a  $P_{app}$  comparable to those of the brain penetrating compounds 52 and 57 (Figure 4B), supporting the assessment of its BBB permeability using *in vivo* models.

**Pharmacological Parameters.** To evaluate the *in vivo* BBB permeability and oral availability, PK parameters of 8 were determined in male Sprague Dawley rats. 8 was administered orally (5 mg/kg p.o.) and plasma and brain concentrations were assessed after the application of a single dose (Figure 5A). After 30 min, the maximal concentration

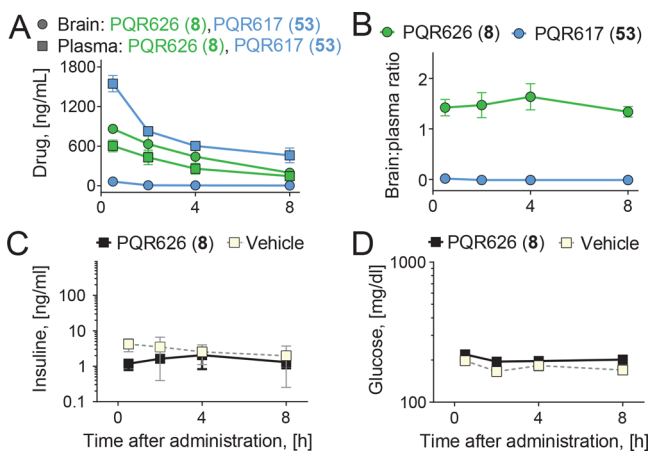


**Figure 5.** Pharmacokinetics and pharmacodynamics in male Sprague Dawley rats. (A) Plasma (square) and brain (circle) levels of 8 and 53 after p.o. dosing at 5 mg/kg. (B) Calculation of brain/plasma ratio over time using the values reported in (A). (C) Insulin and (D) glucose plasma levels after oral administration of 8 in male Sprague Dawley rats ( $n = 3$ ; mean  $\pm$  SEM; error bars not shown when  $<$  symbols). Exact values can be found in Tables S8–S13 in the Supporting Information.

( $C_{max}$ ) of 8 was achieved both in plasma and brain. The total exposure  $AUC_{0-8}$  for compound 8 was in plasma 2429 ng h/mL and in brain 3689 ng h/g after 8 h. The conformationally restricted compound 53 was administered at the same dose and reached an  $AUC_{0-8}$  of  $>5500$  ng h/mL in plasma, but only of  $<110$  ng h/g in brain ( $\sim 1:55$  brain/plasma ratio).<sup>27</sup> While the brain uptake of 53 was minimal, compound 8 showed

excellent brain exposure (Figure 5A). Compound 8 had a brain/plasma ratio of  $\sim 1.5:1$  (Figure 5B).

PI3K $\alpha$  inhibitors are known to trigger a rapid increase in insulin and glucose plasma levels.<sup>46</sup> We have previously reported on 57,<sup>30</sup> PQR530,<sup>35</sup> and PQR514,<sup>32</sup> which are potent pan-PI3K inhibitors, and insulin and glucose peaks were reliable markers for on-target action. 8 did not cause a rise of insulin and glucose concentration as compared to the vehicle, highlighting the selective inhibition of mTOR kinase (Figure 5C,D). These results match the observations published for the selective and brain penetrant mTOR inhibitor 52.<sup>26</sup>

**Comparative PK Studies: PQR626 versus Everolimus and AZD2014.** As 56 (see Figure 1 for chemical structure) has been approved for the treatment of TSC-associated seizures, the pharmacokinetic parameters of 8 were first assessed in comparison with those of 56.<sup>22</sup> Compound 8 was orally administered (p.o.) to female C57BL/6J mice at 10 mg/kg, either as single dose or once a day for 4 consecutive days (qd4), while 56 was dosed at 10 mg/kg p.o. qd4. The plasma and brain concentrations of the compounds were monitored. The dose of compound 8 was doubled with respect to the experiments carried out in male Sprague Dawley rats (see Figure 5) aiming to achieve higher  $C_{max}$ . The PK parameters for 8 were assessed both in mice and rats because significant species differences were observed with other compounds previously investigated.<sup>30,47</sup> In mice dosed at 10 mg/kg, compound 8 reached a  $C_{max}$  of 1096 and 947 ng/mL in plasma and of 1425 and 1317 ng/g in brain, after either single or qd4 applications, respectively (Table 4). Applications of 56 once a day for 4 consecutive days at 10 mg/kg led to a  $C_{max}$  of 3941 ng/mL in plasma and of only 43 ng/g in brain (Table 4). Concentrations of 8 were higher in the brain than in the plasma (Figure 6A,B), highlighting the ability of compound 8 to reach the brain and confirming the results obtained in rats. PQR626 (8) showed a  $\sim 1.4:1$  distribution between brain and plasma, whereas the brain permeability of 56 was negligible (brain/plasma ratio  $\sim 1:92$ , Figure 6C).

To confirm the favorable brain distribution of 8 with respect to the currently available drugs and clinical candidates, a study including 8, 56, and 51 (see Figure 1 for chemical structures) was carried out (Table 5 and Figure 6).

Dosed at 25 mg/kg in mice, compound 8 reached a  $C_{max}$  of 1833 ng/mL and 3345 ng/g in plasma and brain, respectively. On the contrary, both 56 and 51 reached a higher concentration in plasma than in the brain ( $C_{max}$  in plasma = 3464 and 7189 ng/mL;  $C_{max}$  in brain = 57 and 286 ng/g; Table 5 and Figure 6D). Administered at the same dose, compound 8

**Table 4.** PK Parameters after Oral Application in Female C57BL/6J Mice<sup>a</sup>

test Item	plasma			brain		
	PQR626 (8)	PQR626 (8)	everolimus (56)	PQR626 (8)	PQR626 (8)	everolimus (56)
p.o. dosage[mg/kg]	10	10 qd4	10 qd4	10	10 qd4	10 qd4
$C_{max}$ [ng/mL]	1096	947	3941	1425	1317	43
$T_{max}$ [h]	0.5	0.5	2.0	0.5	0.5	4.0
$t_{1/2}$ [h]	3.0	2.2	5.7	2.9	2.3	15.8*
$AUC_{0-8h}$ [h·ng/mL]	2936	2371	42,267	4653	3048	640
Cl [mL/h/kg]	3397	3892	225	2144	3012	10,265*

<sup>a</sup>p.o.: per os;  $C_{max}$ : maximal concentration,  $T_{max}$ : time of maximal concentration in hours (derived from minimally 3 time points);  $t_{1/2}$ : half-life elimination in hours; AUC: area under the curve, Cl: clearance; ( $n = 3$ , mean for each time-point); qd4: compound was administered once a day for 4 consecutive days and the blood sampling was performed after the last treatment on day 4. \*values obtained considering only 2 time points following  $T_{max}$  have to be regarded as a rough estimation.



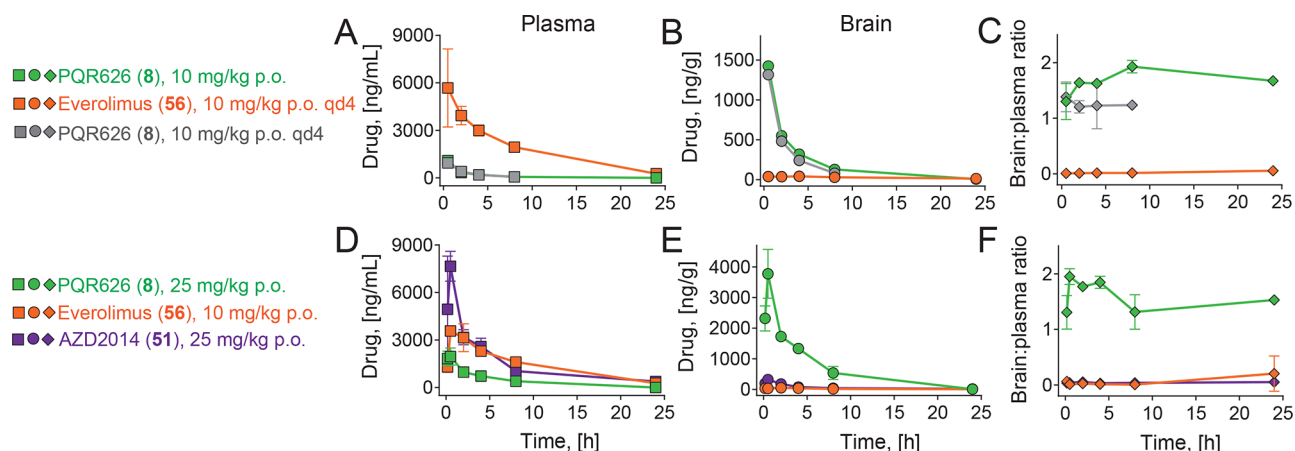


**Figure 6.** Pharmacokinetic study in female C57BL/6J mice. (A–C) **8** was administered at 10 mg/kg in 20% Captisol p.o. either as single dose or administered once a day for 4 consecutive days and the blood sampling performed after the last treatment on day 4 (qd4). **56** was administered at 10 mg/kg in 8% ethanol, 10% PEG 400, and 10% Tween 80 p.o. qd4. (A) Plasma and (B) brain levels of compounds **8** and **56**. (C) Calculation of brain/plasma ratio over time using the values reported in (A,B). Values are reported in Tables S14–S19 in the Supporting Information. (D–F) **8** and **51** were administered p.o. as a single dose of 25 mg/kg. **56** was administered at 10 mg/kg p.o. single dose. (D) Plasma and (E) brain levels of compounds **8**, **51**, and **56**. (C) Brain/plasma ratio over time calculated from the values reported in (D,E). Values are depicted in Tables S20–S25. All values: mean  $\pm$  SEM. Error bars not shown are smaller than the symbols.

**Table 5.** PK Parameters after Oral Application in Female C57BL/6J Mice<sup>a</sup>

test item	plasma			brain		
	PQR626 ( <b>8</b> )	everolimus ( <b>56</b> )	AZD2014 ( <b>51</b> )	PQR626 ( <b>8</b> )	everolimus ( <b>56</b> )	AZD2014 ( <b>51</b> )
p.o. dosage [mg/kg]	25	10	25	25	10	25
$C_{max}$ [ng/mL]	1833	3464	7189	3345	57	286
$T_{max}$ [h]	0.2	0.5	0.5	0.5	24.0	0.5
$t_{1/2}$ [h]	2.4	6.5	7.5	2.4	NC	8.6
AUC <sub>0–8h</sub> [h·ng/mL]	10,295	33,636	33,706	17,103	804	1338
Cl [mL/h/kg]	2427	276	660	1460	NC	15,722

<sup>a</sup>p.o.: per os;  $C_{max}$ : maximal concentration,  $T_{max}$ : time of maximal concentration in hours;  $t_{1/2}$ : half-life elimination in hours; AUC: area under the curve, Cl: clearance; ( $n = 3$ , mean for each time-point). NC = not calculated.

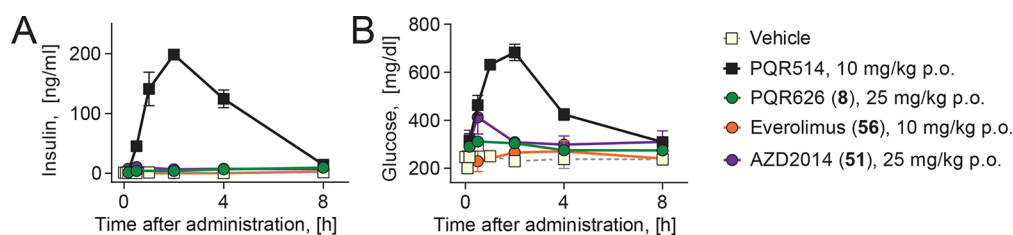


**Figure 7.** (A) Insulin and (B) glucose plasma levels after oral administration of **8** (25 mg/kg), **56** (10 mg/kg), and **51** (25 mg/kg) in female C57BL/6J mice and of PQR514 (10 mg/kg)<sup>32</sup> in male C57BL/6J mice. All values: mean  $\pm$  SEM. Error bars are not shown when smaller than the symbols. Values are reported in Tables S26–S31 in the Supporting Information.

yielded a  $C_{max}$  in brain  $\sim$ 12-fold higher than that of **51** (Figure 6E). **51** showed a higher brain/plasma ratio with respect to **56** [ $\sim$ 1:25 (**51**) and  $\sim$ 1:61 (**56**), Figure 6F]. However, the brain-to-plasma ratio is significantly improved for **8** ( $\sim$ 1.8:1, Figure 6F).

Compared to PQR514,<sup>32</sup> a potent pan-PI3K inhibitor, **8** did not lead to an increase in insulin and glucose plasma levels at a concentration  $>$ 2-fold higher than that of PQR514 (10 vs 25 mg/kg). **56** and **51** also did not trigger an increase in insulin and glucose plasma concentrations (Figure 7A,B). Moreover, metabolic side effects were not present at the same dose at which **8** led to a significant decrease in brain pS6 and pS473 PKB (see next section).

**Pharmacodynamic Evaluation of 8 in the Brain.** The effects of inhibiting the mTOR pathway in the brain using **8**

were investigated in C57BL/6J mice after oral administration at 25 mg/kg and compared with **56** dosed at 10 mg/kg. While **56** is an allosteric inhibitor of TORC1, **8** targets the ATP-binding site and inhibits both mTORC1 and mTORC2. Thus, **8** was expected to impact both pS6<sup>(Ser235/236)</sup> and pPKB<sup>(Ser473)</sup> levels, which, respectively, reflect the activity of mTORC1 and mTORC2 complexes. At 10 mg/kg [same dose as investigated in the vivo efficacy model], **56** did not show a decrease in pS6 levels (Figure 8A). On the contrary, a single administration of compound **8** at 25 mg/kg led to an effective reduction of levels of pS6 30 min after drug dosing in murine cortex (Figure 8A,C). Similarly, **8** significantly reduced the phosphorylation of S473 PKB 30 min after dosing (Figure 8B,C). The pharmacodynamic effect of **8** in the brain was strongly correlated with the brain levels of the compound (Figure

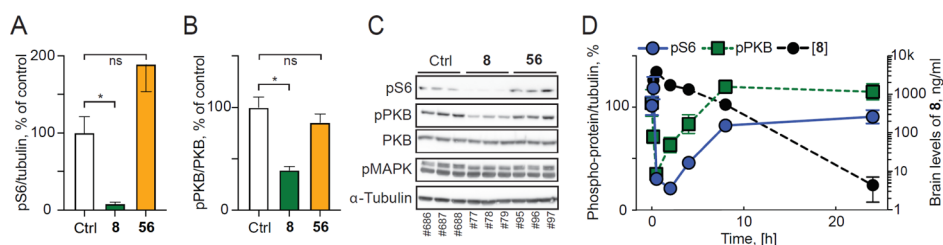


**Figure 8.** Inhibition of mTOR signaling in murine brain cortex by PQR626 (**8**) and everolimus (**56**). (A–C) Brain cortex was collected from female C57BL/6J mice or from mice treated with **8** (25 mg/kg, p.o.) or **56** (10 mg/kg, p.o.) for 30 min. Cortex was lysed and equal amount proteins subjected to sodium dodecyl sulfate-polyacrylamide gel electrophoresis (SDS-PAGE) and western blotting, followed by the detection of pPKB, pS6, phosphorylated MAP kinases, total PKB, or  $\alpha$ -tubulin using specific primary antibodies and respective HRP-coupled secondary antibodies and enhanced chemiluminescence. (A,B) Quantification of (A) pS6 and (B) pPKB levels in compound-treated murine cortex given as % of control cortex. For details, see [Experimental Section](#) [ $n = 3$ , mean  $\pm$  SEM, \* $p$ -value  $< 0.05$ .  $p$ -value using an unpaired  $t$ -test vs control: compound **8**: 0.0125 (pS6); 0.0044 (pPKB)]. (C) Western blot images used for quantification of (A,B). (D) Time-course of inhibition of mTOR signaling in murine brain cortex by **8**. Brain cortex was collected from **8** (25 mg/kg, p.o.) treated female C57BL/6J mice at indicated time-points in [h] and from control mice. Western blot images are reported in [Figure S4](#). Phosphorylated proteins and  $\alpha$ -tubulin levels were quantified using ImageJ, and phospho-protein/tubulin levels are presented as % of control cortex (left  $y$ -axis) as a function of time [ $n = 9$  for control animals,  $n = 3$  for each timepoint of **8** treatment, mean  $\pm$  SEM]. Right  $y$ -axis: brain concentration of **8** in ng/mL from the same mice ( $n = 3$ , mean  $\pm$  SEM for each time point).

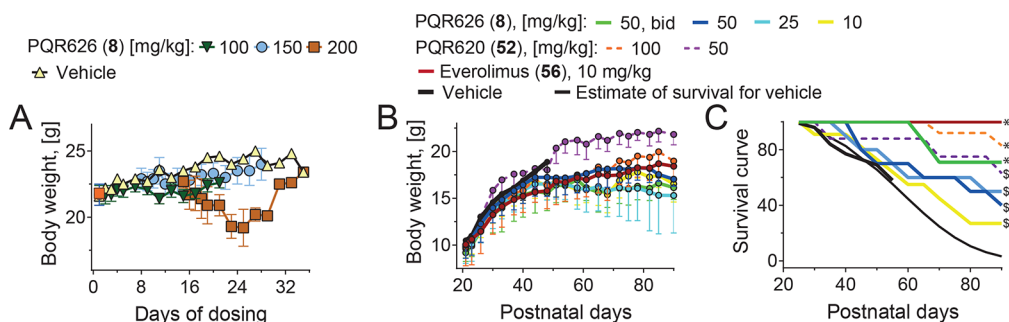


**Figure 9.** (A) Body weight changes in BALB/c nude female mice to assess MTD. Group 1: vehicle (20% Captisol in water) once a day (qd)  $\times 14$  from day 1 p.o. ( $n = 1$ ). Group 2: compound **8** at 100 mg/kg qd  $\times 14$  from day 1 p.o. ( $n = 3$ ). Group 3: compound **8** at 150 mg/kg qd  $\times 14$  from day 8 p.o. ( $n = 3$ ). Group 4: compound **8** at 200 mg/kg qd  $\times 14$  from day 15 p.o. ( $n = 3$ ). Raw data are depicted in [Table S32](#). (B) Body weight of  $Tsc1^{GFAPCKO}$  mice as a function of treatments. Data are shown as mean  $\pm$  SEM. Raw data are depicted in [Table S33](#). (C) Effects of treatments on the survival rate of  $Tsc1^{GFAPCKO}$  mice. All treatments started at P21, with the exception of **52** (50 mg/kg p.o. qd) which started on P27. Compound **56** at 10 mg/kg,  $n = 12$ ; compound **52** at 100 and 50 mg/kg,  $n = 12$  and 8, respectively; compound **8** at 50 bid, 50, 25, and 10 mg/kg,  $n = 7, 10, 10,$  and 10, respectively. Mid-study (day P45) brain and plasma collection: four additional animals per group were dosed and sacrificed on day P45. Data are presented as percent surviving at each time point. Survival was determined from the start of the study (P21) to the day the animal was found dead or until P90 (*i.e.*, animals were censored at P90). A  $\chi^2$  survival analysis was performed in JMP Statistical Software (a division of SAS) with treatment as a factor. The statistical report for survival analysis: [Table S34](#) in the [Supporting Information](#). \* $p$ -value  $< 0.05$ .  $p$ -values using the log-rank test vs vehicle—compound **52** at 50 and 100 mg/kg:  $p$ -value 0.1336 and 0.0093, respectively; compound **8** at 10, 25, 50, and 50 bid mg/kg:  $p$ -value 0.6530, 0.4502, 0.4489, and 0.0469, respectively.  $^{\$}$  $p$ -value  $< 0.05$ .  $p$ -values using the log-rank test vs everolimus (**56**)—compound **52** at 50 and 100 mg/kg:  $p$ -value 0.0228 and 0.1483, respectively; compound **8** at 10, 25, 50, and 50 bid mg/kg: 0.0002, 0.0016, 0.0016, and 0.0542, respectively.

8D). In a time-course experiment, we observed a significant decrease in brain pS6 and pPKB at 0.5–2 h after dosing, while pS6 and pPKB levels returned to pretreated levels after 8 h ([Figure S4](#)).

**Evaluation of In Vivo Efficacy.** *In vivo* toxicokinetic studies were performed in nontumor-bearing BALB/c nude female mice to establish the maximum tolerated dose (MTD). Compound **8** was tested at 100 (group 2), 150 (group 3), and 200 mg/kg (group 4) and compared with vehicle (group 1). Animals were evaluated for 7 days after 2 weeks of once a day (qd) dosing schedule. The body weight changes are shown in [Figure 9A](#). No adverse effect on body weight was observed in groups 2 and 3. Compound **8** had a tolerability in mice at 100 and 150 mg/kg comparable to that of **52** (MTD  $\sim$ 150 mg/kg). Efficacy studies were performed using mice with conditional inactivation of the  $Tsc1$  gene primarily in glia ( $Tsc1^{GFAPCKO}$  mice), which develop glial proliferation and postnatal epilepsy

and show a highly increased mortality. TSC-induced epilepsy originates in the CNS, and compounds must therefore target mTOR behind the BBB.<sup>22</sup> Alterations in BBB permeability are associated with mTOR-mediated inflammation in TSC epileptogenesis.<sup>48</sup> Increased permeability is not always associated with enhanced drug penetration into the brain because an increase in efflux carrier expression (i.g. P-gp) has been observed as the mechanism to protect the brain from toxins.<sup>49,50</sup> While **55** is known to be a P-gp substrate,<sup>51</sup> **8** was not affected by P-gp-mediated efflux ([Figure 4](#)), highlighting its potential advantage in the treatment of TSC-associated seizures. **55** decreased seizures and prolonged survival in  $Tsc1^{GFAPCKO}$  mice.<sup>13</sup> Everolimus (**56**) is currently available under the trend name Afinitor Disperz for the treatment of TSC-associated seizures.<sup>52</sup> However, the limited BBB penetration of **56** leads to the need of a very high dose causing serious systemic side effects (immunosuppression). Moreover,

56 forms quasi-irreversible complexes with TORC1 (FRB–Rapalog–FKBP12 complexes) that act as a sink for the drug. A brain-penetrant, reversible mTOR inhibitor is expected to have a lower systemic impact on immune responses.

In a dose-range finding study, the efficacy of compound 8 (10, 25, and 50 mg/kg) on survival in *Tsc1*<sup>GFAP</sup>CKO mice was assessed and compared to vehicle and treatment with 56 (10 mg/kg) and 52 (50 and 100 mg/kg). Significant changes in body weight were not observed across all compounds and doses  $\leq 150$  mg/kg (Figure 9B). Compounds 8 and 52 showed a positive dose–response effect on survival. Both compounds 8 at 50 mg/kg, bid (twice a day) and 52 at 100 mg/kg significantly decreased mortality as compared to vehicle control mortality data (*p*-values using the log-rank test: 0.0469 and 0.0093, respectively). 56 at 10 mg/kg prevented mortality in *Tsc1*<sup>GFAP</sup>CKO mice. Compounds 8 at 50 mg/kg bid and 52 at 100 mg/kg were not statistically different from 56, suggesting noninferiority under these study conditions (*p*-values using the log-rank test: 0.0542 and 0.1483, respectively; Figure 9C and Table S34 in the Supporting Information). The effectiveness of 8 administered twice a day at 50 mg/kg is highly encouraging. 52 at 100 mg/kg had been previously exploited as a proof-of-concept compound to prove the ability of mTOR inhibitors in eliminating seizures in *Tsc1*<sup>GFAP</sup>CKO mice. The almost complete elimination of seizures by 52 proved that ATP-competitive mTOR inhibitors are able to counteract TSC-dependent overactivation of the mTOR pathway<sup>26,53</sup> and supports the further investigation of the novel, metabolically optimized TORKi 8 for TSC treatment.

## CONCLUSIONS

Recently, epileptic seizures in TSC-patients have been shown to be reduced by treatment with everolimus. A limited clinical success has, however, been reported. The discovery of novel, brain-penetrant, and highly selective mTOR inhibitors could prevent epilepsy, improve treatment, and mitigate comorbidities. Previously, we had discovered PQR620 (52), a first-in-class brain-penetrant ATP-competitive TORKi able to attenuate seizures in a TSC mouse model.<sup>26</sup>

The ethylene-bridged morpholines of 52 have been replaced in PQR626 (8) because they were found to be the primary site of metabolism in human liver microsomes,<sup>34</sup> human hepatocytes, and Cynomolgus monkeys (Figures S1 and S2). Compound 8 achieves a >50% increase in stability in human hepatocytes as compared to 52, favoring 8 as a candidate for further development in neurologic treatment in humans, as metabolically stability of TORKi is a pivotal requirement for long-term inhibition of the mTOR pathway in diseases such as TSC.

Moreover, compound 8 showed a high stability toward degradation by CYP1A1 as compared to 4, which was extensively metabolized. The proven stability of 8 against the CYP1A1 isoenzyme is an asset in drug development, as CYP1A1 is highly variable in individual patients: liver and extrahepatic expression of this enzyme can be induced by many substrates, leading to a significant variation in pharmacokinetics of drugs metabolized by CYP1A1. Compound 8 has been discovered through an extensive triazine-scaffold exploration focused on the morpholine moiety pointing toward the solvent exposed region of the ATP-binding site. 8 is a potent, selective mTORC1/2 inhibitor and showed a good exposure both in plasma and brain after oral dosing. The lack of metabolic side effects in rats and mice, such as hyper-

glycemia and hyperinsulinemia, suggests its potential application in the treatment of chronic diseases. Compound 8 at 50 mg/kg twice a day significantly reduced the loss of *Tsc1*-induced mortality as compared to vehicle. The effectiveness of 8 in a *Tsc1*<sup>GFAP</sup>CKO mouse model, its excellent brain penetration, optimized stability in human hepatocytes, and CYP profile are highly encouraging and suggest further preclinical and clinical investigations of the compound for the treatment of CNS disorders.

## EXPERIMENTAL SECTION

**General Information.** Reagents were purchased at the highest commercial quality from Acros, Combi-blocks, Sigma-Aldrich, or Fluorochem and used without further purification. Solvents were purchased from Acros Organics in AcroSeal bottles over molecular sieves. Cross-coupling reactions were performed under a nitrogen atmosphere using anhydrous solvents, and glassware was oven-dried prior to use. Thin-layer chromatography (TLC) plates were purchased from Merck KGaA (Polygram SIL/UV254, 0.2 mm silica with fluorescence indicator), and UV light (254 nm) was used to visualize the compounds. Column chromatographic purifications were performed on the Merck KGaA silica gel (pore size 60 Å, 230–400 mesh particle size). Alternatively, flash chromatography was performed with Isco CombiFlash Companion systems using prepacked silica gel columns (40–60  $\mu$ m particle size RediSep). <sup>1</sup>H, <sup>19</sup>F, and <sup>13</sup>C NMR spectra were recorded on a Bruker AVANCE 400 spectrometer. NMR spectra were obtained in deuterated solvents, such as CDCl<sub>3</sub>, (CD<sub>3</sub>)<sub>2</sub>SO, or CD<sub>3</sub>OD. The chemical shifts ( $\delta$  values) are reported in parts-per-million and corrected to the signal of the deuterated solvents [7.26 ppm (<sup>1</sup>H NMR) and 77.16 ppm (<sup>13</sup>C NMR) for CDCl<sub>3</sub>; 2.50 ppm (<sup>1</sup>H NMR) and 39.52 ppm (<sup>13</sup>C NMR) for (CD<sub>3</sub>)<sub>2</sub>SO; and 3.31 ppm (<sup>1</sup>H NMR) and 49.00 ppm (<sup>13</sup>C NMR) for CD<sub>3</sub>OD]. <sup>19</sup>F NMR spectra are calibrated relative to CFCl<sub>3</sub> ( $\delta$  = 0 ppm) as the external standard. Peak multiplicities are reported as: s (singlet), d (doublet), dd (doublet of doublets), t (triplet), td (triplet of doublets), q (quartet), m (multiplet), br (broadened). Coupling constants are reported in Hertz (Hz). High-resolution mass spectra (HRMS) were recorded on a Bruker maxis 4G, high-resolution ESI-QTOF. Analyses were performed in positive ion mode, and MeOH +0.1% formic acid was used as the solvent. Sodium formate was used as the calibration standard. MALDI-ToF mass spectra were obtained on a Voyager-De Pro measured in *m/z*. The purity of final compounds was assessed by high-performance liquid chromatography (HPLC) analyses on an Ultimate 3000SD System from Thermo Fisher with a LPG-3400SD pump system, ACC-3000 autosampler and column oven, and DAD-3000 diode array detector. An Acclaim-120 C18 reversed-phase column from Thermo Fisher was used as the stationary phase. Gradient elution (5:95 for 0.2 min, 5:95  $\rightarrow$  100:0 over 10 min, 100:0 for 3 min) of the mobile phase consisting of CH<sub>3</sub>CN/MeOH/H<sub>2</sub>O<sub>(10:90)</sub> was used at a flow rate of 0.5 mL/min at 40 °C. The purity of all final compounds was >95%. Melting points were determined with a Stuart SMP20 apparatus.

**General Procedure 1.** Under a nitrogen atmosphere, boronate 48 (1.0–1.3 equiv) was charged in a flask and dissolved in dioxane (approx. 1 mL/0.15 mmol). The respective chlorotriazine derivative (24, 25, 27–46, 1.0 equiv), K<sub>3</sub>PO<sub>4</sub> (2 equiv), and chloro(2-dicyclohexylphosphino-2',4',6'-triisopropyl-1,1'-biphenyl)[2-(2'-amino-1,1'-biphenyl)]-palladium(II) (XPhos Pd G2, 0.05 equiv) and degassed distilled H<sub>2</sub>O (H<sub>2</sub>O/dioxane 1:2) were added. The reaction mixture was placed in a preheated oil bath at 95 °C and stirred at this temperature for 2–16 h. After completion of the reaction monitored by TLC, a 3 M aqueous HCl solution (10 equiv) was added and the mixture was stirred at 60 °C for 3–16 h. A 2 M aqueous NaOH solution was added until pH 9–10. The aqueous layer was extracted with EtOAc (3 $\times$ ). The combined organic layers were dried over anhydrous Na<sub>2</sub>SO<sub>4</sub> and filtered, and the solvent was evaporated under reduced pressure. The crude product was purified by column chromatography on a silica gel.



**General Procedure 2.** To a solution of the respective morpholine (free base or hydrochloride, 1.05 equiv) and DIPEA (2.1 equiv) in DCM (approx. 1 mL/0.15 mmol) at 0 °C, (R)-4-(4,6-dichloro-1,3,5-triazin-2-yl)-3-methylmorpholine (**26**, 1.0 equiv) was added dropwise. After completion of the addition, the reaction mixture was stirred at r.t. overnight. After completion of the reaction monitored by TLC, the reaction mixture was washed with NaHSO<sub>4</sub> (2×). The organic layer was dried over anhydrous Na<sub>2</sub>SO<sub>4</sub> and filtered, and the solvent was evaporated under reduced pressure. The crude product was purified by column chromatography on a silica gel.

**General Procedure 3.** To a solution of the respective morpholine (free base, 1.05 equiv) and DIPEA (2.1 equiv) in THF (approx. 1 mL/0.15 mmol) at 0 °C, (R)-4-(4,6-dichloro-1,3,5-triazin-2-yl)-3-methylmorpholine (**26**, 1.0 equiv) was added dropwise. After completion of the addition, the reaction mixture was stirred at 70 °C overnight. After completion of the reaction monitored by TLC, the reaction mixture was washed with NaHSO<sub>4</sub> (2×). The organic layer was dried over anhydrous Na<sub>2</sub>SO<sub>4</sub> and filtered, and the solvent was evaporated under reduced pressure. The crude product was purified by column chromatography on a silica gel.

**General Procedure 4.** To a solution of the respective morpholine (free base, 1.05 equiv) and DIPEA (2.1 equiv) in EtOH (approx. 1 mL/0.15 mmol) at 0 °C, (R)-4-(4,6-dichloro-1,3,5-triazin-2-yl)-3-methylmorpholine (**26**, 1.0 equiv) was added dropwise. After completion of the addition, the reaction mixture was stirred at r.t. overnight. After completion of the reaction monitored by TLC, the reaction mixture was washed with NaHSO<sub>4</sub> (2×). The organic layer was dried over anhydrous Na<sub>2</sub>SO<sub>4</sub> and filtered, and the solvent was evaporated under reduced pressure. The crude product was purified by column chromatography on a silica gel.

(R)-4-(Difluoromethyl)-5-(4-(3-methylmorpholino)-6-morpholino-1,3,5-triazin-2-yl)pyridin-2-amine (**1**) was prepared according to general procedure 1 from intermediate **24** (250 mg, 0.83 mmol, 1.0 equiv) and boronate **48** (298 mg, 0.92 mmol, 1.1 equiv). Purification by column chromatography on a silica gel (cyclohexane/ethyl acetate 1:0 → 3:1) gave compound **1** as a colorless solid (248 mg, 0.61 mmol, 73%). <sup>1</sup>H NMR (400 MHz, CDCl<sub>3</sub>): δ 9.03 (s, 1H), 7.68 (t, <sup>1</sup>J<sub>H,F</sub> = 55.3 Hz, 1H), 6.84 (s, 1H), 4.91 (br s, 2H), 4.78–4.70 (m, 1H), 4.45–4.37 (m, 1H), 3.98 (dd, <sup>1</sup>J<sub>H,H</sub> = 11.4, 3.7 Hz, 1H), 3.89–3.80 (m, 4H), 3.79–3.72 (m, 5H), 3.68 (dd, <sup>1</sup>J<sub>H,H</sub> = 11.5, 3.3 Hz, 1H), 3.53 (ddd, <sup>1</sup>J<sub>H,H</sub> = 12.4, 11.4, 3.0 Hz, 1H), 3.28 (td, <sup>1</sup>J<sub>H,H</sub> = 13.0, 3.9 Hz, 1H), 1.32 (d, <sup>1</sup>J<sub>H,H</sub> = 6.8 Hz, 3H). <sup>19</sup>F{<sup>1</sup>H} NMR (376 MHz, CDCl<sub>3</sub>): δ -115.99 (s, 2F). <sup>13</sup>C{<sup>1</sup>H} NMR (101 MHz, CDCl<sub>3</sub>): δ 169.24 (s, 1C), 164.72 (s, 1C), 164.34 (s, 1C), 160.22 (s, 1C), 152.30 (s, 1C), 143.49 (t, <sup>2</sup>J<sub>C,F</sub> = 22.2 Hz, 1C), 121.34 (t, <sup>3</sup>J<sub>C,F</sub> = 4.8 Hz, 1C), 111.35 (t, <sup>1</sup>J<sub>C,F</sub> = 238.6 Hz, 1C), 104.00 (t, <sup>3</sup>J<sub>C,F</sub> = 7.9 Hz, 1C), 71.04 (s, 1C), 66.99 (s, 1C), 66.77 (s, 1C), 46.40 (s, 1C), 43.62 (s, 1C), 38.55 (s, 1C), 30.93 (s, 1C), 26.90 (s, 1C), 14.26 (s, 1C). HRMS (*m/z*): [M + H]<sup>+</sup> calcd for C<sub>18</sub>H<sub>24</sub>F<sub>2</sub>N<sub>7</sub>O<sub>2</sub>, 408.1954; found, 408.1958. HPLC: *t*<sub>R</sub> = 7.81 min (>99.9% purity). mp 189.8 °C (dec).

5-(4,6-Bis((R)-3-methylmorpholino)-1,3,5-triazin-2-yl)-4-(difluoromethyl)pyridin-2-amine (**2**) was prepared according to general procedure 1 from intermediate **25** (250 mg, 0.80 mmol, 1.0 equiv) and boronate **48** (285 mg, 0.88 mmol, 1.1 equiv). Purification by column chromatography on a silica gel (cyclohexane/ethyl acetate 1:0 → 3:1) gave compound **2** as a colorless solid (327 mg, 0.78 mmol, 97%). <sup>1</sup>H NMR (400 MHz, CDCl<sub>3</sub>): δ 9.04 (s, 1H), 7.70 (t, <sup>1</sup>J<sub>H,F</sub> = 55.4 Hz, 1H), 6.83 (s, 1H), 5.01 (br s, 2H), 4.78–4.71 (m, 2H), 4.41 (d, <sup>1</sup>J<sub>H,H</sub> = 13.7 Hz, 2H), 3.98 (dd, <sup>1</sup>J<sub>H,H</sub> = 11.4, 3.7 Hz, 2H), 3.78 (d, <sup>1</sup>J<sub>H,H</sub> = 11.4 Hz, 2H), 3.68 (dd, <sup>1</sup>J<sub>H,H</sub> = 11.5, 3.3 Hz, 2H), 3.53 (td, <sup>1</sup>J<sub>H,H</sub> = 11.7, 3.0 Hz, 2H), 3.27 (td, <sup>1</sup>J<sub>H,H</sub> = 13.0, 3.9 Hz, 2H), 1.33 (d, <sup>1</sup>J<sub>H,H</sub> = 6.9 Hz, 6H). <sup>19</sup>F{<sup>1</sup>H} NMR (376 MHz, CDCl<sub>3</sub>): δ -115.98 (s, 2F). <sup>13</sup>C{<sup>1</sup>H} NMR (101 MHz, CDCl<sub>3</sub>): δ 169.20 (s, 1C), 164.37 (s, 1C), 160.14 (s, 1C), 152.33 (s, 1C), 149.13 (s, 1C), 143.52 (t, <sup>2</sup>J<sub>C,F</sub> = 22.1 Hz, 1C), 121.46 (s, 1C), 111.36 (t, <sup>1</sup>J<sub>C,F</sub> = 238.7 Hz, 1C), 103.98 (t, <sup>3</sup>J<sub>C,F</sub> = 7.8 Hz, 1C), 71.07 (s, 2C), 67.01 (s, 2C), 46.39 (s, 2C), 38.53 (s, 2C), 14.26 (s, 2C). HRMS (*m/z*): [M + H]<sup>+</sup> calcd for C<sub>19</sub>H<sub>26</sub>F<sub>2</sub>N<sub>7</sub>O<sub>2</sub>, 422.2111; found, 422.21117. HPLC: *t*<sub>R</sub> = 8.34 min (>99.9% purity). mp 147.3 °C (dec).

4-(Difluoromethyl)-5-(4-((R)-3-methylmorpholino)-6-((S)-3-methylmorpholino)-1,3,5-triazin-2-yl)pyridin-2-amine (**3**). Compound **3** was prepared according to the literature.<sup>35</sup> mp 214.0 °C.

(R)-4-(Difluoromethyl)-5-(4-(3,3-dimethylmorpholino)-6-(3-methylmorpholino)-1,3,5-triazin-2-yl)pyridin-2-amine (**4**) was prepared according to general procedure 1 from intermediate **28** (189 mg, 0.58 mmol, 1.0 equiv) and boronate **48** (188 mg, 0.58 mmol, 1.0 equiv). Purification by column chromatography on a silica gel (cyclohexane/ethyl acetate 1:0 → 0:1) gave compound **4** as a colorless solid (178 mg, 0.41 mmol, 71%). <sup>1</sup>H NMR (400 MHz, CDCl<sub>3</sub>): δ 9.02 (s, 1H), 7.68 (t, <sup>1</sup>J<sub>H,F</sub> = 55.3 Hz, 1H), 6.84 (s, 1H), 4.94 (br s, 2H), 4.71–4.64 (m, 1H), 4.39–4.32 (m, 1H), 3.99 (dd, <sup>1</sup>J<sub>H,H</sub> = 11.4, 3.8 Hz, 1H), 3.94–3.87 (d, <sup>1</sup>J<sub>H,H</sub> = 3.2 Hz, 4H), 3.79 (dt, <sup>1</sup>J<sub>H,H</sub> = 11.4, 1.0 Hz, 1H), 3.69 (dd, <sup>1</sup>J<sub>H,H</sub> = 11.5, 3.2 Hz, 1H), 3.54 (ddd, <sup>1</sup>J<sub>H,H</sub> = 12.3, 11.4, 3.0 Hz, 1H), 3.49 (s, 2H), 3.29 (ddd, <sup>1</sup>J<sub>H,H</sub> = 13.7, 12.4, 3.8 Hz, 1H), 1.56 (d, <sup>1</sup>J<sub>H,H</sub> = 2.6 Hz, 6H), 1.33 (d, <sup>1</sup>J<sub>H,H</sub> = 6.8 Hz, 3H). <sup>19</sup>F{<sup>1</sup>H} NMR (376 MHz, CDCl<sub>3</sub>): δ -116.11 (s, 2F). <sup>13</sup>C{<sup>1</sup>H} NMR (101 MHz, CDCl<sub>3</sub>): δ 168.65 (s, 1C), 166.78 (s, 1C), 164.00 (s, 1C), 160.02 (s, 1C), 152.29 (s, 1C), 143.46 (t, <sup>2</sup>J<sub>C,F</sub> = 22.1 Hz, 1C), 121.68 (t, <sup>3</sup>J<sub>C,F</sub> = 4.9 Hz, 1C), 111.31 (t, <sup>1</sup>J<sub>C,F</sub> = 238.6 Hz, 1C), 103.98 (t, <sup>3</sup>J<sub>C,F</sub> = 7.9 Hz, 1C), 76.68 (s, 1C), 71.05 (s, 1C), 66.98 (s, 1C), 66.96 (s, 1C), 55.42 (s, 1C), 46.61 (s, 1C), 41.19 (s, 1C), 38.76 (s, 1C), 23.05 (s, 2C), 14.26 (s, 1C). HRMS (*m/z*): [M + H]<sup>+</sup> calcd for C<sub>20</sub>H<sub>28</sub>F<sub>2</sub>N<sub>7</sub>O<sub>2</sub>, 436.2267; found, 436.2272. HPLC: *t*<sub>R</sub> = 8.77 min (98.7% purity). mp 152.4 °C.

(R)-4-(Difluoromethyl)-5-(4-(3-methylmorpholino)-6-(8-oxa-5-azaspiro[3.5]nonan-5-yl)-1,3,5-triazin-2-yl)pyridin-2-amine (**5**) was prepared according to general procedure 1 from intermediate **29** (249 mg, 0.73 mmol, 1.0 equiv) and boronate **48** (239 mg, 0.73 mmol, 1.0 equiv). Purification by column chromatography on a silica gel (cyclohexane/ethyl acetate 1:0 → 0:1) gave compound **5** as a colorless solid (163 mg, 0.36 mmol, 50%). <sup>1</sup>H NMR (400 MHz, CDCl<sub>3</sub>): δ 8.99 (s, 1H), 7.67 (t, <sup>1</sup>J<sub>H,F</sub> = 55.3 Hz, 1H), 6.83 (s, 1H), 5.00 (br s, 2H), 4.75–4.56 (m, 1H), 4.40–4.25 (m, 1H), 3.97 (dd, <sup>1</sup>J<sub>H,H</sub> = 11.5, 3.7 Hz, 1H), 3.91–3.88 (m, 2H), 3.80–3.74 (m, 3H), 3.68 (dd, <sup>1</sup>J<sub>H,H</sub> = 11.5, 3.2 Hz, 1H), 3.59 (t, <sup>1</sup>J<sub>H,H</sub> = 4.7 Hz, 2H), 3.53 (td, <sup>1</sup>J<sub>H,H</sub> = 11.9, 3.0 Hz, 2H), 2.61–2.52 (m, 2H), 2.40–2.32 (m, 2H), 1.85–1.77 (m, 1H), 1.71 (tdd, <sup>1</sup>J<sub>H,H</sub> = 10.8, 8.2, 2.5 Hz, 1H), 1.31 (d, <sup>1</sup>J<sub>H,H</sub> = 6.9 Hz, 3H). <sup>19</sup>F{<sup>1</sup>H} NMR (376 MHz, CDCl<sub>3</sub>): δ -115.31 (–116.65) (m, 2F). <sup>13</sup>C{<sup>1</sup>H} NMR (101 MHz, CDCl<sub>3</sub>): δ 169.12 (s, 1C), 164.27 (s, 1C), 160.12 (s, 1C), 152.32 (s, 1C), 149.13 (s, 1C), 143.47 (t, <sup>2</sup>J<sub>C,F</sub> = 22.2 Hz, 1C), 121.45 (t, <sup>3</sup>J<sub>C,F</sub> = 4.9 Hz, 1C), 111.31 (t, <sup>1</sup>J<sub>C,F</sub> = 238.6 Hz, 1C), 103.97 (t, <sup>3</sup>J<sub>C,F</sub> = 7.9 Hz, 1C), 71.03 (s, 1C), 70.73 (s, 1C), 66.96 (s, 1C), 66.14 (s, 1C), 60.59 (s, 1C), 46.50 (s, 1C), 43.43 (s, 1C), 38.66 (s, 1C), 31.26 (s, 1C), 31.18 (s, 1C), 14.97 (s, 1C), 14.25 (s, 1C). HRMS (*m/z*): [M + H]<sup>+</sup> calcd for C<sub>21</sub>H<sub>28</sub>F<sub>2</sub>N<sub>7</sub>O<sub>2</sub>, 448.2267; found, 448.2273. HPLC: *t*<sub>R</sub> = 9.00 min (99.6% purity). mp 87.6 °C.

4-(Difluoromethyl)-5-(4-((3R,5R)-3,5-dimethylmorpholino)-6-((R)-3-methylmorpholino)-1,3,5-triazin-2-yl)pyridin-2-amine (**6**) was prepared according to general procedure 1 from intermediate **30** (267 mg, 0.82 mmol, 1.0 equiv) and boronate **48** (265 mg, 0.82 mmol, 1.0 equiv). Purification by column chromatography on a silica gel (cyclohexane/ethyl acetate 1:0 → 0:1) gave compound **6** as a colorless solid (253 mg, 0.58 mmol, 71%). <sup>1</sup>H NMR (400 MHz, CDCl<sub>3</sub>): δ 9.08 (s, 1H), 7.78 (t, <sup>1</sup>J<sub>H,F</sub> = 55.4 Hz, 1H), 6.84 (s, 1H), 5.03 (br s, 2H), 4.77–4.70 (m, 1H), 4.45–4.36 (m, 3H), 4.25 (dd, <sup>1</sup>J<sub>H,H</sub> = 11.2, 3.4 Hz, 2H), 3.98 (dd, <sup>1</sup>J<sub>H,H</sub> = 11.4, 3.7 Hz, 1H), 3.80–3.74 (m, 3H), 3.68 (dd, <sup>1</sup>J<sub>H,H</sub> = 11.4, 3.2 Hz, 1H), 3.54 (td, <sup>1</sup>J<sub>H,H</sub> = 12.0, 3.0 Hz, 1H), 3.27 (td, <sup>1</sup>J<sub>H,H</sub> = 12.8, 3.8 Hz, 1H), 1.46 (d, <sup>1</sup>J<sub>H,H</sub> = 6.7 Hz, 6H), 1.34 (d, <sup>1</sup>J<sub>H,H</sub> = 6.8 Hz, 3H). <sup>19</sup>F{<sup>1</sup>H} NMR (376 MHz, CDCl<sub>3</sub>): δ -115.28 (–118.15) (m, 2F). <sup>13</sup>C{<sup>1</sup>H} NMR (101 MHz, CDCl<sub>3</sub>): δ 168.92 (s, 1C), 164.16 (s, 1C), 163.97 (s, 1C), 160.14 (s, 1C), 152.42 (s, 1C), 143.57 (t, <sup>2</sup>J<sub>C,F</sub> = 22.1 Hz, 1C), 121.42 (s, 1C), 111.37 (t, <sup>1</sup>J<sub>C,F</sub> = 238.6 Hz, 1C), 103.95 (t, <sup>3</sup>J<sub>C,F</sub> = 8.0 Hz, 1C), 71.11 (s, 1C), 67.68 (s, 2C), 67.02 (s, 1C), 47.95 (s, 2C), 46.42 (s, 1C), 38.47 (s, 1C), 19.66 (s, 2C), 14.26 (s, 1C). HRMS (*m/z*): [M + H]<sup>+</sup> calcd for C<sub>20</sub>H<sub>28</sub>F<sub>2</sub>N<sub>7</sub>O<sub>2</sub>, 436.2267; found, 436.2273. HPLC: *t*<sub>R</sub> = 8.73 min (99.4% purity). mp 102.2 °C.



4-(Difluoromethyl)-5-(4-((3S,5S)-3,5-dimethylmorpholino)-6-((R)-3-methylmorpholino)-1,3,5-triazin-2-yl)pyridin-2-amine (7) was prepared according to general procedure 1 from intermediate 31 (244 mg, 0.75 mmol, 1.0 equiv) and boronate 48 (243 mg, 0.75 mmol, 1.0 equiv). Purification by column chromatography on a silica gel (cyclohexane/ethyl acetate 1:0 → 0:1) gave compound 7 as a colorless solid (213 mg, 0.49 mmol, 65%). <sup>1</sup>H NMR (400 MHz, CDCl<sub>3</sub>): δ 9.09 (s, 1H), 7.78 (t, <sup>1</sup>J<sub>H,F</sub> = 55.4 Hz, 1H), 6.84 (s, 1H), 5.02 (br s, 2H), 4.77–4.70 (m, 1H), 4.44–4.36 (m, 3H), 4.25 (dd, *J*<sub>H,H</sub> = 11.2, 3.4 Hz, 2H), 3.99 (dd, *J*<sub>H,H</sub> = 11.4, 3.7 Hz, 1H), 3.80–3.74 (m, 3H), 3.69 (dd, *J*<sub>H,H</sub> = 11.4, 3.3 Hz, 1H), 3.57–3.48 (m, 1H), 3.29 (td, *J*<sub>H,H</sub> = 13.0, 3.8 Hz, 1H), 1.45 (d, *J*<sub>H,H</sub> = 6.7 Hz, 6H), 1.33 (d, *J*<sub>H,H</sub> = 6.9 Hz, 3H). <sup>19</sup>F{<sup>1</sup>H} NMR (376 MHz, CDCl<sub>3</sub>): δ -116.24–(-116.51) (m, 2F). <sup>13</sup>C{<sup>1</sup>H} NMR (101 MHz, CDCl<sub>3</sub>): δ 168.91 (s, 1C), 164.19 (s, 1C), 163.99 (s, 1C), 160.15 (s, 1C), 152.45 (s, 1C), 143.58 (t, <sup>2</sup>J<sub>C,F</sub> = 22.1 Hz, 1C), 121.40 (s, 1C), 111.36 (t, <sup>1</sup>J<sub>C,F</sub> = 238.6 Hz, 1C), 103.94 (t, <sup>3</sup>J<sub>C,F</sub> = 8.0 Hz, 1C), 71.05 (s, 1C), 67.68 (s, 2C), 67.03 (s, 1C), 47.94 (s, 2C), 38.57 (s, 1C), 26.91 (s, 1C), 19.64 (s, 2C), 14.31 (s, 1C). HRMS (*m/z*): [M + H]<sup>+</sup> calcd for C<sub>20</sub>H<sub>28</sub>F<sub>2</sub>N<sub>7</sub>O<sub>2</sub>, 436.2267; found, 436.2271. HPLC: *t*<sub>R</sub> = 8.89 min (97.5% purity). mp 168.7 °C.

4-(Difluoromethyl)-5-(4-((3R,5S)-3,5-dimethylmorpholino)-6-((R)-3-methylmorpholino)-1,3,5-triazin-2-yl)pyridin-2-amine (PQR626, 8) was prepared according to general procedure 1 from intermediate 32 (149 mg, 0.46 mmol, 1.0 equiv) and boronate 48 (148 mg, 0.46 mmol, 1.0 equiv). Purification by column chromatography on a silica gel (cyclohexane/ethyl acetate 1:0 → 0:1) gave compound 8 as a colorless solid (149 mg, 0.34 mmol, 74%; mp 100 °C). To generate the HCl salt, compound 8 was dissolved in *tert*-butyl methyl ether (30 equiv) and a 5 N solution of HCl in isopropanol (1.5 equiv) was added dropwise. The suspension was stirred at r.t. for 1 h. The solid was collected *via* Buchner filtration and dried in high vacuum. <sup>1</sup>H NMR (400 MHz, DMSO-*d*<sub>6</sub>): δ 9.01 (br s, 2H), 8.82 (s, 1H), 7.83 (t, <sup>1</sup>J<sub>H,F</sub> = 54.3 Hz, 1H), 7.41 (s, 1H), 4.75–4.58 (m, 1H), 4.56–4.44 (m, 2H), 4.39–4.27 (m, 1H), 3.92 (dd, *J*<sub>H,H</sub> = 11.4, 3.6 Hz, 1H), 3.76 (d, *J*<sub>H,H</sub> = 11.5 Hz, 2H), 3.71 (d, *J*<sub>H,H</sub> = 11.4 Hz, 1H), 3.59–3.51 (m, 3H), 3.44–3.36 (m, 1H), 3.18 (td, *J*<sub>H,H</sub> = 13.2, 3.8 Hz, 1H), 1.27 (d, *J*<sub>H,H</sub> = 6.9 Hz, 6H), 1.22 (d, *J*<sub>H,H</sub> = 6.8 Hz, 3H). <sup>19</sup>F{<sup>1</sup>H} NMR (376 MHz, DMSO-*d*<sub>6</sub>): δ -116.14–(-119.51) (m, 2F). <sup>13</sup>C{<sup>1</sup>H} NMR (101 MHz, DMSO-*d*<sub>6</sub>): δ 167.00 (s, 1C), 164.01 (s, 1C), 163.63 (s, 1C), 155.53 (s, 1C), 146.95 (t, <sup>2</sup>J<sub>C,F</sub> = 22.0 Hz, 1C), 140.68 (s, 1C), 120.00 (s, 1C), 111.15 (t, <sup>1</sup>J<sub>C,F</sub> = 239.3 Hz, 1C), 110.80 (t, <sup>3</sup>J<sub>C,F</sub> = 9.7 Hz, 1C), 70.89 (s, 1C), 70.61 (s, 1C), 66.81 (s, 1C), 66.56 (s, 1C), 49.17 (s, 1C), 46.42 (s, 1C), 45.75 (s, 1C), 38.70 (s, 1C), 27.25 (s, 1C), 19.19 (s, 1C), 14.52 (s, 1C). HRMS (*m/z*): [M + H]<sup>+</sup> calcd for C<sub>20</sub>H<sub>28</sub>F<sub>2</sub>N<sub>7</sub>O<sub>2</sub>, 436.2267; found, 436.2274. HPLC: *t*<sub>R</sub> = 8.96 min (>99.9% purity). mp 192.2 °C.

4-(Difluoromethyl)-5-(4-((2S,6R)-2,6-dimethylmorpholino)-6-((R)-3-methylmorpholino)-1,3,5-triazin-2-yl)pyridin-2-amine (9) was prepared according to general procedure 1 from intermediate 33 (150 mg, 0.46 mmol, 1.0 equiv) and boronate 48 (149 mg, 0.46 mmol, 1.0 equiv). Purification by column chromatography on a silica gel (cyclohexane/ethyl acetate 1:0 → 0:1) gave compound 9 as a colorless solid (142 mg, 0.33 mmol, 71%). <sup>1</sup>H NMR (400 MHz, CDCl<sub>3</sub>): δ 9.03 (s, 1H), 7.67 (t, <sup>1</sup>J<sub>H,F</sub> = 55.3 Hz, 1H), 6.84 (s, 1H), 4.98 (br s, 2H), 4.78–4.49 (m, 3H), 4.40 (d, *J*<sub>H,H</sub> = 13.6 Hz, 1H), 3.99 (dd, *J*<sub>H,H</sub> = 11.4, 3.7 Hz, 1H), 3.78 (d, *J*<sub>H,H</sub> = 11.2 Hz, 1H), 3.68 (dd, *J*<sub>H,H</sub> = 11.5, 3.3 Hz, 1H), 3.62 (dddd, *J*<sub>H,H</sub> = 10.6, 6.3, 2.6, 1.7 Hz, 1H), 3.65–3.58 (m, 2H), 3.28 (td, *J*<sub>H,H</sub> = 12.7, 3.8 Hz, 1H), 2.60 (t, *J*<sub>H,H</sub> = 11.5 Hz, 2H), 1.33 (d, *J*<sub>H,H</sub> = 6.8 Hz, 3H), 1.26 (d, *J*<sub>H,H</sub> = 6.2 Hz, 6H). <sup>19</sup>F{<sup>1</sup>H} NMR (376 MHz, CDCl<sub>3</sub>): δ -115.97–(-116.64) (m, 2F). <sup>13</sup>C{<sup>1</sup>H} NMR (101 MHz, CDCl<sub>3</sub>): δ 169.18 (s, 1C), 164.38 (s, 2C), 160.13 (s, 1C), 152.30 (s, 1C), 143.51 (t, <sup>2</sup>J<sub>C,F</sub> = 22.2 Hz, 1C), 121.51 (t, <sup>3</sup>J<sub>C,F</sub> = 4.9 Hz, 1C), 111.34 (t, <sup>1</sup>J<sub>C,F</sub> = 238.6 Hz, 1C), 103.99 (t, <sup>3</sup>J<sub>C,F</sub> = 7.8 Hz, 1C), 71.74 (br s, 2C), 71.07 (s, 1C), 67.01 (s, 1C), 48.69 (br s, 2C), 46.41 (s, 1C), 38.57 (s, 1C), 18.90 (s, 1C), 14.27 (s, 1C), 14.20 (s, 1C). HRMS (*m/z*): [M + H]<sup>+</sup> calcd for C<sub>20</sub>H<sub>28</sub>F<sub>2</sub>N<sub>7</sub>O<sub>2</sub>, 436.2267; found, 436.2273. HPLC: *t*<sub>R</sub> = 8.79 min (>99.9% purity). mp 106.4 °C.

4-(Difluoromethyl)-5-(4-((S)-3-ethylmorpholino)-6-((R)-3-methylmorpholino)-1,3,5-triazin-2-yl)pyridin-2-amine (10) was prepared according to general procedure 1 from intermediate 34 (309 mg, 0.95 mmol, 1.0 equiv) and boronate 48 (307 mg, 0.95 mmol, 1.0 equiv). Purification by column chromatography on a silica gel (cyclohexane/ethyl acetate 1:0 → 0:1) gave compound 10 as a colorless solid (192 mg, 0.44 mmol, 47%). <sup>1</sup>H NMR (400 MHz, CDCl<sub>3</sub>): δ 9.04 (s, 1H), 7.70 (t, <sup>1</sup>J<sub>H,F</sub> = 55.3 Hz, 1H), 6.83 (s, 1H), 5.00 (br s, 2H), 4.78–4.68 (m, 1H), 4.59–4.34 (m, 3H), 4.01–3.87 (m, 3H), 3.78 (d, *J*<sub>H,H</sub> = 11.4 Hz, 1H), 3.69 (dd, *J*<sub>H,H</sub> = 11.5, 3.3 Hz, 1H), 3.61 (dd, *J*<sub>H,H</sub> = 11.6, 3.2 Hz, 1H), 3.56–3.48 (m, 2H), 3.32–3.18 (m, 2H), 1.88–1.77 (m, 2H), 1.32 (d, *J*<sub>H,H</sub> = 6.8 Hz, 3H), 0.94 (t, *J*<sub>H,H</sub> = 7.5 Hz, 3H). <sup>19</sup>F{<sup>1</sup>H} NMR (376 MHz, CDCl<sub>3</sub>): δ -116.26 (s, 2F). <sup>13</sup>C{<sup>1</sup>H} NMR (101 MHz, CDCl<sub>3</sub>): δ 169.13 (s, 1C), 164.68 (s, 1C), 164.36 (s, 1C), 160.14 (s, 1C), 152.34 (s, 1C), 143.53 (t, <sup>2</sup>J<sub>C,F</sub> = 22.1 Hz, 1C), 121.49 (t, <sup>3</sup>J<sub>C,F</sub> = 5.0 Hz, 1C), 111.33 (t, <sup>1</sup>J<sub>C,F</sub> = 238.6 Hz, 1C), 103.97 (t, <sup>3</sup>J<sub>C,F</sub> = 7.8 Hz, 1C), 71.06 (s, 1C), 68.44 (br s, 1C), 67.00 (s, 1C), 52.09 (br s, 1C), 46.38 (s, 1C), 38.91 (br s, 1C), 38.57 (s, 1C), 24.87 (s, 1C), 21.53 (s, 1C), 14.23 (s, 1C), 10.86 (s, 1C). HRMS (*m/z*): [M + H]<sup>+</sup> calcd for C<sub>20</sub>H<sub>28</sub>F<sub>2</sub>N<sub>7</sub>O<sub>2</sub>, 436.2267; found, 436.2271. HPLC: *t*<sub>R</sub> = 8.82 min (>99.9% purity). mp 101.3 °C.

4-(Difluoromethyl)-5-(4-((S)-3-ethylmorpholino)-6-((R)-3-methylmorpholino)-1,3,5-triazin-2-yl)pyridin-2-amine (11) was prepared according to general procedure 1 from intermediate 35 (345 mg, 1.06 mmol, 1.0 equiv) and boronate 48 (343 mg, 1.06 mmol, 1.0 equiv). Purification by column chromatography on a silica gel (cyclohexane/ethyl acetate 1:0 → 0:1) gave compound 11 as a colorless solid (241 mg, 0.55 mmol, 52%). <sup>1</sup>H NMR (400 MHz, CDCl<sub>3</sub>): δ 9.04 (s, 1H), 7.70 (t, <sup>1</sup>J<sub>H,F</sub> = 55.3 Hz, 1H), 6.83 (s, 1H), 5.05 (br s, 2H), 4.80–4.67 (m, 1H), 4.61–4.36 (m, 3H), 3.96 (ddd, *J*<sub>H,H</sub> = 14.5, 11.4, 3.6 Hz, 2H), 3.90 (d, *J*<sub>H,H</sub> = 11.6 Hz, 1H), 3.78 (d, *J*<sub>H,H</sub> = 11.4 Hz, 1H), 3.69 (dd, *J*<sub>H,H</sub> = 11.4, 3.3 Hz, 1H), 3.61 (dd, *J*<sub>H,H</sub> = 11.6, 3.2 Hz, 1H), 3.53 (ddt, *J*<sub>H,H</sub> = 15.2, 12.2, 3.2 Hz, 2H), 3.32–3.19 (m, 2H), 1.93–1.76 (m, 2H), 1.32 (d, *J*<sub>H,H</sub> = 6.8 Hz, 3H), 0.94 (t, *J*<sub>H,H</sub> = 7.4 Hz, 3H). <sup>19</sup>F{<sup>1</sup>H} NMR (376 MHz, CDCl<sub>3</sub>): δ -116.25 (s, 2F). <sup>13</sup>C{<sup>1</sup>H} NMR (101 MHz, CDCl<sub>3</sub>): δ 169.14 (s, 1C), 164.68 (s, 1C), 164.36 (s, 1C), 160.19 (s, 1C), 152.33 (s, 1C), 143.52 (t, <sup>2</sup>J<sub>C,F</sub> = 22.2 Hz, 1C), 121.44 (t, <sup>3</sup>J<sub>C,F</sub> = 4.9 Hz, 1C), 111.34 (t, <sup>1</sup>J<sub>C,F</sub> = 238.5 Hz, 1C), 103.98 (t, <sup>3</sup>J<sub>C,F</sub> = 7.8 Hz, 1C), 71.06 (s, 1C), 68.45 (br s, 1C), 67.00 (s, 1C), 52.09 (s, 1C), 46.38 (s, 1C), 38.91 (s, 1C), 38.58 (s, 1C), 24.87 (s, 1C), 21.53 (s, 1C), 14.23 (s, 1C), 10.87 (s, 1C). HRMS (*m/z*): [M + H]<sup>+</sup> calcd for C<sub>20</sub>H<sub>28</sub>F<sub>2</sub>N<sub>7</sub>O<sub>2</sub>, 436.2267; found, 436.2275. HPLC: *t*<sub>R</sub> = 8.69 min (99.7% purity). mp 93.5 °C.

(R)-4-(4-(6-Amino-4-(difluoromethyl)pyridin-3-yl)-6-((R)-3-methylmorpholino)-1,3,5-triazin-2-yl)morpholin-3-yl)methanol (12) was prepared according to general procedure 1 from intermediate 36 (170 mg, 0.52 mmol, 1.0 equiv) and boronate 48 (168 mg, 0.52 mmol, 1.0 equiv). Purification by column chromatography on a silica gel (cyclohexane/ethyl acetate 1:0 → 0:1) gave compound 12 as a colorless solid (105 mg, 0.24 mmol, 44%). <sup>1</sup>H NMR (400 MHz, CDCl<sub>3</sub>): δ 9.02 (s, 1H), 7.66 (t, <sup>1</sup>J<sub>H,F</sub> = 55.1 Hz, 1H), 6.83 (s, 1H), 4.96 (br s, 2H), 4.79–4.66 (m, 2H), 4.59–4.32 (m, 2H), 4.07 (d, *J*<sub>H,H</sub> = 11.9 Hz, 1H), 4.03–3.92 (m, 4H), 3.77 (d, *J*<sub>H,H</sub> = 11.4 Hz, 1H), 3.70–3.62 (m, *J*<sub>H,H</sub> = 11.9, 6.2, 3.4 Hz, 2H), 3.60–3.48 (m, 2H), 3.35–3.24 (m, 2H), 2.57 (br s, 1H), 1.32 (d, *J*<sub>H,H</sub> = 6.8 Hz, 3H). <sup>19</sup>F{<sup>1</sup>H} NMR (376 MHz, CDCl<sub>3</sub>): δ -114.79–(-118.05) (s, 2F). <sup>13</sup>C{<sup>1</sup>H} NMR (101 MHz, CDCl<sub>3</sub>): δ 169.21 (s, 1C), 165.47 (s, 1C), 164.20 (s, 1C), 160.16 (s, 1C), 152.33 (s, 1C), 143.54 (t, <sup>2</sup>J<sub>C,F</sub> = 22.1 Hz, 1C), 121.18 (t, <sup>3</sup>J<sub>C,F</sub> = 4.9 Hz, 1C), 111.33 (t, <sup>1</sup>J<sub>C,F</sub> = 238.6 Hz, 1C), 104.08 (t, <sup>3</sup>J<sub>C,F</sub> = 8.1 Hz, 1C), 71.04 (s, 1C), 66.93–66.88 (m, 1C), 66.68 (s, 1C), 60.96 (s, 1C), 51.87 (s, 1C), 46.52 (s, 1C), 39.56 (s, 1C), 38.60 (s, 1C), 30.94 (s, 1C), 14.34 (s, 1C). HRMS (*m/z*): [M + H]<sup>+</sup> calcd for C<sub>19</sub>H<sub>26</sub>F<sub>2</sub>N<sub>7</sub>O<sub>3</sub>, 438.2060; found, 438.2066. HPLC: *t*<sub>R</sub> = 6.72 min (97.7% purity). mp 118.9 °C.

(S)-4-(4-(6-Amino-4-(difluoromethyl)pyridin-3-yl)-6-((R)-3-methylmorpholino)-1,3,5-triazin-2-yl)morpholin-3-yl)methanol (13) was prepared according to general procedure 1 from intermediate 37 (253 mg, 0.77 mmol, 1.0 equiv) and boronate 48 (250 mg, 0.77 mmol, 1.0 equiv). Purification by column chromatography on a silica

gel (cyclohexane/ethyl acetate 1:0 → 0:1) gave compound **13** as a colorless solid (162 mg, 0.37 mmol, 48%).  $^1\text{H}$  NMR (400 MHz,  $\text{CDCl}_3$ ):  $\delta$  9.00 (s, 1H), 7.66 (t,  $J_{\text{H,F}} = 55.2$  Hz, 1H), 6.81 (s, 1H), 5.13 (br s, 2H), 4.77–4.68 (m, 2H), 4.57–4.34 (m, 2H), 4.10 (d,  $J_{\text{H,H}} = 12.5$  Hz, 1H), 4.01–3.92 (m, 4H), 3.76 (d,  $J_{\text{H,H}} = 11.4$  Hz, 1H), 3.69–3.62 (m, 2H), 3.60–3.48 (m, 2H), 3.34–3.22 (m, 2H), 3.05 (br s, 1H), 1.32 (d,  $J_{\text{H,H}} = 6.9$  Hz, 3H).  $^{19}\text{F}\{^1\text{H}\}$  NMR (376 MHz,  $\text{CDCl}_3$ ):  $\delta$  -113.80–(-117.87) (s, 2F).  $^{13}\text{C}\{^1\text{H}\}$  NMR (101 MHz,  $\text{CDCl}_3$ ):  $\delta$  169.20 (s, 1C), 165.37 (s, 1C), 164.22 (s, 1C), 160.27 (s, 1C), 152.22 (s, 1C), 143.53 (t,  $J_{\text{C,F}} = 22.1$  Hz, 1C), 121.04 (t,  $J_{\text{C,F}} = 4.8$  Hz, 1C), 111.34 (t,  $J_{\text{C,F}} = 238.7$  Hz, 1C), 104.15 (t,  $J_{\text{C,F}} = 8.0$  Hz, 1C), 70.98 (s, 1C), 66.95–66.85 (m, 1C), 66.53 (s, 1C), 60.43 (s, 1C), 51.85 (s, 1C), 46.47 (s, 1C), 39.58 (s, 1C), 38.61 (s, 1C), 21.05 (s, 1C), 14.30 (s, 1C). HRMS ( $m/z$ ):  $[\text{M} + \text{H}]^+$  calcd for  $\text{C}_{19}\text{H}_{26}\text{F}_2\text{N}_7\text{O}_3$ , 438.2060; found, 438.2068. HPLC (ACN with 0.1% TFA):  $t_{\text{R}} = 5.66$  min (98.1% purity). mp 100.5 °C.

4-(Difluoromethyl)-5-(4-((R)-3-(methoxymethyl)morpholino)-6-((R)-3-methylmorpholino)-1,3,5-triazin-2-yl)pyridin-2-amine (**14**) was prepared according to general procedure 1 from intermediate **38** (309 mg, 0.90 mmol, 1.0 equiv) and boronate **48** (293 mg, 0.90 mmol, 1.0 equiv). Purification by column chromatography on a silica gel (cyclohexane/ethyl acetate 1:0 → 0:1) gave compound **14** as a colorless solid (275 mg, 0.61 mmol, 68%).  $^1\text{H}$  NMR (400 MHz,  $\text{CDCl}_3$ ):  $\delta$  9.03 (s, 1H), 7.71 (t,  $J_{\text{H,F}} = 55.1$  Hz, 1H), 6.83 (s, 1H), 4.93 (br s, 2H), 4.81–4.69 (m, 2H), 4.56–4.36 (m, 2H), 4.13–4.08 (m, 1H), 4.00–3.94 (m, 2H), 3.80–3.73 (m, 2H), 3.67 (dd,  $J_{\text{H,H}} = 11.5$ , 3.2 Hz, 1H), 3.62–3.49 (m, 4H), 3.40 (s, 3H), 3.31–3.14 (m, 2H), 1.33 (d,  $J_{\text{H,H}} = 6.8$  Hz, 3H).  $^{19}\text{F}\{^1\text{H}\}$  NMR (376 MHz,  $\text{CDCl}_3$ ):  $\delta$  -115.36–(-118.20) (m, 2F).  $^{13}\text{C}\{^1\text{H}\}$  NMR (101 MHz,  $\text{CDCl}_3$ ):  $\delta$  169.28 (s, 1C), 164.76 (s, 1C), 164.36 (s, 1C), 160.11 (s, 1C), 152.35 (s, 1C), 144.77 (s, 1C), 121.44 (s, 1C), 111.40 (t,  $J_{\text{C,F}} = 238.7$  Hz, 1C), 103.98 (t,  $J_{\text{C,F}} = 8.0$  Hz, 1C), 71.06 (s, 1C), 68.75–68.11 (m, 1C), 66.99 (s, 1C), 66.75 (s, 1C), 66.44–66.08 (m, 1C), 59.06 (s, 1C), 49.76–49.25 (m, 1C), 46.44 (s, 1C), 39.99–39.51 (m, 1C), 38.56 (s, 1C), 14.30 (s, 1C). HRMS ( $m/z$ ):  $[\text{M} + \text{H}]^+$  calcd for  $\text{C}_{20}\text{H}_{28}\text{F}_2\text{N}_7\text{O}_3$ , 452.2216; found, 452.2222. HPLC:  $t_{\text{R}} = 7.91$  min (97.2% purity). mp 101.4 °C.

5-(4-(3-Oxa-6-azabicyclo[3.1.1]heptan-6-yl)-6-((R)-3-methylmorpholino)-1,3,5-triazin-2-yl)-4-(difluoromethyl)pyridin-2-amine (**15**) was prepared according to general procedure 1 from intermediate **39** (228 mg, 0.73 mmol, 1.0 equiv) and boronate **48** (238 mg, 0.73 mmol, 1.0 equiv). Purification by column chromatography on a silica gel (cyclohexane/ethyl acetate 1:0 → 0:1) gave compound **15** as a colorless solid (159 mg, 0.38 mmol, 52%).  $^1\text{H}$  NMR (400 MHz,  $\text{CDCl}_3$ ):  $\delta$  9.06 (s, 1H), 7.74 (t,  $J_{\text{H,F}} = 55.4$  Hz, 1H), 6.82 (s, 1H), 5.06 (br s, 2H), 4.77–4.68 (m, 1H), 4.50–4.30 (m, 5H), 4.00–3.94 (m, 1H), 3.84–3.74 (m, 3H), 3.67 (dd,  $J_{\text{H,H}} = 11.5$ , 3.3 Hz, 1H), 3.52 (td,  $J_{\text{H,H}} = 11.9$ , 3.0 Hz, 1H), 3.32–3.21 (m, 1H), 2.76 (q,  $J_{\text{H,H}} = 6.8$  Hz, 1H), 1.94 (d,  $J_{\text{H,H}} = 8.2$  Hz, 1H), 1.32 (d,  $J_{\text{H,H}} = 6.8$  Hz, 3H).  $^{19}\text{F}\{^1\text{H}\}$  NMR (376 MHz,  $\text{CDCl}_3$ ):  $\delta$  -115.05–(-118.48) (m, 2F).  $^{13}\text{C}\{^1\text{H}\}$  NMR (101 MHz,  $\text{CDCl}_3$ ):  $\delta$  169.30 (s, 1C), 166.12 (s, 1C), 164.18 (s, 1C), 160.28 (s, 1C), 152.40 (s, 1C), 143.67 (t,  $J_{\text{C,F}} = 22.1$  Hz, 1C), 120.89 (t,  $J_{\text{C,F}} = 4.8$  Hz, 1C), 111.31 (t,  $J_{\text{C,F}} = 238.7$  Hz, 1C), 104.02 (t,  $J_{\text{C,F}} = 8.1$  Hz, 1C), 71.01 (s, 1C), 66.96 (s, 1C), 65.78 (s, 1C), 65.21 (s, 1C), 61.85 (s, 1C), 61.47 (s, 1C), 46.31 (s, 1C), 38.47 (s, 1C), 27.76 (s, 1C), 14.34 (s, 1C). HRMS ( $m/z$ ):  $[\text{M} + \text{H}]^+$  calcd for  $\text{C}_{19}\text{H}_{24}\text{F}_2\text{N}_7\text{O}_2$ , 420.1954; found, 420.1962. HPLC (ACN with 0.1% TFA):  $t_{\text{R}} = 6.26$  min (98.2% purity). mp 186.2 °C.

5-(4-(6-Oxa-3-azabicyclo[3.1.1]heptan-3-yl)-6-((R)-3-methylmorpholino)-1,3,5-triazin-2-yl)-4-(difluoromethyl)pyridin-2-amine (**16**) was prepared according to general procedure 1 from intermediate **40** (230 mg, 0.74 mmol, 1.0 equiv) and boronate **48** (240 mg, 0.74 mmol, 1.0 equiv). Purification by column chromatography on a silica gel (cyclohexane/ethyl acetate 1:0 → 0:1) gave compound **16** as a colorless solid (113 mg, 0.27 mmol, 36%).  $^1\text{H}$  NMR (400 MHz,  $\text{CDCl}_3$ ):  $\delta$  9.11 (s, 1H), 7.82 (t,  $J_{\text{H,F}} = 55.4$  Hz, 1H), 6.84 (s, 1H), 4.98 (br s, 2H), 4.83–4.69 (m, 3H), 4.46 (d,  $J_{\text{H,H}} = 13.7$  Hz, 1H), 4.05 (d,  $J_{\text{H,H}} = 13.3$  Hz, 1H), 4.01–3.93 (m, 2H), 3.87 (dt,  $J_{\text{H,H}} = 13.2$ , 2.9 Hz, 1H), 3.82–3.75 (m, 2H), 3.69 (dd,  $J_{\text{H,H}} = 11.4$ , 3.3 Hz, 1H), 3.54 (tt,  $J_{\text{H,H}} = 12.0$ , 3.2 Hz, 1H), 3.34–3.24 (m, 2H), 1.93 (dd,

$J_{\text{H,H}} = 8.9$ , 4.7 Hz, 1H), 1.34 (d,  $J_{\text{H,H}} = 6.8$  Hz, 3H).  $^{19}\text{F}\{^1\text{H}\}$  NMR (376 MHz,  $\text{CDCl}_3$ ):  $\delta$  -115.62–(-116.97) (m, 2F).  $^{13}\text{C}\{^1\text{H}\}$  NMR (101 MHz,  $\text{CDCl}_3$ ):  $\delta$  168.84 (s, 1C), 165.35 (s, 1C), 164.11–164.09 (m, 1C), 160.14 (s, 1C), 152.42 (s, 1C), 143.67 (t,  $J_{\text{C,F}} = 22.1$  Hz, 1C), 121.38 (t,  $J_{\text{C,F}} = 4.8$  Hz, 1C), 111.41 (t,  $J_{\text{C,F}} = 238.6$  Hz, 1C), 103.99 (t,  $J_{\text{C,F}} = 8.1$  Hz, 1C), 78.14 (s, 1C), 77.98 (s, 1C), 71.09 (s, 1C), 67.04 (s, 1C), 48.65 (s, 1C), 48.59 (s, 1C), 46.39 (s, 1C), 38.53 (s, 1C), 32.30–32.28 (m, 1C), 14.25 (s, 1C). HRMS ( $m/z$ ):  $[\text{M} + \text{H}]^+$  calcd for  $\text{C}_{19}\text{H}_{24}\text{F}_2\text{N}_7\text{O}_2$ , 420.1954; found, 420.1956. HPLC (ACN with 0.1% TFA):  $t_{\text{R}} = 6.17$  min (98.9% purity). mp 205.3 °C.

5-(4-((1R,4R)-2-Oxa-5-azabicyclo[2.2.1]heptan-5-yl)-6-((R)-3-methylmorpholino)-1,3,5-triazin-2-yl)-4-(difluoromethyl)pyridin-2-amine (**17**) was prepared according to general procedure 1 from intermediate **41** (257 mg, 0.83 mmol, 1.0 equiv) and boronate **48** (209 mg, 0.83 mmol, 1.0 equiv). Purification by column chromatography on a silica gel (cyclohexane/ethyl acetate 1:0 → 0:1) gave compound **17** as a colorless solid (182 mg, 0.43 mmol, 52%).  $^1\text{H}$  NMR (400 MHz,  $\text{CDCl}_3$ ):  $\delta$  9.07/9.04 (2 × s, 1H), 7.76 (2 × t,  $J_{\text{H,F}} = 55.4$  Hz, 1H), 6.83 (s, 1H), 5.10–5.00 (m, 1H), 4.98 (br s, 2H), 4.80–4.73 (m, 1H), 4.72–4.67 (m, 1H), 4.43 (d,  $J_{\text{H,H}} = 12.2$  Hz, 1H), 3.97 (dd,  $J_{\text{H,H}} = 11.4$ , 3.6 Hz, 1H), 3.92–3.86 (m, 2H), 3.77 (d,  $J_{\text{H,H}} = 11.5$  Hz, 1H), 3.71–3.48 (m, 4H), 3.31–3.22 (m, 1H), 1.99–1.90 (m, 2H), 1.33 (2 × d,  $J_{\text{H,H}} = 6.9$  Hz, 3H).  $^{19}\text{F}\{^1\text{H}\}$  NMR (376 MHz,  $\text{CDCl}_3$ ):  $\delta$  -116.10–(-116.89) (m, 2F).  $^{13}\text{C}\{^1\text{H}\}$  NMR (101 MHz,  $\text{CDCl}_3$ ):  $\delta$  169.25/168.83 (2 × s, 1C), 164.29/164.06 (2 × s, 1C), 163.37/163.30 (2 × s, 1C), 160.20/160.16 (2 × s, 1C), 152.36/152.28 (2 × s, 1C), 143.94–143.31 (m, 1C), 121.39–121.16 (2 × s, 1C), 111.38 (t,  $J_{\text{C,F}} = 238.6$  Hz, 1C), 104.00 (t,  $J_{\text{C,F}} = 8.0$  Hz, 1C), 76.42/76.34 (2 × s, 1C), 74.06/73.80 (2 × s, 1C), 71.07 (s, 1C), 67.02 (s, 1C), 56.63/56.26 (2 × s, 1C), 55.06/54.98 (2 × s, 1C), 46.33 (s, 1C), 38.47 (s, 1C), 36.67/36.47 (2 × s, 1C), 14.28 (s, 1C). HRMS ( $m/z$ ):  $[\text{M} + \text{H}]^+$  calcd for  $\text{C}_{19}\text{H}_{24}\text{F}_2\text{N}_7\text{O}_2$ , 420.1954; found, 420.1960. HPLC (ACN with 0.1% TFA):  $t_{\text{R}} = 6.13$  min (99.0% purity). mp 122.1 °C.

5-(4-((1S,4S)-2-Oxa-5-azabicyclo[2.2.1]heptan-5-yl)-6-((R)-3-methylmorpholino)-1,3,5-triazin-2-yl)-4-(difluoromethyl)pyridin-2-amine (**18**) was prepared according to general procedure 1 from intermediate **42** (217 mg, 0.70 mmol, 1.0 equiv) and boronate **48** (227 mg, 0.70 mmol, 1.0 equiv). Purification by column chromatography on a silica gel (cyclohexane/ethyl acetate 1:0 → 0:1) gave compound **18** as a colorless solid (129 mg, 0.31 mmol, 44%).  $^1\text{H}$  NMR (400 MHz,  $\text{CDCl}_3$ ):  $\delta$  9.06/9.04 (2 × s, 1H), 7.76 (2 × t,  $J_{\text{H,F}} = 55.4$  Hz, 1H), 6.83 (2 × s, 1H), 5.10–5.02 (m, 3H), 4.78–4.69 (m, 1H), 4.70 (d,  $J_{\text{H,H}} = 5.5$  Hz, 1H), 4.42 (d,  $J_{\text{H,H}} = 13.4$  Hz, 1H), 3.97 (dt,  $J_{\text{H,H}} = 11.4$ , 3.8 Hz, 1H), 3.89–3.86 (m, 2H), 3.77 (dd,  $J_{\text{H,H}} = 11.4$ , 3.1 Hz, 1H), 3.71–3.48 (m, 4H), 3.27 (td,  $J_{\text{H,H}} = 13.0$ , 3.8 Hz, 1H), 2.00–1.89 (m, 2H), 1.32 (d,  $J_{\text{H,H}} = 6.8$  Hz, 3H).  $^{19}\text{F}\{^1\text{H}\}$  NMR (376 MHz,  $\text{CDCl}_3$ ):  $\delta$  -115.72–(-116.88) (m, 2F).  $^{13}\text{C}\{^1\text{H}\}$  NMR (101 MHz,  $\text{CDCl}_3$ ):  $\delta$  169.22/168.83 (2 × s, 1C), 164.30/164.04 (2 × s, 1C), 163.40/163.25 (2 × s, 1C), 160.16/160.14 (2 × s, 1C), 152.36/152.29 (2 × s, 1C), 143.54 (t,  $J_{\text{C,F}} = 22.1$  Hz, 1C), 121.40 (s, 1C), 111.38 (t,  $J_{\text{C,F}} = 238.6$  Hz, 1C), 104.01 (t,  $J_{\text{C,F}} = 8.0$  Hz, 1C), 76.43/76.34 (s × 2, 1C), 74.05/73.86 (s × 2, 1C), 71.08 (s, 1C), 67.02 (s, 1C), 56.65/56.22 (2 × s, 1C), 55.01 (s, 1C), 46.30 (s, 1C), 38.52/38.47 (2 × s, 1C), 36.68/36.49 (2 × s, 1C), 14.26 (s, 1C). HRMS ( $m/z$ ):  $[\text{M} + \text{H}]^+$  calcd for  $\text{C}_{19}\text{H}_{24}\text{F}_2\text{N}_7\text{O}_2$ , 420.1954; found, 420.1960. HPLC (ACN with 0.1% TFA):  $t_{\text{R}} = 6.12$  min (95.5% purity). mp 115.2 °C.

5-(4-(3-Oxa-8-azabicyclo[3.2.1]octan-8-yl)-6-((R)-3-methylmorpholino)-1,3,5-triazin-2-yl)-4-(difluoromethyl)pyridin-2-amine (**19**) was prepared according to general procedure 1 from intermediate **43** (200 mg, 0.61 mmol, 1.0 equiv) and boronate **48** (259 mg, 0.80 mmol, 1.3 equiv). Purification by column chromatography on a silica gel (cyclohexane/ethyl acetate 1:0 → 0:1) gave compound **19** as a colorless solid (187 mg, 0.43 mmol, 71%).  $^1\text{H}$  NMR (400 MHz,  $\text{CDCl}_3$ ):  $\delta$  9.00 (s, 1H), 7.71 (t,  $J_{\text{H,F}} = 55.4$  Hz, 1H), 6.83 (s, 1H), 5.29 (br s, 2H), 4.77–4.63 (m, 3H), 4.41 (d,  $J_{\text{H,H}} = 13.7$  Hz, 1H), 3.97 (dd,  $J_{\text{H,H}} = 11.4$ , 3.7 Hz, 1H), 3.81–3.75 (m, 3H), 3.70–3.62 (m, 3H), 3.53 (td,  $J_{\text{H,H}} = 11.9$ , 3.0 Hz, 1H), 3.27 (td,  $J_{\text{H,H}} = 13.0$ , 3.8 Hz, 1H), 2.11–1.97 (m, 4H), 1.32 (d,  $J_{\text{H,H}} = 6.8$  Hz, 3H).  $^{19}\text{F}\{^1\text{H}\}$  NMR

(376 MHz, CDCl<sub>3</sub>):  $\delta$  -115.57–(-116.57) (m, 2F). <sup>13</sup>C{<sup>1</sup>H} NMR (101 MHz, CDCl<sub>3</sub>):  $\delta$  176.21 (s, 1C), 169.34 (s, 1C), 164.48 (s, 1C), 160.16 (s, 1C), 151.68 (s, 1C), 143.80 (t, <sup>2</sup>J<sub>C,F</sub> = 22.1 Hz, 1C), 121.22 (s, 1C), 111.31 (t, <sup>1</sup>J<sub>C,F</sub> = 238.8 Hz, 1C), 104.40 (t, <sup>3</sup>J<sub>C,F</sub> = 8.1 Hz, 1C), 71.91–71.84 (m, 1C), 71.57 (br s, 1C), 71.07 (s, 1C), 67.01 (s, 1C), 54.93 (br s, 1C), 54.55–54.48 (m, 1C), 46.34 (s, 1C), 38.52 (s, 1C), 26.97 (br s, 1C), 26.83 (br s, 1C), 14.27 (s, 1C). HRMS (*m/z*): [M + H]<sup>+</sup> calcd for C<sub>20</sub>H<sub>26</sub>F<sub>2</sub>N<sub>7</sub>O<sub>2</sub>, 434.2111; found, 434.2111. HPLC: *t*<sub>R</sub> = 8.29 min (98.6% purity). mp 106.1 °C.

5-(4-(8-Oxa-3-azabicyclo[3.2.1]octan-3-yl)-6-((*R*)-3-methylmorpholino)-1,3,5-triazin-2-yl)-4-(difluoromethyl)pyridin-2-amine (20) was prepared according to general procedure 1 from intermediate 44 (200 mg, 0.61 mmol, 1.0 equiv) and boronate 48 (259 mg, 0.80 mmol, 1.3 equiv). Purification by column chromatography on a silica gel (cyclohexane/ethyl acetate 1:0 → 0:1) gave compound 20 as a colorless solid (172 mg, 0.40 mmol, 65%). <sup>1</sup>H NMR (400 MHz, CDCl<sub>3</sub>):  $\delta$  9.00 (s, 1H), 7.70 (t, <sup>1</sup>J<sub>H,F</sub> = 55.3 Hz, 1H), 6.83 (s, 1H), 5.18 (br s, 2H), 4.77–4.68 (m, 1H), 4.48–4.27 (m, 5H), 3.97 (dd, *J*<sub>H,H</sub> = 11.4, 3.7 Hz, 1H), 3.77 (d, *J*<sub>H,H</sub> = 11.4 Hz, 1H), 3.68 (dd, *J*<sub>H,H</sub> = 11.5, 3.2 Hz, 1H), 3.53 (ddd, *J*<sub>H,H</sub> = 12.3, 11.4, 3.0 Hz, 1H), 3.31–3.14 (m, 3H), 1.95 (dd, *J*<sub>H,H</sub> = 7.8, 3.8 Hz, 2H), 1.81–1.73 (m, 2H), 1.32 (d, *J* = 6.8 Hz, 3H). <sup>19</sup>F{<sup>1</sup>H} NMR (376 MHz, CDCl<sub>3</sub>):  $\delta$  -115.52–(-117.61) (m, 2F). <sup>13</sup>C{<sup>1</sup>H} NMR (101 MHz, CDCl<sub>3</sub>):  $\delta$  168.90 (s, 1C), 165.73 (s, 1C), 164.20 (s, 1C), 160.11 (s, 1C), 151.86 (s, 1C), 143.72 (t, <sup>2</sup>J<sub>C,F</sub> = 22.1 Hz, 1C), 121.36 (t, <sup>3</sup>J<sub>C,F</sub> = 4.7 Hz, 1C), 111.30 (t, <sup>1</sup>J<sub>C,F</sub> = 238.8 Hz, 1C), 104.28 (t, <sup>3</sup>J<sub>C,F</sub> = 8.1 Hz, 1C), 73.89 (br s, 2C), 71.07 (s, 1C), 67.00 (s, 1C), 49.32 (s, 1C), 49.08 (s, 1C), 46.38 (s, 1C), 38.54 (s, 1C), 27.70 (s, 1C), 21.54 (s, 1C), 14.20 (s, 1C). HRMS (*m/z*): [M + H]<sup>+</sup> calcd for C<sub>20</sub>H<sub>26</sub>F<sub>2</sub>N<sub>7</sub>O<sub>2</sub>, 434.2111; found, 434.2118. HPLC: *t*<sub>R</sub> = 8.14 min (96.2% purity). mp 124.0 °C.

(*R*)-4-(Difluoromethyl)-5-(4-(3-methylmorpholino)-6-(2-oxa-6-azaspiro[3.3]heptan-6-yl)-1,3,5-triazin-2-yl)pyridin-2-amine (21) was prepared according to general procedure 1 from intermediate 45 (212 mg, 0.68 mmol, 1.0 equiv) and boronate 48 (222 mg, 0.68 mmol, 1.0 equiv). Purification by column chromatography on a silica gel (cyclohexane/ethyl acetate 1:0 → 0:1) gave compound 21 as a colorless solid (151 mg, 0.36 mmol, 53%). <sup>1</sup>H NMR (400 MHz, CDCl<sub>3</sub>):  $\delta$  9.04 (s, 1H), 7.78 (t, <sup>1</sup>J<sub>H,F</sub> = 55.4 Hz, 1H), 6.82 (s, 1H), 5.04 (br s, 2H), 4.84 (s, 4H), 4.79–4.72 (m, 1H), 4.44–4.38 (m, 1H), 4.29 (s, 4H), 3.97 (dd, *J*<sub>H,H</sub> = 11.4, 3.7 Hz, 1H), 3.76 (d, *J*<sub>H,H</sub> = 11.4 Hz, 1H), 3.66 (dd, *J*<sub>H,H</sub> = 11.5, 3.2 Hz, 1H), 3.51 (td, *J*<sub>H,H</sub> = 11.7, 3.0 Hz, 1H), 3.25 (td, *J*<sub>H,H</sub> = 13.0, 3.8 Hz, 1H), 1.31 (d, *J*<sub>H,H</sub> = 6.8 Hz, 3H). <sup>19</sup>F{<sup>1</sup>H} NMR (376 MHz, CDCl<sub>3</sub>):  $\delta$  -113.75–(-116.94) (m, 2F). <sup>13</sup>C{<sup>1</sup>H} NMR (101 MHz, CDCl<sub>3</sub>):  $\delta$  169.13 (s, 1C), 165.33 (s, 1C), 164.08 (s, 1C), 160.26 (s, 1C), 152.33 (s, 1C), 143.69 (t, <sup>2</sup>J<sub>C,F</sub> = 22.1 Hz, 1C), 120.96 (s, 1C), 111.38 (t, <sup>1</sup>J<sub>C,F</sub> = 238.7 Hz, 1C), 104.02 (t, <sup>3</sup>J<sub>C,F</sub> = 8.1 Hz, 1C), 81.05 (s, 2C), 71.02 (s, 1C), 66.98 (s, 1C), 58.89 (s, 2C), 46.29 (s, 1C), 38.81 (s, 1C), 38.46 (s, 1C), 14.27 (s, 1C). HRMS (*m/z*): [M + H]<sup>+</sup> calcd for C<sub>19</sub>H<sub>24</sub>F<sub>2</sub>N<sub>7</sub>O<sub>2</sub>, 420.1954; found, 420.1957. HPLC (ACN with 0.1% TFA): *t*<sub>R</sub> = 5.89 min (97.8% purity). mp 174.9 °C.

(*R*)-4-(Difluoromethyl)-5-(4-(3-methylmorpholino)-6-(1,4-oxazepan-4-yl)-1,3,5-triazin-2-yl)pyridin-2-amine (22) was prepared according to general procedure 1 from intermediate 46 (252 mg, 0.81 mmol, 1.0 equiv) and boronate 48 (262 mg, 0.81 mmol, 1.0 equiv). Purification by column chromatography on a silica gel (cyclohexane/ethyl acetate 1:0 → 0:1) gave compound 22 as a colorless solid (145 mg, 0.34 mmol, 43%). <sup>1</sup>H NMR (400 MHz, CDCl<sub>3</sub>):  $\delta$  9.08/9.05 (2 × s, 1H), 7.76/7.70 (2 × t, <sup>1</sup>J<sub>H,F</sub> = 55.4 Hz, 1H), 6.83 (s, 1H), 4.99 (br s, 2H), 4.78–4.69 (m, 1H), 4.45–4.36 (m, 1H), 4.01–3.66 (m, 11H), 3.58–3.49 (m, 1H), 3.32–3.22 (m, 1H), 2.04–1.96 (m, 2H), 1.32 (d, *J*<sub>H,H</sub> = 6.1 Hz, 3H). <sup>19</sup>F{<sup>1</sup>H} NMR (376 MHz, CDCl<sub>3</sub>):  $\delta$  -115.59–(-117.25) (m, 2F). <sup>13</sup>C{<sup>1</sup>H} NMR (101 MHz, CDCl<sub>3</sub>):  $\delta$  169.11/168.99 (2 × s, 1C), 164.63 (s, 1C), 164.43/164.32 (2 × s, 1C), 160.11 (s, 1C), 152.39/152.34 (2 × s, 1C), 143.58/143.52 (2 × t, <sup>2</sup>J<sub>C,F</sub> = 22.2 Hz, 1C), 121.51 (t, <sup>3</sup>J<sub>C,F</sub> = 4.8 Hz, 1C), 111.39 (t, <sup>1</sup>J<sub>C,F</sub> = 238.8 Hz, 1C), 103.94 (t, <sup>3</sup>J<sub>C,F</sub> = 7.9 Hz, 1C), 71.08 (s, 1C), 70.90 (s, 1C), 70.14–70.06 (m, 1C), 67.02 (s, 1C), 49.51/49.21 (2 × s, 1C), 46.35 (s, 1C), 45.27/45.25 (2 × s, 1C), 38.52 (s, 1C), 29.54/28.93 (2 × s, 1C), 14.22 (s, 1C). HRMS (*m/z*): [M + H]<sup>+</sup> calcd for

C<sub>19</sub>H<sub>26</sub>F<sub>2</sub>N<sub>7</sub>O<sub>2</sub>, 422.2111; found, 422.2117. HPLC: *t*<sub>R</sub> = 8.06 min (99.2% purity). mp 157.5 °C.

4-(4,6-Dichloro-1,3,5-triazin-2-yl)morpholine (23). Compound 23 was prepared according to the literature.<sup>29</sup>

(*R*)-4-(4-Chloro-6-morpholino-1,3,5-triazin-2-yl)-3-methylmorpholine (24). Compound 24 was prepared according to the literature.<sup>26</sup>

(3*R*,3'*R*)-4,4'-(6-Chloro-1,3,5-triazine-2,4-diyl)bis(3-methylmorpholine) (25). Compound 25 was prepared according to the literature.<sup>26</sup>

(*R*)-4-(4,6-Dichloro-1,3,5-triazin-2-yl)-3-methylmorpholine (26). Compound 26 was prepared according to the literature.<sup>35</sup>

(*S*)-4-(4-Chloro-6-((*R*)-3-methylmorpholino)-1,3,5-triazin-2-yl)-3-methylmorpholine (27). Compound 27 was prepared according to the literature.<sup>35</sup>

(*R*)-4-(4-Chloro-6-(3-methylmorpholino)-1,3,5-triazin-2-yl)-3,3-dimethylmorpholine (28). Compound 28 was prepared according to general procedure 2 from 3,3-dimethylmorpholine hydrochloride (192 mg, 1.27 mmol, 1.05 equiv) and compound 26 (300 mg, 1.20 mmol, 1.0 equiv). Purification by column chromatography on a silica gel (cyclohexane/ethyl acetate 1:0 → 0:1) gave compound 28 as a colorless solid (189 mg, 0.58 mmol, 48%). <sup>1</sup>H NMR (400 MHz, DMSO-*d*<sub>6</sub>):  $\delta$  4.53–4.45 (m, 1H), 4.15 (dd, *J*<sub>H,H</sub> = 13.8, 2.7 Hz, 1H), 3.93–3.86 (m, 1H), 3.80–3.73 (m, 4H), 3.73–3.65 (m, 1H), 3.57–3.52 (m, 1H), 3.46–3.42 (m, 2H), 3.44–3.34 (m, 1H), 3.23–3.13 (m, 1H), 1.44 (s, 6H), 1.21 (d, *J*<sub>H,H</sub> = 6.8 Hz, 3H). MALDI-MS: *m/z* 328.896 [M + H]<sup>+</sup>.

(*R*)-5-(4-Chloro-6-(3-methylmorpholino)-1,3,5-triazin-2-yl)-8-oxa-5-azaspiro[3.5]nonane (29). Compound 29 was prepared according to general procedure 2 from 8-oxa-5-azaspiro[3.5]nonane (161 mg, 1.27 mmol, 1.05 equiv) and compound 26 (300 mg, 1.20 mmol, 1.0 equiv). Purification by column chromatography on a silica gel (cyclohexane/ethyl acetate 1:0 → 0:1) gave compound 29 as a colorless solid (249 mg, 0.73 mmol, 61%). <sup>1</sup>H NMR (400 MHz, DMSO-*d*<sub>6</sub>):  $\delta$  4.454–4.35 (m, 1H), 4.17–4.07 (m, 1H), 3.87 (dd, *J*<sub>H,H</sub> = 11.5, 3.7 Hz, 1H), 3.73–3.61 (m, 5H), 3.56–3.45 (m, 3H), 3.41–3.35 (m, 1H), 3.19–3.10 (m, 1H), 2.49–2.40 (m, 2H), 2.25–2.16 (m, 2H), 1.75–1.65 (m, 2H), 1.19 (d, *J*<sub>H,H</sub> = 6.8 Hz, 3H). MALDI-MS: *m/z* 340.577 [M + H]<sup>+</sup>.

(3*R*,5*R*)-4-(4-Chloro-6-((*R*)-3-methylmorpholino)-1,3,5-triazin-2-yl)-3,5-dimethylmorpholine (30). Compound 30 was prepared according to general procedure 3 from (3*R*,5*R*)-3,5-dimethylmorpholine (193 mg, 1.27 mmol, 1.05 equiv) and compound 26 (300 mg, 1.20 mmol, 1.0 equiv). Purification by column chromatography on a silica gel (cyclohexane/ethyl acetate 1:0 → 0:1) gave compound 30 as a colorless solid (267 mg, 0.81 mmol, 68%). <sup>1</sup>H NMR (400 MHz, DMSO-*d*<sub>6</sub>):  $\delta$  4.56–4.49 (m, 1H), 4.27–4.17 (m, 3H), 4.09 (dd, *J*<sub>H,H</sub> = 11.4, 3.3 Hz, 2H), 3.88 (dd, *J*<sub>H,H</sub> = 11.6, 3.6 Hz, 1H), 3.72–3.62 (m, 3H), 3.53 (d, *J*<sub>H,H</sub> = 11.7 Hz, 1H), 3.38 (td, *J*<sub>H,H</sub> = 12.0, 3.0 Hz, 1H), 3.17 (td, *J*<sub>H,H</sub> = 13.0, 3.9 Hz, 1H), 1.33 (d, *J*<sub>H,H</sub> = 6.7 Hz, 6H), 1.21 (d, *J*<sub>H,H</sub> = 6.8 Hz, 3H). MALDI-MS: *m/z* 328.675 [M + H]<sup>+</sup>.

(3*S*,5*S*)-4-(4-Chloro-6-((*R*)-3-methylmorpholino)-1,3,5-triazin-2-yl)-3,5-dimethylmorpholine (31). Compound 31 was prepared according to general procedure 3 from (3*S*,5*S*)-3,5-dimethylmorpholine (193 mg, 1.27 mmol, 1.05 equiv) and compound 26 (300 mg, 1.20 mmol, 1.0 equiv). Purification by column chromatography on a silica gel (cyclohexane/ethyl acetate 1:0 → 0:1) gave compound 31 as a colorless solid (244 mg, 0.74 mmol, 62%). <sup>1</sup>H NMR (400 MHz, DMSO-*d*<sub>6</sub>):  $\delta$  4.60–4.50 (m, 1H), 4.26–4.13 (m, 3H), 4.09 (dd, *J*<sub>H,H</sub> = 11.4, 3.4 Hz, 2H), 3.89 (d, *J*<sub>H,H</sub> = 11.2 Hz, 1H), 3.73–3.66 (m, 1H), 3.65 (dd, *J*<sub>H,H</sub> = 11.4, 2.2 Hz, 2H), 3.53 (dd, *J*<sub>H,H</sub> = 11.6, 3.3 Hz, 1H), 3.43–3.33 (m, 1H), 3.22–3.12 (m, 1H), 1.33 (d, *J*<sub>H,H</sub> = 6.6 Hz, 6H), 1.21 (d, *J*<sub>H,H</sub> = 6.8 Hz, 3H). MALDI-MS: *m/z* 328.692 [M + H]<sup>+</sup>.

(3*R*,5*S*)-4-(4-Chloro-6-((*R*)-3-methylmorpholino)-1,3,5-triazin-2-yl)-3,5-dimethylmorpholine (32). Compound 32 was prepared according to general procedure 2 from (*R*)-3-methylmorpholine (86 mg, 0.85 mmol, 1.05 equiv) and compound 47 (214 mg, 0.81 mmol, 1.0 equiv). Purification by column chromatography on a silica gel (cyclohexane/ethyl acetate 1:0 → 0:1) gave compound 32 as a colorless solid (232 mg, 0.71 mmol, 87%). <sup>1</sup>H NMR (400 MHz,



DMSO- $d_6$ ):  $\delta$  4.57–4.50 (m, 1H), 4.44–4.35 (m, 2H), 4.27–4.12 (m, 1H), 3.88 (dd,  $J_{\text{H,H}} = 11.6, 3.6$  Hz, 1H), 3.76–3.65 (m, 3H), 3.56–3.50 (m, 3H), 3.38 (td,  $J_{\text{H,H}} = 11.9, 3.0$  Hz, 1H), 3.21–3.12 (m, 1H), 1.25 (d,  $J_{\text{H,H}} = 6.8$  Hz, 6H), 1.21 (d,  $J_{\text{H,H}} = 6.8$  Hz, 3H). MALDI-MS:  $m/z$  328.828 [M + H] $^+$ .

(2*S*,6*R*)-4-(4-Chloro-6-((*R*)-3-methylmorpholino)-1,3,5-triazin-2-yl)-2,6-dimethylmorpholine (33). Compound 33 was prepared according to general procedure 4 from (2*S*,6*R*)-2,6-dimethylmorpholine (145 mg, 1.27 mmol, 1.05 equiv) and compound 26 (300 mg, 1.20 mmol, 1.0 equiv). Purification by column chromatography on a silica gel (cyclohexane/ethyl acetate 1:0  $\rightarrow$  0:1) gave compound 33 as a colorless solid (220 mg, 0.67 mmol, 56%).  $^1\text{H}$  NMR (400 MHz, DMSO- $d_6$ ):  $\delta$  4.64–4.48 (m, 1H), 4.47–4.32 (m, 2H), 4.30–4.12 (m, 1H), 3.88 (dd,  $J_{\text{H,H}} = 11.6, 3.7$  Hz, 1H), 3.68 (d,  $J_{\text{H,H}} = 11.5$  Hz, 1H), 3.58–3.46 (m, 3H), 3.41–3.33 (m, 1H), 3.16 (td,  $J_{\text{H,H}} = 13.1, 3.8$  Hz, 1H), 2.60–2.51 (m, 2H), 1.20 (d,  $J_{\text{H,H}} = 6.8$  Hz, 3H), 1.13 (d,  $J_{\text{H,H}} = 6.2$  Hz, 6H). MALDI-MS:  $m/z$  328.788 [M + H] $^+$ .

(*R*)-4-(4-Chloro-6-((*R*)-3-ethylmorpholino)-1,3,5-triazin-2-yl)-3-methylmorpholine (34). Compound 34 was prepared according to general procedure 2 from (*R*)-3-ethylmorpholine hydrochloride (193 mg, 1.27 mmol, 1.05 equiv) and compound 26 (300 mg, 1.20 mmol, 1.0 equiv). Purification by column chromatography on a silica gel (cyclohexane/ethyl acetate 1:0  $\rightarrow$  0:1) gave compound 34 as a colorless solid (317 mg, 0.97 mmol, 81%).  $^1\text{H}$  NMR (400 MHz, DMSO- $d_6$ ):  $\delta$  4.60–4.47 (m, 1H), 4.46–4.10 (m, 3H), 3.92–3.80 (m, 2H), 3.77 (d,  $J_{\text{H,H}} = 11.7$  Hz, 1H), 3.71–3.62 (m, 1H), 3.57–3.43 (m, 2H), 3.41–3.31 (m, 2H), 3.21–3.08 (m, 2H), 1.80–1.65 (m, 2H), 1.19 (d,  $J_{\text{H,H}} = 6.8$  Hz, 3H), 0.87–0.78 (m, 3H). MALDI-MS:  $m/z$  328.709 [M + H] $^+$ .

(*S*)-4-(4-Chloro-6-((*R*)-3-methylmorpholino)-1,3,5-triazin-2-yl)-3-ethylmorpholine (35). Compound 35 was prepared according to general procedure 2 from (*S*)-3-ethylmorpholine hydrochloride (191 mg, 1.27 mmol, 1.05 equiv) and compound 26 (300 mg, 1.20 mmol, 1.0 equiv). Purification by column chromatography on a silica gel (cyclohexane/ethyl acetate 1:0  $\rightarrow$  0:1) gave compound 35 as a colorless solid (345 mg, 1.06 mmol, 88%).  $^1\text{H}$  NMR (400 MHz, DMSO- $d_6$ ):  $\delta$  4.59–4.47 (m, 1H), 4.46–4.10 (m, 3H), 3.91–3.80 (m, 2H), 3.77 (d,  $J_{\text{H,H}} = 11.7$  Hz, 1H), 3.71–3.63 (m, 1H), 3.57–3.43 (m, 2H), 3.41–3.31 (m, 2H), 3.21–3.07 (m, 2H), 1.80–1.65 (m, 2H), 1.19 (d,  $J_{\text{H,H}} = 6.8$  Hz, 3H), 0.88–0.77 (m, 3H). MALDI-MS:  $m/z$  328.635 [M + H] $^+$ .

(*R*)-4-(4-Chloro-6-((*R*)-3-methylmorpholino)-1,3,5-triazin-2-yl)-morpholin-3-yl)methanol (36). Compound 36 was prepared according to general procedure 2 from (*R*)-morpholin-3-ylmethanol hydrochloride (195 mg, 1.27 mmol, 1.05 equiv) and compound 26 (300 mg, 1.20 mmol, 1.0 equiv). Purification by column chromatography on a silica gel (cyclohexane/ethyl acetate 1:0  $\rightarrow$  0:1) gave compound 36 as a colorless solid (338 mg, 1.03 mmol, 86%).  $^1\text{H}$  NMR (400 MHz, DMSO- $d_6$ ):  $\delta$  4.97–4.84 (m, 1H), 4.64–4.47 (m, 1H), 4.43–4.11 (m, 3H), 4.01–3.94 (m, 1H), 3.91–3.80 (m, 2H), 3.75–3.62 (m, 2H), 3.56–3.49 (m, 1H), 3.48–3.32 (m, 4H), 3.22–3.04 (m, 2H), 1.20 (d,  $J_{\text{H,H}} = 7.3$  Hz, 3H). MALDI-MS:  $m/z$  330.797 [M + H] $^+$ .

(*S*)-4-(4-Chloro-6-((*R*)-3-methylmorpholino)-1,3,5-triazin-2-yl)-morpholin-3-yl)methanol (37). Compound 37 was prepared according to general procedure 2 from (*S*)-morpholin-3-ylmethanol hydrochloride (124 mg, 1.05 mmol, 1.05 equiv) and compound 26 (250 mg, 1.00 mmol, 1.0 equiv). Purification by column chromatography on a silica gel (cyclohexane/ethyl acetate 1:0  $\rightarrow$  0:1) gave compound 37 as a colorless solid (253 mg, 0.77 mmol, 77%).  $^1\text{H}$  NMR (400 MHz, DMSO- $d_6$ ):  $\delta$  4.97–4.84 (m, 1H), 4.60–4.46 (m, 1H), 4.45–4.32 (m, 1H), 4.30–4.11 (m, 2H), 3.98 (d,  $J_{\text{H,H}} = 11.5$  Hz, 1H), 3.93–3.81 (m, 2H), 3.73–3.63 (m, 2H), 3.57–3.49 (m, 1H), 3.48–3.35 (m, 4H), 3.21–3.04 (m, 2H), 1.20 (d,  $J_{\text{H,H}} = 6.8$  Hz, 3H). MALDI-MS:  $m/z$  330.661 [M + H] $^+$ .

(*R*)-4-(4-Chloro-6-((*R*)-3-(methoxymethyl)morpholino)-1,3,5-triazin-2-yl)-3-methylmorpholine (38). Compound 38 was prepared according to general procedure 2 from (*R*)-3-(methoxymethyl)morpholine hydrochloride (224 mg, 1.27 mmol, 1.05 equiv) and compound 26 (300 mg, 1.20 mmol, 1.0 equiv). Purification by

column chromatography on a silica gel (cyclohexane/ethyl acetate 1:0  $\rightarrow$  0:1) gave compound 38 as a colorless solid (309 mg, 0.90 mmol, 75%).  $^1\text{H}$  NMR (400 MHz, DMSO- $d_6$ ):  $\delta$  4.65–4.49 (m, 2H), 4.33–4.13 (m, 2H), 3.92–3.81 (m, 3H), 3.71–3.56 (m, 2H), 3.55–3.44 (m, 3H), 3.43–3.34 (m, 2H), 3.28 (s, 3H), 3.21–3.08 (m, 2H), 1.21 (d,  $J_{\text{H,H}} = 6.9$  Hz, 3H). MALDI-MS:  $m/z$  344.159 [M + H] $^+$ .

6-(4-Chloro-6-((*R*)-3-methylmorpholino)-1,3,5-triazin-2-yl)-3-oxa-6-azabicyclo[3.1.1]heptane (39). Compound 39 was prepared according to general procedure 2 from 3-oxa-6-azabicyclo[3.1.1]heptane (344 mg, 1.27 mmol, 1.05 equiv) and compound 26 (300 mg, 1.20 mmol, 1.0 equiv). Purification by column chromatography on a silica gel (cyclohexane/ethyl acetate 1:0  $\rightarrow$  0:1) gave compound 39 as a colorless solid (228 mg, 0.73 mmol, 61%).  $^1\text{H}$  NMR (400 MHz, DMSO- $d_6$ ):  $\delta$  4.57–4.49 (m, 1H), 4.41–4.34 (m, 2H), 4.24–4.11 (m, 2H), 4.04 (d,  $J_{\text{H,H}} = 10.1$  Hz, 1H), 3.87 (dd,  $J_{\text{H,H}} = 11.6, 3.7$  Hz, 1H), 3.79–3.72 (m, 2H), 3.67 (d,  $J_{\text{H,H}} = 11.5$  Hz, 1H), 3.53 (dd,  $J_{\text{H,H}} = 11.3, 2.9$  Hz, 1H), 3.42–3.33 (m, 1H), 3.21–3.12 (m, 1H), 2.67 (q,  $J_{\text{H,H}} = 6.9$  Hz, 1H), 1.81 (d,  $J_{\text{H,H}} = 8.3$  Hz, 1H), 1.20 (d,  $J_{\text{H,H}} = 6.9$  Hz, 3H). MALDI-MS:  $m/z$  312.708 [M + H] $^+$ .

3-(4-Chloro-6-((*R*)-3-methylmorpholino)-1,3,5-triazin-2-yl)-6-oxa-3-azabicyclo[3.1.1]heptane (40). Compound 40 was prepared according to general procedure 2 from 6-oxa-3-azabicyclo[3.1.1]heptane (344 mg, 1.27 mmol, 1.05 equiv) and compound 26 (300 mg, 1.20 mmol, 1.0 equiv). Purification by column chromatography on a silica gel (cyclohexane/ethyl acetate 1:0  $\rightarrow$  0:1) gave compound 40 as a colorless solid (230 mg, 0.74 mmol, 62%).  $^1\text{H}$  NMR (400 MHz, DMSO- $d_6$ ):  $\delta$  4.69–4.52 (m, 3H), 4.34–4.15 (m, 1H), 3.93–3.79 (m, 3H), 3.73–3.50 (m, 4H), 3.43–3.34 (m, 1H), 3.24–3.14 (m, 1H), 3.14–3.07 (m, 1H), 1.81 (d,  $J_{\text{H,H}} = 9.0$  Hz, 1H), 1.22 (d,  $J_{\text{H,H}} = 6.9$  Hz, 3H). MALDI-MS:  $m/z$  312.749 [M + H] $^+$ .

(1*R*,4*R*)-5-(4-Chloro-6-((*R*)-3-methylmorpholino)-1,3,5-triazin-2-yl)-2-oxa-5-azabicyclo[2.2.1]heptane (41). Compound 41 was prepared according to general procedure 2 from (1*R*,4*R*)-2-oxa-5-azabicyclo[2.2.1]heptane (171 mg, 1.27 mmol, 1.05 equiv) and compound 26 (300 mg, 1.20 mmol, 1.0 equiv). Purification by column chromatography on a silica gel (cyclohexane/ethyl acetate 1:0  $\rightarrow$  0:1) gave compound 41 as a colorless solid (268 mg, 0.87 mmol, 72%).  $^1\text{H}$  NMR (400 MHz, DMSO- $d_6$ ):  $\delta$  4.95–4.87 (m, 1H), 4.69–4.63 (m, 1H), 4.63–4.49 (m, 1H), 4.29–4.13 (m, 1H), 3.88 (dd,  $J_{\text{H,H}} = 11.5, 3.6$  Hz, 1H), 3.79–3.74 (m, 1H), 3.72–3.63 (m, 2H), 3.57–3.49 (m, 1H), 3.46–3.33 (m, 3H), 3.22–3.11 (m, 1H), 1.92–1.80 (m, 2H), 1.20 (d,  $J_{\text{H,H}} = 6.8$  Hz, 3H). MALDI-MS:  $m/z$  312.199 [M + H] $^+$ .

(1*S*,4*S*)-5-(4-Chloro-6-((*R*)-3-methylmorpholino)-1,3,5-triazin-2-yl)-2-oxa-5-azabicyclo[2.2.1]heptane (42). Compound 42 was prepared according to general procedure 2 from (1*S*,4*S*)-2-oxa-5-azabicyclo[2.2.1]heptane (171 mg, 1.27 mmol, 1.05 equiv) and compound 26 (300 mg, 1.20 mmol, 1.0 equiv). Purification by column chromatography on a silica gel (cyclohexane/ethyl acetate 1:0  $\rightarrow$  0:1) gave compound 42 as a colorless solid (271 mg, 0.87 mmol, 73%).  $^1\text{H}$  NMR (400 MHz, DMSO- $d_6$ ):  $\delta$  4.99–4.86 (m, 1H), 4.66–4.51 (m, 2H), 4.34–4.11 (m, 1H), 3.92–3.84 (dd,  $J_{\text{H,H}} = 11.3, 3.7$  Hz, 1H), 3.76 (dd,  $J_{\text{H,H}} = 7.4, 1.6$  Hz, 1H), 3.71–3.63 (m, 2H), 3.55–3.48 (m, 1H), 3.45–3.33 (m, 3H), 3.21–3.11 (m, 1H), 1.92–1.83 (m, 2H), 1.21 (d,  $J_{\text{H,H}} = 7.0$  Hz, 3H). MALDI-MS:  $m/z$  312.216 [M + H] $^+$ .

8-(4-Chloro-6-((*R*)-3-methylmorpholino)-1,3,5-triazin-2-yl)-3-oxa-8-azabicyclo[3.2.1]octane (43). Compound 43 was prepared according to general procedure 2 from 3-oxa-8-azabicyclo[3.2.1]octane hydrochloride (439 mg, 2.94 mmol, 1.05 equiv) and compound 26 (700 mg, 2.80 mmol, 1.0 equiv). Purification by column chromatography on a silica gel (cyclohexane/ethyl acetate 1:0  $\rightarrow$  0:1) gave compound 43 as a colorless solid (672 mg, 2.06 mmol, 74%).  $^1\text{H}$  NMR (400 MHz, CDCl $_3$ ):  $\delta$  4.71–4.57 (m, 3H), 4.36–4.28 (m, 1H), 3.93 (dd,  $J_{\text{H,H}} = 11.5, 3.8$  Hz, 1H), 3.75–3.70 (m, 3H), 3.66–3.61 (m, 3H), 3.48 (td,  $J_{\text{H,H}} = 11.9, 3.0$  Hz, 1H), 3.24 (td,  $J_{\text{H,H}} = 13.0, 3.8$  Hz, 1H), 2.09–1.93 (m, 4H), 1.30 (d,  $J_{\text{H,H}} = 6.9$  Hz, 3H). MALDI-MS:  $m/z$  326.645 [M + H] $^+$ .

3-(4-Chloro-6-((*R*)-3-methylmorpholino)-1,3,5-triazin-2-yl)-8-oxa-3-azabicyclo[3.2.1]octane (44). Compound 44 was prepared



according to general procedure 2 from 8-oxa-3-azabicyclo[3.2.1]-octane hydrochloride (253 mg, 2.23 mmol, 1.05 equiv) and compound 26 (500 mg, 2.03 mmol, 1.0 equiv). Purification by column chromatography on a silica gel (cyclohexane/ethyl acetate 1:0 → 0:1) gave compound 44 as a colorless solid (504 mg, 1.55 mmol, 76%). <sup>1</sup>H NMR (400 MHz, CDCl<sub>3</sub>): δ 4.73–4.59 (m, 1H), 4.43–4.38 (m, 2H), 4.34–4.18 (m, 3H), 3.93 (dd, *J*<sub>H,H</sub> = 11.5, 3.7 Hz, 1H), 3.73 (d, *J*<sub>H,H</sub> = 11.5 Hz, 1H), 3.63 (dd, *J*<sub>H,H</sub> = 11.5, 3.2 Hz, 1H), 3.48 (td, *J*<sub>H,H</sub> = 11.9, 3.0 Hz, 1H), 3.26 (dd, *J*<sub>H,H</sub> = 13.2, 3.8 Hz, 1H), 3.22–3.12 (m, 2H), 1.99–1.88 (m, 2H), 1.84–1.68 (m, 2H), 1.30 (d, *J*<sub>H,H</sub> = 7.1 Hz, 3H). MALDI-MS: *m/z* 326.679 [M + H]<sup>+</sup>.

(*R*)-6-(4-Chloro-6-(3-methylmorpholino)-1,3,5-triazin-2-yl)-2-oxa-6-azaspiro[3.3]heptane (45). Compound 45 was prepared according to general procedure 2 from 2-oxa-6-azaspiro[3.3]heptane oxalate (2:1, 183 mg, 1.27 mmol, 1.05 equiv) and compound 26 (300 mg, 1.21 mmol, 1.0 equiv). Purification by column chromatography on a silica gel (cyclohexane/ethyl acetate 1:0 → 0:1) gave compound 45 as a colorless solid (212 mg, 0.68 mmol, 57%). <sup>1</sup>H NMR (400 MHz, DMSO-*d*<sub>6</sub>): δ 4.69 (br s, 4H), 4.57–4.49 (m, 1H), 4.24–4.11 (m, 5H), 3.88 (d, *J*<sub>H,H</sub> = 9.8 Hz, 1H), 3.67 (d, *J*<sub>H,H</sub> = 11.6 Hz, 1H), 3.50 (dd, *J*<sub>H,H</sub> = 11.6, 3.2 Hz, 1H), 3.39–3.32 (m, 1H), 3.15 (ddd, *J*<sub>H,H</sub> = 13.7, 12.3, 3.9 Hz, 1H), 1.19 (d, *J*<sub>H,H</sub> = 6.9 Hz, 3H). MALDI-MS: *m/z* 312.598 [M + H]<sup>+</sup>.

(*R*)-4-(4-Chloro-6-(3-methylmorpholino)-1,3,5-triazin-2-yl)-1,4-oxazepane (46). Compound 46 was prepared according to general procedure 2 from 1,4-oxazepane (128 mg, 1.27 mmol, 1.05 equiv) and compound 26 (300 mg, 1.21 mmol, 1.0 equiv). Purification by column chromatography on a silica gel (cyclohexane/ethyl acetate 1:0 → 0:1) gave compound 46 as a colorless solid (252 mg, 0.81 mmol, 67%). <sup>1</sup>H NMR (400 MHz, DMSO-*d*<sub>6</sub>): δ 4.59–4.50 (m, 1H), 4.30–4.11 (m, 1H), 3.92–3.85 (m, 1H), 3.86–3.59 (m, 8H), 3.56–3.49 (m, 1H), 3.42–3.35 (m, 1H), 3.21–3.11 (m, 2H), 1.88–1.76 (m, 2H), 1.23–1.18 (m, 3H). MALDI-MS: *m/z* 314.342 [M + H]<sup>+</sup>.

(3*R*,5*S*)-4-(4,6-Dichloro-1,3,5-triazin-2-yl)-3,5-dimethylmorpholine (47). To a solution of cyanuric chloride (479 mg, 2.60 mmol, 1.0 equiv) in DCM (10 mL) at –50 °C, a solution of (3*R*,5*S*)-3,5-dimethylmorpholine (300 mg, 2.60 mmol, 1.0 equiv) and DIPEA (1 mL, 742 mg, 5.75 mmol, 2.1 equiv) in DCM (5 mL) was added dropwise over 20 min. The mixture was stirred at –50 °C for 2 h. After completion of the reaction monitored by TLC, the mixture was washed with NaHSO<sub>4</sub>, the organic layer was separated, dried over Na<sub>2</sub>S<sub>2</sub>O<sub>4</sub>, filtered, and concentrated under reduced pressure. Recrystallization from dichloromethane/heptanes gave compound 47 as a colorless solid (423 mg, 1.60 mmol, 62%). <sup>1</sup>H NMR (400 MHz, CDCl<sub>3</sub>): δ 4.55 (qd, *J*<sub>H,H</sub> = 7.0, 3.8 Hz, 2H), 3.84 (d, *J*<sub>H,H</sub> = 11.8 Hz, 2H), 3.63 (dd, *J*<sub>H,H</sub> = 11.7, 3.9 Hz, 2H), 1.41 (dd, *J*<sub>H,H</sub> = 7.1, 0.7 Hz, 3H).

*N*'-[4-(Difluoromethyl)-5-(4,4,5,5-tetramethyl-1,3,2-dioxaborolan-2-yl)pyridin-2-yl]-*N,N*-dimethylmethanimidamide (48). Compound 48 was prepared according to the literature.<sup>35,54</sup>

#### Structure Modeling of PI3K and mTOR Kinase Complexes.

The coordinates of mTOR kinase bound to PI103 (PDB code 4JT6; 3.6 Å) and PQR530 in PI3K $\alpha$  complex (PDB code 6OAC, resolution of 3.15 Å) were used as starting points for docking the molecules into the kinase ATP-binding site. Compounds were manually replaced/modified in crystal structures using Maestro 11.1, and energy minimization of the resulting protein-inhibitor complex was carried out. Measurements and figures were generated using Maestro Schrödinger 11.1 and Chimera UCSF.

**Determination of Inhibitor Dissociation Constants.** The library's dissociation constants (*K*<sub>d</sub>) for p110 $\alpha$  and mTOR were determined using a commercial LanthaScreen (Life Technologies) assay. The assays were performed as described in ref 30, and data analysis was carried out as previously reported in ref 29. Briefly, AlexaFluor647-labeled Kinase Tracer314 (#PV6087) with a *K*<sub>d</sub> of 2.2 nM was used at 20 nM for p110 $\alpha$  and at a final concentration of 10 nM for mTOR (*K*<sub>d</sub> of 19 nM; modifications see Table S1). Recombinant N-terminally (His)<sub>6</sub>-tagged p110 $\alpha$  was captured with biotinylated anti-(His)<sub>6</sub>-tag antibody (2 nM, #PV6089) and detected with LanthaScreen Eu-streptavidin (2 nM, #PV5899); N-terminal

GST fused to truncated mTOR (amino acids 1360–2549; #PR8683B) was detected with a LanthaScreen Eu-labeled anti-GST antibody (2 nM, #PV5594). The p110 $\alpha$  assay buffer was composed of 50 mM HEPES pH 7.5, 10 mM MgCl<sub>2</sub>, 1 mM EGTA, and 0.01% (v/v) Brij-35, and the mTOR assay buffer contained 50 mM HEPES; 5 mM MgCl<sub>2</sub>; 1 mM EGTA; 0.01% Pluronic F-127. IC<sub>50</sub>s were measured using a 10-point 1:4 serial dilution. Values at each concentration were determined in independent duplicate experiments.

**Kinome Profiling.** Compounds' binding affinity and selectivity were determined using the ScanMax platform of DiscoverX.<sup>55</sup> Experiments were performed at DiscoverX, 11180 Roselle Street, Suite D, San Diego, using an automated and standardized *in vitro* assay. Inhibitor binding constants (*K*<sub>d</sub> values) were calculated from duplicate 11-point dose–response curves. As described in the standard DiscoverX protocol, kinase-tagged T7 phage strains were grown in parallel in 24-well blocks in an *Escherichia coli* host derived from the BL21 strain. *E. coli* were grown to log-phase and infected with T7 phage from a frozen stock (multiplicity of infection = 0.4) and incubated with shaking at 32 °C until lysis (90–150 min). The lysates were centrifuged (6000g) and filtered (0.2  $\mu$ m) to remove cell debris. The remaining kinases were produced in HEK-293 cells and subsequently tagged with DNA for qPCR detection. Streptavidin-coated magnetic beads were treated with biotinylated small-molecule ligands for 30 min at room temperature to generate affinity resins for kinase assays. The liganded beads were blocked with excess biotin and washed with a blocking buffer [SeaBlock (Pierce), 1% BSA, 0.05% Tween 20, 1 mM DTT] to remove unbound ligand and to reduce nonspecific phage binding. Binding reactions were assembled by combining kinases, liganded affinity beads, and test compounds in 1 $\times$  binding buffer (20% SeaBlock, 0.17 $\times$  PBS, 0.05% Tween 20, 6 mM DTT). Test compounds were prepared as 40 $\times$  stocks in 100% DMSO and directly diluted into the assay. All reactions were performed in polypropylene 384-well plates in a final volume of 0.02 mL. The assay plates were incubated at room temperature with shaking for 1 h, and the affinity beads were washed with a wash buffer (1 $\times$  PBS, 0.05% Tween 20). The beads were then resuspended in an elution buffer (1 $\times$  PBS, 0.05% Tween 20, 0.5  $\mu$ M non-biotinylated affinity ligand) and incubated at room temperature with shaking for 30 min. The kinase concentration in the eluates was measured by qPCR. Binding of the immobilized ligand to DNA-tagged kinases was competed with 10  $\mu$ M compound. The amount of kinase bound to the immobilized ligand was measured by quantitative PCR of the respective DNA tags and was reported as % of control. The compounds' binding constants for selected kinases were determined by competing the immobilized ligand kinase interactions with an 11-point threefold serial dilution of compound starting from 30  $\mu$ M and subsequent quantitative PCR of DNA tags. Binding constants were calculated by a standard dose–response curve using the Hill equation (with Hill slope set to –1)

$$\text{response} = \text{background} + (\text{signal-background})$$

$$/(1 + 10^{([\text{lg } K_d - \text{lg dose}] * \text{Hill slope})})$$

Selectivity scores<sup>44</sup> were calculated as reported below

$$S = \text{number of hits/number of tested kinases} \\ (\text{excluding mutant variants})$$

where S35, S10, and S1 were calculated using % Ctrl as a potency threshold (35, 10, 1%); for example, S(35) = (number of nonmutant kinases with % Ctrl < 35)/(number of nonmutant kinases tested).

**Cellular PI3K and mTOR Signaling.** In-cell western assays were used to measure phosphorylation of PKB/Akt at Ser473 and phosphorylation of ribosomal protein S6 at Ser235/236. ICW experiments and determination of IC<sub>50</sub> were performed as described in ref 30. Briefly, A2058 cells were seeded at 2  $\times$  10<sup>4</sup> cells/well in 96-well plates (Cell Carrier, Perkin Elmer) and grown for 24 h at 37 °C (at 5% CO<sub>2</sub>). Cells were then exposed to inhibitors or DMSO for 1 h. At this time, cells were fixed (4% PFA in PBS for 30 min at r.t.), blocked (1% BSA/0.1% Triton X-100/5% goat serum in PBS for 30 min, r.t.), and stained with CST primary anti-phosphoprotein

antibodies [1:500; phosphorylation of Ser473 of PKB/Akt was detected with rabbit polyclonal antibody from Cell Signaling Technology (CST, #4058) and mTORC1 activity as phosphorylation of Ser235/236 on the ribosomal protein S6 with rabbit monoclonal antibody from CST, #4856]. Tubulin staining was assessed as the internal standard with mouse anti- $\alpha$ -tubulin, 1:2000, from Sigma (#T9026). Fluorescence outputs were detected on an Odyssey CLx infrared imaging scanner (LICOR) using secondary, species-specific antibodies, IR-dye-labeled antibodies (IRDye680-conjugated goat anti-mouse, and IRDye800-conjugated goat anti-rabbit antibodies [LICOR # 926-68070 and # 926-32211], both 1:500). Remaining phospho-protein signals were normalized to cellular tubulin and related to DMSO controls.  $IC_{50}$ s were measured using a 7- or 11-point 1:2 serial dilution and each concentration was measured in independent triplicate (7-point dilution) or independent duplicate (11-point dilution).

**Hepatocyte Stability Assay.** The hepatocyte stability was assessed using primary hepatocytes from mice (CD-1), rats (Sprague-Dawley, SD), dogs (Beagle), and humans. Assays were performed using cryopreserved hepatocytes in suspension, and each experiment was performed in duplicate. Stock solution of compound **8** was prepared with 10 mM in DMSO and diluted to the final concentration of 5  $\mu$ M. 7-EC has been used as a positive control. Negative control incubations were run in line with all experiments using the incubation medium in the absence of hepatocytes to exclude nonmetabolic degradation processes. Further experimental details are reported in ref 27. As described in the standard Pharmacelsus protocol, 25  $\mu$ L of a 10-fold stock of **8** or 7-EC (reference compound) was added to 225  $\mu$ L of cell suspension, yielding a final concentration of 5  $\mu$ M for **8** and 7-EC. The final solvent concentrations did not exceed 0.5% DMSO (for **8**) or 1% ACN (for 7-EC). Samples were collected after 0, 15, 60, 90, and 180 min of incubation for **8** and after 0, 60, and 180 min for 7-EC. Subsequently, proteins were precipitated using ACN (200  $\mu$ L cell suspension plus 200  $\mu$ L ACN/ISTD3). After centrifugation for 5 min at 4800g, particle-free supernatant was diluted with one volume of  $H_2O$  and analyzed by LC-MS. To exclude nonmetabolic degradation processes, negative controls were performed. For example, the finding that the concentrations remained stable over the investigated time suggested that the decrease of the parent compound was mainly due to metabolism. Negative control incubations were performed in line with all experiments using the incubation medium in the absence of hepatocytes.

A HPLC system consisting of a LC pump Surveyor Plus and an auto sampler Surveyor Plus (Thermo Fisher, USA) was used to quantify compound **8** in samples from primary hepatocytes. Mass spectrometry was carried out on a TSQ Quantum Discovery Max triple quadrupole mass spectrometer equipped with an electro-spray ion source (ESI, Thermo Fisher Scientific, USA). Xcalibur 2.0.7. was used as software for data analysis.

**CYP Reactive Phenotyping with Human Recombinant CYP1A1 and CYP1A2 Isoenzymes.** Human recombinant isoenzymes from insect cells infected by baculovirus and containing cDNA of a single human CYP isoenzyme (Supersomes, Corning) were employed. The compounds were tested in the CYP-reactive phenotyping at a concentration of 1  $\mu$ M in the presence of 0.25% DMSO. The assays were performed in duplicate using human recombinant enzymes systems from Corning (BD Gentest P450 High Throughput Inhibitor Screening Kits). Further experimental details are reported in ref 27.

As described in standard Pharmacelsus protocol, the cofactor-mix, containing the NADP<sup>+</sup>-regenerating system, was prepared according to the manufacturer's instructions. For CYP1A1 and CYP1A2, 4  $\mu$ L of the 50-fold concentrated working solution was added to 96  $\mu$ L of the cofactor mix. The cofactor mix and test item were pipetted into the respective wells of a prewarmed 96-well plate and prewarmed for 10 min on a shaker with fitted heating block. The reactions were initiated by addition of 100  $\mu$ L of prewarmed enzyme-mix. By default, the final protein concentration of all CYP isoenzymes was 25 pmol/mL. Incubations with a final volume of 200  $\mu$ L were performed at 37 °C. After 0 and 60 min (30 min for positive control substrates), the

reactions were stopped by the addition of 200  $\mu$ L of stop solution, that is, ACN containing the internal standard. Two control groups were evaluated in parallel for each assay: specific substrates for each CYP isoform were used as positive controls (CYP1A1, melatonin and CYP1A2, phenacetin). Negative controls ( $n = 2$ ) were performed without cofactors and glucose-6-phosphate-dehydrogenase to ensure that the potential loss of parent compound is due to the CYP-mediated metabolism.

For quantitative analysis of compounds **8** and **4**, the following equipment have been used: (1) LC-MS consisting of an Accela U-HPLC pump and an Accela auto sampler connected to an Exactive mass spectrometer (Orbitrap with accurate mass, Thermo Fisher Scientific, USA). Data analysis was performed with Xcalibur 2.1 software. (2) LC-HRMS consisting of an Accela U-HPLC pump and an Accela Open auto sampler (Thermo Fisher Scientific, USA) connected to a Q Exactive mass spectrometer (Orbitrap). Data analysis was performed with Xcalibur 2.2. (3) LC-MS consisting of a Surveyor MS Plus HPLC system connected to a TSQ Quantum Discovery Max (Thermo Electron) triple quadrupole mass spectrometer equipped with an electrospray (ESI) or APCI interface (Thermo Fisher Scientific, USA). Software used: Xcalibur 2.0.7.

**MDCK TransWell Assays.** MDCK-hMDR1<sup>cMDR1-ko</sup> and MDCK<sup>cMDR1-ko</sup> cells were obtained from Karlgren *et al.*, Uppsala University,<sup>45</sup> and cultured according to the provided protocol. Briefly, cells were cultured in DMEM with Glutamax (cat. no. 14190), 10% fetal bovine serum (cat. no. 10270), and 5% penicillin-streptomycin (cat. no. 10687). Hygromycin B (cat no 10687) was used as selection antibiotic for cells expressing hMDR1. Cells (100,000/well) were seeded into 12-well TransWell plates (cat. no. CLS3401) and grown for 5 days prior to experiments. Cell culture medium was exchanged every second day and the day before the experiment. For  $P_{app}$  experiments, the cell culture medium was replaced with prewarmed HBSS for 30 min at 37 °C under gentle stirring (300 rpm). The experiment was started by the addition of 0.4 mL of 1  $\mu$ M drug solution in HBSS to the apical side ( $P_{app}$  A to B) or 1.2 mL of 1  $\mu$ M drug solution to the basolateral side ( $P_{app}$  B to A). Samples of 100  $\mu$ L were retrieved from the receiver chamber at time points 5, 10, and 20 min and replaced with fresh buffer. Samples (100  $\mu$ L) were retrieved from the donor chamber at the end of the experiment for calculation of mass balance. Trans-epithelial electrical resistance (TEER) values were measured prior to addition of drug and 30 min after sampling of last time point [Epithelial Volt/Ohm Meter (EVOM), World Precision Instrument, equipped with Chopstick Electrode STX2].

Immediately after the final sampling, the samples and calibration standards were diluted 1:1 with ACN containing the internal standard, vortexed, and centrifuged at 2000g for 15 min, and the supernatant was analyzed by UPLC-MS/MS. The UPLC-MS/MS system consisted of an Agilent 1290 Infinity Binary Pump coupled to an Agilent 6460 Triple Quad Mass Spectrometer with an AJS ESI interface. Mobile phases consisted of (A) water with 5% ACN, 0.05% formic acid, and 10 mM ammonium formate and (B) ACN with 0.05% formic acid. Separation was performed on an Acquity UPLC column (BEH C18 1.7  $\mu$ m, 2.1  $\times$  50 mm) with an integrated prefilter. Acquisition and quantification were performed with the Agilent MassHunter Workstation (Version 10.1).

Finally,  $P_{app}$  was calculated according to the literature<sup>56</sup> using the equation

$$P_{app} = (dQ/dt)(1/AC_0)$$

where  $dQ/dt$  is the steady-state flux ( $\mu$ mol/s),  $A$  is the surface area of the filter ( $cm^2$ ), and  $C_0$  is the initial concentration in the donor chamber ( $\mu$ M).

The ER is the ratio between the secretory permeability and the absorptive permeability

$$ER = P_{app} B \text{ to } A / P_{app} A \text{ to } B$$

Experiments were performed in triplicates on at least two independent occasions.  $P_{app}$  values were retained for experiments with a mass balance >75% and TEER in the range of 160–180  $\Omega$ - $cm^2$ .



Citalopram has been used as control because it is a hMDR1 substrate for which literature data using these cell lines are available.<sup>45</sup>

**Pharmacokinetic Studies in Rats.** Male Sprague Dawley rats purchased from Janvier Labs (France) were used for the study. The animals were 8 weeks old at delivery and were housed in a temperature-controlled room (20–24 °C) and kept in a 12 h light/12 h dark cycle. Food and water were available *ad libitum* throughout the duration of the study. Formulation of compound **8** was prepared by dissolving it in Captisol (40% w/w in water). Compound preparation and experiment setup were consistent with the previous literature reports.<sup>27</sup> Briefly, the compounds were administered p.o. at 5 mg/kg (application volume: 5 mL/kg). At each time point (30 min, 2, 4, and 8 h), three rats were anesthetized with isoflurane and 1 mL of blood was collected, *via* heart puncture, in tubes containing lithium-heparin. After blood sampling, the rats were euthanized and brain, liver, and skin were collected.

**Quantification of Plasma Insulin.** Plasma insulin was determined using an immunoassay kit (Rat/Mouse Insulin ELISA from Merck Millipore, cat. no. EZRMI-13K, lot 2688510, Germany), according to the manufacturer's instructions. This Rat/Mouse Insulin ELISA kit was used for the nonradioactive quantification of insulin in rat sera. At each time point, three rats were anesthetized with isoflurane and 1 mL of blood was collected. Blood samples were stored on dry ice until centrifugation at 3000g (10 min, 4 °C). Plasma supernatants and tissue samples were stored at –80 °C until being assayed.

**Quantification of Plasma Glucose.** Plasma glucose was determined using a glucose colorimetric assay (Cayman, cat. no. 10009582, lot 0478964, USA). The glucose assay uses the glucose oxidase–peroxide reaction for the determination of glucose concentrations. In this assay, glucose is oxidized to  $\delta$ -gluconolactone with concomitant reduction of the flavin adenine dinucleotide-dependent enzyme glucose oxidase. The reduced form of glucose oxidase is regenerated to its oxidized form by molecular oxygen to produce hydrogen peroxide. Finally, hydrogen peroxide reacts with 3,5-dichloro-2-hydroxybenzenesulfonic acid and 4-aminoantipyrine to generate a pink dye with an optimal absorption at 514 nm. The plasma was collected and stored in ice or at –80 °C until being assayed.

**Pharmacokinetic Studies in Mice.** Female C57BL/6J mice purchased from Janvier Labs (France) were used for the study. The animals were 8 weeks old at delivery and were housed in a temperature-controlled room (20–24 °C) and maintained in a 12 h light/12 h dark cycle. Food and water were available *ad libitum* before and throughout the duration of the study. The animals were checked for clinical signs throughout the study. No adverse effects were observed. Dose formulations were prepared freshly on the day of the in-life phase.

**Study PQR626 (8) versus Everolimus (56).** The compounds were orally administered the following: compound **8** at 10 mg/kg, either as single or multiple (qd4) application in 20% Captisol and compound **56** at 10 mg/kg qd4 in 8% ethanol, 10% PEG 400, 10% Tween 80.

**Study PQR626 (8) versus Everolimus (56) and AZD2014 (51).** The compounds were orally administered the following: compound **8** at 25 mg/kg in 20% Captisol; compound **56** at 10 mg/kg in 8% ethanol, 10% PEG 400, 10% Tween 80 and 72% water; and compound **51** at 25 mg/kg in 20% Captisol (SBECD).

At each of the designated time points, three mice were subjected to isoflurane anesthesia to obtain about 0.5 mL of Li heparin blood by puncture of the retrobulbar venous plexus. Blood samples were stored on ice until centrifugation at 3000g (6000 rpm) for 10 min at 4 °C for the preparation of plasma samples. Subsequently, mice were sacrificed by inhalation of an overdose of isoflurane for the collection of the brain and muscles. All samples were frozen on dry ice and stored at –80 °C.

The HPLC system consisted of a U-HPLC pump (Ultimate 3000 RS) and an Accela Open auto sampler (Thermo Fisher Scientific, USA). Mass spectrometry was performed on a Q Exactive (Orbitrap) accurate mass spectrometer equipped with a heated electrospray (HESI) interface (Thermo Fisher Scientific, USA). Xcalibur 4.0. software was used for data collection and analysis.

For the quantification of plasma insulin and glucose, see the section above.

All experimental procedures in male Sprague Dawley rats and in female C57BL/6J mice were approved by and conducted in accordance with the regulations of the local Animal Welfare authorities (Landesamt für Gesundheit und Verbraucherschutz, Abteilung Lebensmittel und Veterinärwesen, Saarbrücken).

**Determination of Phospho-Protein Levels in the Murine Cortex. Tissue Lysis.** Snap-frozen murine cortical brain pieces of compound-treated animals were obtained from studies described in **Experimental Section** in “Pharmacokinetic Studies in Mice” above and control animals were obtained from the same supplier and were stored at –80 °C. Cortical tissue was homogenized and lysed in 400  $\mu$ L of ice-cold RIPA lysis buffer + protease/phosphatase inhibitor cocktail (Halt Protease Inhibitor Cocktail #87786; Halt Phosphatase Inhibitor Cocktail #78420, Thermo Fisher Scientific) in precooled 2 mL ScrewCup tubes by mechanical disruption using a bead mill [MP Fast-Prep 24 with beads (#11079124zx, Biospec products), 1 cycle: 20s, speed 6 m/s]. The lysate was cleared in a cooled centrifuge (4 °C, 5 min, 16 000 g) and cleared lysate transferred and aliquoted in cooled Eppendorf tubes and snap frozen until further processing.

**SDS-PAGE.** The total protein content of cortex lysates was determined using a Bradford assay (Bio-Rad DC Protein Assay). Equal amounts of lysates were denatured in a SDS-PAGE sample buffer and heated to 97 °C for 5 min. Denatured protein samples were subjected to SDS-PAGE and transferred to Immobilon FL membranes (Millipore).

**Immunodetection by Western Blotting.** Primary antibodies to pSer473-PKB/Akt (#4058L), PKB/AKT (#2929S), pS235/236 ribosomal protein S6 (#4856S), and ribosomal protein S6 (#2317S) were from Cell Signaling Technology; mouse monoclonal anti activated MAP Kinase (#M8159) and primary antibody to  $\alpha$ -tubulin (#T9026) was from Sigma. HRP-conjugated secondary antibodies were visualized using enhanced chemiluminescence (Millipore) on a Fusion FX (Vilber Lourmat) imaging system. Levels of phosphorylated protein and total protein and  $\alpha$ -tubulin signals were quantified using ImageJ. Phospho-protein levels in each sample were corrected for unequal loading using  $\alpha$ -tubulin or total PKB signals. Resulting phospho-protein signals of compound-treated samples were subsequently normalized to control-treated samples and illustrated and analyzed using a GraphPad Prism. Statistical analysis was performed using unpaired *t*-test and the probability value (*p*-value) used to identify significance (*p* < 0.05).

**Toxicokinetic Studies in Mice.** Female Balb/c nude mice were purchased from Beijing Anikeeper Biological Technology Co. Ltd. (AK, Beijing, China). The animals were housed in a temperature-controlled room (20–26 °C) and maintained in a 12 h light/12 h dark cycle. Food and water were available *ad libitum* before and throughout the duration of the study. Treatment with compound **8** at 100, 150, and 200 mg/kg was carried out and compared to vehicle (20% Captisol). Ten mice, 6–8 weeks old at inoculation, were enrolled in the study. All animals were randomly allocated to the four different study groups. Randomization was performed based on body weight and randomized block design on day 1. The animals were checked daily for morbidity and mortality. At the time of routine monitoring, the animals were checked for treatments on normal behavior such as mobility, visual estimation of food and water consumption, body weight gain/loss, eye/hair matting, and any other abnormalities. The body weights were recorded daily. The entire procedure of dosing and body weight measurement was conducted in a laminar flow cabinet. Animals showing obvious signs of severe distress were euthanized. Gross necropsy was performed on euthanized animals, and observations on the major organs (heart, lung, liver, kidney, spleen, and intestine) were reported.

All studies were conducted following an approved Institutional Animal Care and Use Committee (IACUC) protocol of CrownBio. During the study, the care and use of animals were conducted in accordance with the regulations of the Association for Assessment and Accreditation of Laboratory Animal Care (AAALAC). All experimental data management and reporting procedures were in strict

accordance with applicable Crown Bioscience, Inc. Guidelines and Standard Operating Procedures.

**Efficacy on Survival in *Tsc1*<sup>GFAP</sup> Knockout Mice.** The study was performed at PsychoGenics, Inc., headquartered at 215 College Road, Paramus, NJ 07652, USA. Animals were used in accordance with humane laboratory animal care and used based on the Guide for the Care and Use of Laboratory Animals (NRC 2011) and PsychoGenics, Inc. internal IACUC program. PsychoGenics achieved AAALAC accreditation (Unit #001213) and holds PHS OLAW Assurance (#D16-00732 [A4471-0]).

*Tsc1*<sup>fllox/fllox</sup>-GFAP-Cre<sup>+</sup> (*Tsc1*<sup>GFAP</sup> conditional knockout) male and female mice were bred at PsychoGenics using breeding pairs obtained from Prof. Michael Wong, MD, Ph.D. (Washington University, St. Louis, MO). Genotyping of mice was performed using PCR and primers for TSC1 and CRE according to the procedure provided by Dr. Wong. Kits were purchased from Lambda Biotech (catalog number D124R). All mice were acclimated to the environment, examined, handled, and weighed prior to the initiation of the study to assure adequate health and suitability and to minimize nonspecific stress associated with human handling. During the course of the study, 12 h/12 h light/dark cycles were maintained. The room temperature was maintained at 20–23 °C with a relative humidity maintained around 50%. Food and water were provided *ad libitum* for the duration of the study. Each mouse was randomly assigned to designated treatment groups. The dosing was performed during the animals' light cycle phase. Body weights were determined twice per week from P21 to P90. Twice a week all mice were assessed for general health including biweekly body weights.

Animals were checked at least once daily for survival. Survival curves were generated and represented as a percent of surviving animals for each treatment group over the course of the study. The first death was observed at P26, therefore data are plotted from P25 to P90 and recorded in intervals of 5 days. At end of study at P90, surviving mice were euthanized for plasma and brain collection 2 h after last dose.

Blood was collected from submandibular vein in K2EDTA tubes and kept on ice for short-term storage. Within 15 min of blood collection, tubes were centrifuged for 10 min at 10 000 rpm in a refrigerated centrifuge. The plasma was extracted using a pipette and transferred into pre-labeled tubes. Plasma were stored at –80 °C until shipment to Sponsor-designated laboratory.

Whole brains were perfused by PBS first and then 4% PFA and collected into 4% PFA filled vials and stored at 4 °C overnight. Fixed brains were transferred to 30% sucrose and 0.05% sodium azide for storage and shipment. Brains were stored at –4 °C.

With the exception of compound **52** at 50 mg/kg, all compounds were dosed p.o. and daily from P21 to P90. A treatment group with **52** at 50 mg/kg was added at P27, and 6 days post-study comparing with compound **8** at 50 mg/kg was started. Four additional animals per group were dosed and sacrificed on day P45 for brain and plasma collection. See [Supporting Information](#) Table S33 for additional information (P21 and P23 were not measured for **52** at 50 mg/kg). Details on animals used in the study are reported in Table S35 of the [Supporting Information](#). Vehicle was 20% SBEC (sulfobutyl-ether- $\beta$ -cyclodextrin, Captisol, Dexolve) pH 3.0. Compounds **52** and **8** were dissolved in vehicle. Compound **56** was dissolved in 10% PEG400/10% Tween-80/8% ethanol.

**Statistical Reports for Survival Analysis.** Survival was determined from the start of the study (P21) to the day the animal was found dead or until P90 (*i.e.*, animals were censored at P90). A Chi-square survival analysis was performed in JMP Statistical Software (a division of SAS) with treatment as a factor. The log-rank test places more weight on larger survival times and is more useful when the ratio of hazard functions in the groups being compared is approximately constant where the hazard function is the instantaneous failure rate at a given time. Data are reported as percent of survival across days.

## ■ ASSOCIATED CONTENT

### SI Supporting Information

The Supporting Information is available free of charge at <https://pubs.acs.org/doi/10.1021/acs.jmedchem.0c00620>.

Comparison of PQR620 (**52**) PK profile in mice and cynomolgus monkeys; metabolites analysis of **52** in cynomolgus monkey; final compounds SAR studies: activity data and standard errors (SEM); TREEspot data visualization of KINOMEScan interactions of compounds PQR626 (**8**), PQR617 (**53**), PQR620 (**52**) and INK128 (**50**); selectivity profile calculated from KinomeScan data; kinase interactions (KINOMEScan data); *in vitro* pharmacology I—ligand binding assays with compound **8** at 10  $\mu$ M; *in vitro* pharmacology II—enzyme assays with compound **8** at 10  $\mu$ M; stability of compounds **8** and **52** in primary mouse, rat, dog, and human hepatocytes; plasma and brain concentration of compound **8** after a single p.o. dose of 5 mg/kg in rats; plasma insulin and glucose concentration after a single p.o. dose of 5 mg/kg of compound **8** and after vehicle administration in rats; plasma concentration of compound **8** after a p.o. single dosing and multiple dosing at 10 mg/kg and of everolimus (**56**) after a p.o. multiple dosing at 10 mg/kg in mice; brain concentration of compound **8** after a p.o. single dosing and multiple dosing at 10 mg/kg and of compound **56** after a p.o. multiple dosing at 10 mg/kg in mice; plasma and brain concentration after a p.o. single dosing of compound **8** at 25 mg/kg, of compound **56** at 10 mg/kg, and of AZD2014 (**51**) at 25 mg/kg in mice; plasma insulin and glucose concentration after a p.o. single dosing of compound **8** at 25 mg/kg, of compound **56** at 10 mg/kg, and of compound **51** at 25 mg/kg in mice; time-course of inhibition of mTOR signaling in murine brain cortex by compound **8**; body weight changes in nontumor bearing Balb/c mice; body weight of mice as a function of treatments in *Tsc1*<sup>GFAP</sup> knockout mice; statistical reports for survival analysis in *Tsc1*<sup>GFAP</sup> knockout mice; details on *Tsc1*<sup>GFAP</sup> knockout mice used in the experiments; <sup>1</sup>H NMR spectra; <sup>13</sup>C{<sup>1</sup>H} NMR spectra; MALDI spectra; HRMS spectra; HPLC chromatograms; final compounds (chemical structures); intermediates (chemical structures); and reference compounds (chemical structures) (PDF)

Molecular formula strings of compounds 1–21 (CSV)

3D PDB Files for Figure 2 (PDF)

Compound **8**\_methyl up-mTOR (PDB)

Compound **8**\_methyl down-mTOR (PDB)

Compound **8**\_methyl up-PI3K $\alpha$  (PDB)

Compound **8**\_methyl down-PI3K $\alpha$  (PDB)

Compound **4**\_methyl right-mTOR (PDB)

Compound **4**\_methyl left-mTOR (PDB)

Compound **4**\_methyl right-PI3K $\alpha$  (PDB)

Compound **4**\_methyl left-PI3K $\alpha$  (PDB)

### Accession Codes

PDB code 4JT6 was used for docking of compounds PQR626 (**8**) and **4** into mTOR kinase. PDB code 6OAC was used for docking of PQR626 (**8**) and **4** into PI3K $\alpha$ .



## AUTHOR INFORMATION

### Corresponding Author

Matthias P. Wymann – Department of Biomedicine, University of Basel, 4058 Basel, Switzerland; [orcid.org/0000-0003-3349-4281](https://orcid.org/0000-0003-3349-4281); Phone: +41 61 207 5046; Email: [matthias.wymann@unibas.ch](mailto:matthias.wymann@unibas.ch); Fax: +41 61 207 3566

### Authors

Chiara Borsari – Department of Biomedicine, University of Basel, 4058 Basel, Switzerland; [orcid.org/0000-0002-4688-8362](https://orcid.org/0000-0002-4688-8362)  
Erhan Keles – Department of Biomedicine, University of Basel, 4058 Basel, Switzerland  
Denise Rageot – Department of Biomedicine, University of Basel, 4058 Basel, Switzerland  
Andrea Treyer – Pharmaceutical Biology, Pharmacenter, University of Basel, 4056 Basel, Switzerland; [orcid.org/0000-0002-4533-7761](https://orcid.org/0000-0002-4533-7761)  
Thomas Bohnacker – Department of Biomedicine, University of Basel, 4058 Basel, Switzerland  
Lukas Bissegger – Department of Biomedicine, University of Basel, 4058 Basel, Switzerland  
Martina De Pascale – Department of Biomedicine, University of Basel, 4058 Basel, Switzerland  
Anna Melone – Department of Biomedicine, University of Basel, 4058 Basel, Switzerland  
Rohitha Sriramarnam – Department of Biomedicine, University of Basel, 4058 Basel, Switzerland  
Florent Beaufils – PIQR Therapeutics AG, 4057 Basel, Switzerland  
Matthias Hamburger – Pharmaceutical Biology, Pharmacenter, University of Basel, 4056 Basel, Switzerland; [orcid.org/0000-0001-9331-273X](https://orcid.org/0000-0001-9331-273X)  
Paul Hebeisen – PIQR Therapeutics AG, 4057 Basel, Switzerland  
Wolfgang Löscher – Department of Pharmacology, Toxicology and Pharmacy and Center for Systems Neuroscience, University of Veterinary Medicine, 30559 Hannover, Germany  
Doriano Fabbro – PIQR Therapeutics AG, 4057 Basel, Switzerland  
Petra Hillmann – PIQR Therapeutics AG, 4057 Basel, Switzerland

Complete contact information is available at:

<https://pubs.acs.org/10.1021/acs.jmedchem.0c00620>

### Author Contributions

The manuscript was written through contributions of all authors. All authors have given approval to the final version of the manuscript.

### Funding

This work was supported by the Innosuisse grant 37213.1 IP-LS, EU Horizon 2020, ITN 675392—Ph.D; the Novartis Foundation for medical-biological Research grant 14B095; the Swiss Commission for Technology and Innovation (CTI) by PFLS-LS grant 17241.1; the Stiftung für Krebsbekämpfung grant 341, the Swiss National Science Foundation grant 310030\_189065 to MPW, the Peter and Traudl Engelhorn Foundation to RS, and a grant from the Epilepsy Foundation of America to WL.

### Notes

The authors declare the following competing financial interest(s): PHe, PHi, and DF are past employees of PIQR Therapeutics AG, Basel; and PHe, DF, and MPW are shareholders of PIQR Therapeutics AG.

### ACKNOWLEDGMENTS

We thank A. Pfaltz and A. M. Sele for advice and discussions; A. Dall'Asen and E. Teillet for contributions to synthetic efforts; and S. Büniger for technical assistance.

### ABBREVIATIONS

mTOR, mechanistical (or mammalian) target of rapamycin; TORC1, mTOR complex 1; TORC2, mTOR complex 2; PI3K, phosphoinositide 3-kinase; PKB, protein kinase B/Akt; S6RP, ribosomal protein S6; S6K, p70 S6 kinase; VPS34, vacuolar protein sorting 34 (the class III PI3K); TORKi, mTOR kinase inhibitors; PK, pharmacokinetic; TR-FRET, time-resolved Förster resonance energy transfer; TSC1, hamartin; TSC2, tuberlin; TSC, tuberous sclerosis complex; FKBP12, TORC1/rapalog/FK506 binding protein 12; BBB, blood–brain barrier; CNS, central nervous system; DCM, dichloromethane; THF, tetrahydrofuran; EtOH, ethanol; DIPEA, *N,N*-diisopropylethylamine; CRISPR, clustered regularly interspaced short palindromic repeats; Cas9, CRISPR-associated protein 9; ER, efflux ratio; MDCK, Madin–Darby canine kidney II cells; MDR1, multidrug resistance protein 1, often referred to as P-glycoprotein;  $P_{app}$ , apparent permeability

### REFERENCES

- (1) Wymann, M. P.; Schreiner, R. Lipid signalling in disease. *Nat. Rev. Mol. Cell Biol.* **2008**, *9*, 162–176.
- (2) Yang, H.; Rudge, D. G.; Koos, J. D.; Vaidialingam, B.; Yang, H. J.; Pavletich, N. P. mTOR kinase structure, mechanism and regulation. *Nature* **2013**, *497*, 217–223.
- (3) Sarbassov, D. D.; Guertin, D. A.; Ali, S. M.; Sabatini, D. M. Phosphorylation and regulation of Akt/PKB by the rictor-mTOR complex. *Science* **2005**, *307*, 1098–1101.
- (4) Wymann, M. P.; Marone, R. Phosphoinositide 3-kinase in disease: timing, location, and scaffolding. *Curr. Opin. Cell Biol.* **2005**, *17*, 141–149.
- (5) Magnuson, B.; Ekim, B.; Fingar, D. C. Regulation and function of ribosomal protein S6 kinase (S6K) within mTOR signalling networks. *Biochem. J.* **2012**, *441*, 1–21.
- (6) Laplante, M.; Sabatini, D. M. mTOR signaling in growth control and disease. *Cell* **2012**, *149*, 274–293.
- (7) Huang, J.; Manning, B. D. The TSC1-TSC2 complex: a molecular switchboard controlling cell growth. *Biochem. J.* **2008**, *412*, 179–190.
- (8) Saxton, R. A.; Sabatini, D. M. mTOR signaling in growth, metabolism, and disease. *Cell* **2017**, *168*, 960–976.
- (9) Chong, Z. Z.; Shang, Y. C.; Wang, S.; Maiese, K. A critical kinase cascade in neurological disorders: PI 3-K, Akt, and mTOR. *Future Neurol.* **2012**, *7*, 733–748.
- (10) Curatolo, P.; Moavero, R. mTOR inhibitors in tuberous sclerosis complex. *Curr. Neuropharmacol.* **2012**, *10*, 404–415.
- (11) Choi, J.; Chen, J.; Schreiber, S. L.; Clardy, J. Structure of the FKBP12-rapamycin complex interacting with the binding domain of human FRAP. *Science* **1996**, *273*, 239–242.
- (12) Lamming, D. W.; Ye, L.; Sabatini, D. M.; Baur, J. A. Rapalogs and mTOR inhibitors as anti-aging therapeutics. *J. Clin. Invest.* **2013**, *123*, 980–989.
- (13) Zeng, L.-H.; Xu, L.; Gutmann, D. H.; Wong, M. Rapamycin prevents epilepsy in a mouse model of tuberous sclerosis complex. *Ann. Neurol.* **2008**, *63*, 444–453.

- (14) Meikle, L.; Pollizzi, K.; Egnor, A.; Kramvis, I.; Lane, H.; Sahin, M.; Kwiatkowski, D. J. Response of a neuronal model of tuberous sclerosis to mammalian target of rapamycin (mTOR) inhibitors: effects on mTORC1 and Akt signaling lead to improved survival and function. *J. Neurosci.* **2008**, *28*, 5422–5432.
- (15) Lechuga, L.; Franz, D. N. Everolimus as adjunctive therapy for tuberous sclerosis complex-associated partial-onset seizures. *Expert Rev. Neurother.* **2019**, *19*, 913–925.
- (16) French, J. A.; Lawson, J. A.; Yapici, Z.; Ikeda, H.; Polster, T.; Nabbout, R.; Curatolo, P.; de Vries, P. J.; Dlugos, D. J.; Berkowitz, N.; Voi, M.; Peyrard, S.; Pelov, D.; Franz, D. N. Adjunctive everolimus therapy for treatment-resistant focal-onset seizures associated with tuberous sclerosis (EXIST-3): a phase 3, randomised, double-blind, placebo-controlled study. *Lancet* **2016**, *388*, 2153–2163.
- (17) Ravikumar, B.; Vacher, C.; Berger, Z.; Davies, J. E.; Luo, S.; Oroz, L. G.; Scaravilli, F.; Easton, D. F.; Duden, R.; O’Kane, C. J.; Rubinsztein, D. C. Inhibition of mTOR induces autophagy and reduces toxicity of polyglutamine expansions in fly and mouse models of Huntington disease. *Nat. Genet.* **2004**, *36*, 585–595.
- (18) Singer, E.; Walter, C.; Fabbro, D.; Rageot, D.; Beaufils, F.; Wymann, M. P.; Rischert, N.; Riess, O.; Hillmann, P.; Nguyen, H. P. Brain-penetrant PQR620 mTOR and PQR530 PI3K/mTOR inhibitor reduce huntingtin levels in cell models of HD. *Neuropharmacology* **2020**, *162*, 107812.
- (19) Talboom, J. S.; Velazquez, R.; Oddo, S. The mammalian target of rapamycin at the crossroad between cognitive aging and Alzheimer’s disease. *npj Aging Mech. Dis.* **2015**, *1*, 15008.
- (20) Zhu, Z.; Yang, C.; Iyaswamy, A.; Krishnamoorthi, S.; Sreenivasamurthy, S. G.; Liu, J.; Wang, Z.; Tong, B. C.-K.; Song, J.; Lu, J.; Cheung, K.-H.; Li, M. Balancing mTOR signaling and autophagy in the treatment of Parkinson’s disease. *Int. J. Mol. Sci.* **2019**, *20*, 728.
- (21) Krueger, D. A.; Wilfong, A. A.; Mays, M.; Talley, C. M.; Agricola, K.; Tudor, C.; Capal, J.; Holland-Bouley, K.; Franz, D. N. Long-term treatment of epilepsy with everolimus in tuberous sclerosis. *Neurology* **2016**, *87*, 2408–2415.
- (22) Brandt, C.; Hillmann, P.; Noack, A.; Römermann, K.; Öhler, L. A.; Rageot, D.; Beaufils, F.; Melone, A.; Sele, A. M.; Wymann, M. P.; Fabbro, D.; Löscher, W. The novel, catalytic mTORC1/2 inhibitor PQR620 and the PI3K/mTORC1/2 inhibitor PQR530 effectively cross the blood-brain barrier and increase seizure threshold in a mouse model of chronic epilepsy. *Neuropharmacology* **2018**, *140*, 107–120.
- (23) Jin, Z.; Niu, H.; Wang, X.; Zhang, L.; Wang, Q.; Yang, A. Preclinical study of CC223 as a potential anti-ovarian cancer agent. *Oncotarget* **2017**, *8*, 58469–58479.
- (24) Slotkin, E. K.; Patwardhan, P. P.; Vasudeva, S. D.; de Stanchina, E.; Tap, W. D.; Schwartz, G. K. MLN0128, an ATP-competitive mTOR kinase inhibitor with potent in vitro and in vivo antitumor activity, as potential therapy for bone and soft-tissue sarcoma. *Mol. Cancer Ther.* **2015**, *14*, 395–406.
- (25) Pike, K. G.; Malagu, K.; Hummersone, M. G.; Menear, K. A.; Duggan, H. M. E.; Gomez, S.; Martin, N. M. B.; Ruston, L.; Pass, S. L.; Pass, M. Optimization of potent and selective dual mTORC1 and mTORC2 inhibitors: the discovery of AZD8055 and AZD2014. *Bioorg. Med. Chem. Lett.* **2013**, *23*, 1212–1216.
- (26) Rageot, D.; Bohnacker, T.; Melone, A.; Langlois, J.-B.; Borsari, C.; Hillmann, P.; Sele, A. M.; Beaufils, F.; Zvelebil, M.; Hebeisen, P.; Löscher, W.; Burke, J.; Fabbro, D.; Wymann, M. P. Discovery and preclinical characterization of 5-[4,6-Bis({3-oxa-8-azabicyclo[3.2.1]octan-8-yl})-1,3,5-triazin-2-yl]-4-(difluoro methyl)pyridin-2-amine (PQR620), a highly potent and selective mTORC1/2 inhibitor for cancer and neurological disorders. *J. Med. Chem.* **2018**, *61*, 10084–10105.
- (27) Borsari, C.; Rageot, D.; Dall’Asen, A.; Bohnacker, T.; Melone, A.; Sele, A. M.; Jackson, E.; Langlois, J.-B.; Beaufils, F.; Hebeisen, P.; Fabbro, D.; Hillmann, P.; Wymann, M. P. A conformational restriction strategy for the identification of a highly selective pyrimido-pyrrolo-oxazine mTOR inhibitor. *J. Med. Chem.* **2019**, *62*, 8609–8630.
- (28) Bonazzi, S.; Goold, C. P.; Gray, A.; Thomsen, N. M.; Nunez, J.; Karki, R. G.; Gorde, A.; Biag, J. D.; Malik, H. A.; Sun, Y.; Liang, G.; Lubicka, D.; Salas, S.; Labbe-Giguere, N.; Keaney, E. P.; McTighe, S.; Liu, S.; Deng, L.; Piuzzi, G.; Lombardo, F.; Burdette, D.; Dodart, J.-C.; Wilson, C. J.; Peukert, S.; Curtis, D.; Hamann, L. G.; Murphy, L. O. Discovery of a brain-penetrant ATP-competitive inhibitor of the mechanistic target of rapamycin (mTOR) for CNS disorders. *J. Med. Chem.* **2020**, *63*, 1068–1083.
- (29) Bohnacker, T.; Prota, A. E.; Beaufils, F.; Burke, J. E.; Melone, A.; Inglis, A. J.; Rageot, D.; Sele, A. M.; Cmiljanovic, V.; Cmiljanovic, N.; Bargsten, K.; Aher, A.; Akhmanova, A.; Diaz, J. F.; Fabbro, D.; Zvelebil, M.; Williams, R. L.; Steinmetz, M. O.; Wymann, M. P. Deconvolution of Buparlisib’s mechanism of action defines specific PI3K and tubulin inhibitors for therapeutic intervention. *Nat. Commun.* **2017**, *8*, 14683.
- (30) Beaufils, F.; Cmiljanovic, N.; Cmiljanovic, V.; Bohnacker, T.; Melone, A.; Marone, R.; Jackson, E.; Zhang, X.; Sele, A.; Borsari, C.; Mestan, J.; Hebeisen, P.; Hillmann, P.; Giese, B.; Zvelebil, M.; Fabbro, D.; Williams, R. L.; Rageot, D.; Wymann, M. P. 5-(4,6-Dimorpholino-1,3,5-triazin-2-yl)-4-(trifluoromethyl)pyridin-2-amine (PQR309), a potent, brain-penetrant, orally bioavailable, pan-class I PI3K/mTOR inhibitor as clinical candidate in oncology. *J. Med. Chem.* **2017**, *60*, 7524–7538.
- (31) Tarantelli, C.; Gaudio, E.; Arribas, A. J.; Kwee, I.; Hillmann, P.; Rinaldi, A.; Cascione, L.; Spriano, F.; Bernasconi, E.; Guidetti, F.; Carrassa, L.; Pittau, R. B.; Beaufils, F.; Ritschard, R.; Rageot, D.; Sele, A.; Dossena, B.; Rossi, F. M.; Zucchetto, A.; Taborelli, M.; Gattei, V.; Rossi, D.; Stathis, A.; Stussi, G.; Broggin, M.; Wymann, M. P.; Wicki, A.; Zucca, E.; Cmiljanovic, V.; Fabbro, D.; Bertoni, F. PQR309 is a novel dual PI3K/mTOR inhibitor with preclinical antitumor activity in lymphomas as a single agent and in combination therapy. *Clin. Cancer Res.* **2018**, *24*, 120–129.
- (32) Borsari, C.; Rageot, D.; Beaufils, F.; Bohnacker, T.; Keles, E.; Buslov, I.; Melone, A.; Sele, A. M.; Hebeisen, P.; Fabbro, D.; Hillmann, P.; Wymann, M. P. Preclinical development of PQR514, a highly potent PI3K inhibitor bearing a difluoromethyl-pyrimidine moiety. *ACS Med. Chem. Lett.* **2019**, *10*, 1473–1479.
- (33) Tarantelli, C.; Gaudio, E.; Hillmann, P.; Spriano, F.; Sartori, G.; Aresu, L.; Cascione, L.; Rageot, D.; Kwee, I.; Beaufils, F.; Zucca, E.; Stathis, A.; Wymann, M. P.; Cmiljanovic, V.; Fabbro, D.; Bertoni, F. The novel TORC1/2 kinase inhibitor PQR620 has anti-tumor activity in lymphomas as a single agent and in combination with venetoclax. *Cancers* **2019**, *11*, 775.
- (34) Venkatesan, A. M.; Chen, Z.; Santos, O. D.; Dehnhardt, C.; Santos, E. D.; Ayral-Kaloustian, S.; Mallon, R.; Hollander, I.; Feldberg, L.; Lucas, J.; Yu, K.; Chaudhary, I.; Mansour, T. S. PKI-179: An orally efficacious dual phosphatidylinositol-3-kinase (PI3K)/mammalian target of rapamycin (mTOR) inhibitor. *Bioorg. Med. Chem. Lett.* **2010**, *20*, 5869–5873.
- (35) Rageot, D.; Bohnacker, T.; Keles, E.; McPhail, J. A.; Hoffmann, R. M.; Melone, A.; Borsari, C.; Sriramaratnam, R.; Sele, A. M.; Beaufils, F.; Hebeisen, P.; Fabbro, D.; Hillmann, P.; Burke, J. E.; Wymann, M. P. (S)-4-(Difluoromethyl)-5-(4-(3-methylmorpholino)-6-morpholino-1,3,5-triazin-2-yl)pyridin-2-amine (PQR530), a potent, orally bioavailable, and brain-penetrable dual inhibitor of class I PI3K and mTOR kinase. *J. Med. Chem.* **2019**, *62*, 6241–6261.
- (36) Zask, A.; Kaplan, J.; Verheijen, J. C.; Richard, D. J.; Curran, K.; Brooijmans, N.; Bennett, E. M.; Toral-Barza, L.; Hollander, I.; Ayral-Kaloustian, S.; Yu, K. Morpholine derivatives greatly enhance the selectivity of mammalian target of rapamycin (mTOR) inhibitors. *J. Med. Chem.* **2009**, *52*, 7942–7945.
- (37) Bohnacker, T.; Marone, R.; Collmann, E.; Calvez, R.; Hirsch, E.; Wymann, M. P. PI3Kγ adaptor subunits define coupling to degranulation and cell motility by distinct PtdIns(3,4,5)P<sub>3</sub> pools in mast cells. *Sci. Signal.* **2009**, *2*, ra27.
- (38) Burger, M. T.; Pecchi, S.; Wagman, A.; Ni, Z.-J.; Knapp, M.; Hendrickson, T.; Atallah, G.; Pfister, K.; Zhang, Y.; Bartulis, S.;

Frazier, K.; Ng, S.; Smith, A.; Verhagen, J.; Haznedar, J.; Huh, K.; Iwanowicz, E.; Xin, X.; Menezes, D.; Merritt, H.; Lee, I.; Wiesmann, M.; Kaufman, S.; Crawford, K.; Chin, M.; Bussiere, D.; Shoemaker, K.; Zaror, I.; Maira, S.-M.; Voliva, C. F. Identification of NVP-BKM120 as a potent, selective, orally bioavailable class I PI3 kinase inhibitor for treating cancer. *ACS Med. Chem. Lett.* **2011**, *2*, 774–779.

(39) Richard, D. J.; Verheijen, J. C.; Yu, K.; Zask, A. Triazines incorporating (R)-3-methylmorpholine are potent inhibitors of the mammalian target of rapamycin (mTOR) with selectivity over PI3K $\alpha$ . *Bioorg. Med. Chem. Lett.* **2010**, *20*, 2654–2657.

(40) Yang, J.; Nie, J.; Ma, X.; Wei, Y.; Peng, Y.; Wei, X. Targeting PI3K in cancer: mechanisms and advances in clinical trials. *Mol. Canc.* **2019**, *18*, 26.

(41) Mortensen, D. S.; Fultz, K. E.; Xu, S.; Xu, W.; Packard, G.; Khambatta, G.; Gamez, J. C.; Leisten, J.; Zhao, J.; Apuy, J.; Ghoreishi, K.; Hickman, M.; Narla, R. K.; Bissonette, R.; Richardson, S.; Peng, S. X.; Perrin-Ninkovic, S.; Tran, T.; Shi, T.; Yang, W. Q.; Tong, Z.; Cathers, B. E.; Moghaddam, M. F.; Canan, S. S.; Worland, P.; Sankar, S.; Raymon, H. K. CC-223, a potent and selective inhibitor of mTOR kinase: in vitro and in vivo characterization. *Mol. Cancer Ther.* **2015**, *14*, 1295–1305.

(42) Dolgin, E. Anticancer autophagy inhibitors attract 'resurgent' interest. *Nat. Rev. Drug Discov.* **2019**, *18*, 408–410.

(43) Dyczynski, M.; Yu, Y.; Otrrocka, M.; Parpal, S.; Braga, T.; Henley, A. B.; Zazzi, H.; Lerner, M.; Wennerberg, K.; Viklund, J.; Martinsson, J.; Grandér, D.; De Milito, A.; Pokrovskaja Tamm, K. Targeting autophagy by small molecule inhibitors of vacuolar protein sorting 34 (Vps34) improves the sensitivity of breast cancer cells to Sunitinib. *Canc. Lett.* **2018**, *435*, 32–43.

(44) Karaman, M. W.; Herrgard, S.; Treiber, D. K.; Gallant, P.; Atteridge, C. E.; Campbell, B. T.; Chan, K. W.; Ciceri, P.; Davis, M. L.; Edeen, P. T.; Faraoni, R.; Floyd, M.; Hunt, J. P.; Lockhart, D. J.; Milanov, Z. V.; Morrison, M. J.; Pallares, G.; Patel, H. K.; Pritchard, S.; Wodicka, L. M.; Zarrinkar, P. P. A quantitative analysis of kinase inhibitor selectivity. *Nat. Biotechnol.* **2008**, *26*, 127–132.

(45) Karlgren, M.; Simoff, L.; Backlund, M.; Wegler, C.; Keiser, M.; Handin, N.; Müller, J.; Lundquist, P.; Jareborg, A.-C.; Oswald, S.; Artursson, P. A CRISPR-Cas9 generated MDCK cell line expressing human MDR1 without endogenous canine MDR1 (cABC1): an improved tool for drug efflux studies. *J. Pharm. Sci.* **2017**, *106*, 2909–2913.

(46) Hopkins, B. D.; Pauli, C.; Du, X.; Wang, D. G.; Li, X.; Wu, D.; Amadiume, S. C.; Goncalves, M. D.; Hodakoski, C.; Lundquist, M. R.; Bareja, R.; Ma, Y.; Harris, E. M.; Sboner, A.; Beltran, H.; Rubin, M. A.; Mukherjee, S.; Cantley, L. C. Suppression of insulin feedback enhances the efficacy of PI3K inhibitors. *Nature* **2018**, *560*, 499–503.

(47) Wicki, A.; Brown, N.; Xyrafas, A.; Bize, V.; Hawle, H.; Berardi, S.; Cmiljanović, N.; Cmiljanović, V.; Stumm, M.; Dimitrijević, S.; Herrmann, R.; Prêtre, V.; Ritschard, R.; Tzankov, A.; Hess, V.; Childs, A.; Hierro, C.; Rodon, J.; Hess, D.; Joerger, M.; von Moos, R.; Sessa, C.; Kristeleit, R. First-in human, phase 1, dose-escalation pharmacokinetic and pharmacodynamic study of the oral dual PI3K and mTORC1/2 inhibitor PQR309 in patients with advanced solid tumors (SAKK 67/13). *Eur. J. Canc.* **2018**, *96*, 6–16.

(48) Gorter, J. A.; Aronica, E.; van Vliet, E. A. The roof is leaking and a storm is raging: repairing the blood-brain barrier in the fight against epilepsy. *Epilepsy Current* **2019**, *19*, 177–181.

(49) Löscher, W.; Potschka, H. Role of drug efflux transporters in the brain for drug disposition and treatment of brain diseases. *Prog. Neurobiol.* **2005**, *76*, 22–76.

(50) Löscher, W.; Potschka, H. Drug resistance in brain diseases and the role of drug efflux transporters. *Nat. Rev. Neurosci.* **2005**, *6*, 591–602.

(51) Anglicheau, D.; Pallet, N.; Rabant, M.; Marquet, P.; Cassinat, B.; Méria, P.; Beaune, P.; Legendre, C.; Thervet, E. Role of P-glycoprotein in cyclosporine cytotoxicity in the cyclosporine–sirolimus interaction. *Kidney Int.* **2006**, *70*, 1019–1025.

(52) Franz, D. N.; Lawson, J. A.; Yapici, Z.; Brandt, C.; Kohrman, M. H.; Wong, M.; Milh, M.; Wiemer-Kruel, A.; Voi, M.; Coello, N.;

Cheung, W.; Grosch, K.; French, J. A. Everolimus dosing recommendations for tuberous sclerosis complex-associated refractory seizures. *Epilepsia* **2018**, *59*, 1188–1197.

(53) Theilmann, W.; Gericke, B.; Schidlitzki, A.; Muneeb Anjum, S. M.; Borsdorf, S.; Harries, T.; Roberds, S. L.; Aguiar, D. J.; Brunner, D.; Leiser, S. C.; Song, D.; Fabbro, D.; Hillmann, P.; Wymann, M. P.; Löscher, W. Novel brain permeant mTORC1/2 inhibitors are as efficacious as rapamycin or everolimus in mouse models of acquired partial epilepsy and tuberous sclerosis complex. *Neuropharmacology* **2020**, *180*, 108297.

(54) Rageot, D.; Beaufile, F.; Borsari, C.; Dall'Asen, A.; Neuburger, M.; Hebeisen, P.; Wymann, M. P. Scalable, economical, and practical synthesis of 4-(difluoromethyl)pyridin-2-amine, a key intermediate for lipid kinase inhibitors. *Org. Process Res. Dev.* **2019**, *23*, 2416–2424.

(55) Fabian, M. A.; Biggs, W. H., 3rd; Treiber, D. K.; Atteridge, C. E.; Azimioara, M. D.; Benedetti, M. G.; Carter, T. A.; Ciceri, P.; Edeen, P. T.; Floyd, M.; Ford, J. M.; Galvin, M.; Gerlach, J. L.; Grotzfeld, R. M.; Herrgard, S.; Insko, D. E.; Insko, M. A.; Lai, A. G.; Lélías, J.-M.; Mehta, S. A.; Milanov, Z. V.; Velasco, A. M.; Wodicka, L. M.; Patel, H. K.; Zarrinkar, P. P.; Lockhart, D. J. A small molecule-kinase interaction map for clinical kinase inhibitors. *Nat. Biotechnol.* **2005**, *23*, 329–336.

(56) Hubatsch, I.; Ragnarsson, E. G. E.; Artursson, P. Determination of drug permeability and prediction of drug absorption in Caco-2 monolayers. *Nat. Protoc.* **2007**, *2*, 2111–2119.